Morphological, physiological and molecular characterization of root senescence in barley

Dissertation

zur Erlangung des
Doktorgrades der Naturwissenschaften (Dr. rer. nat.)

der

Naturwissenschaftlichen Fakultät I – Biowissenschaften –

der Martin-Luther-Universität
Halle-Wittenberg,

vorgelegt

von Herrn Zhaojun Liu

geb. am 28.02.1986 in Deyang, China

eingereicht am: 02.11.2017
verteidigt am: 07.03.2018

Gutachter:

1. Prof. Dr. Nicolaus von Wirén (IPK Gatersleben, Universität Halle-Wittenberg)

2. Prof. Dr. Klaus Humbeck (Universität Halle-Wittenberg)

3. Prof. Dr. Thomas Schmülling (Freie Universität Berlin)

Contents

Acknowledgements

Abbreviations

%	Percent
°C	Celsius
µl	Microliter
µm	Micrometer
µM	Micromolar
nm	Nanometer
min	Minute (s)
ml	Milliliter
mM	Millimolar
Log_2FC	Log_2 Fold change
ACC	1-aminocyclopropane-1-carboxylic acid
ACCO	1-aminocyclopropane-1-carboxylic acid oxidase
ABA	Abscisic acid
ABF	ABA response element binding factor
AP2	AP2 transcription factor
ARZ	Apical root zone
Aux-EC	Auxin efflux carrier
Aux-IP	Auxin induced protein
Aux-TP	Auxin transport protein
B	Boron
BRZ	Basal root zone
C	Carbon
CK	Cytokinins
CKX	Cytokinin oxidase
Cu	Copper
cZR	Cis-zeatin riboside
DW	Dry weight
FW	Fresh weight
GA	Gibberellic acid
GO	Gene Ontology
H_2O_2	Hydrogen peroxide
Hv	*Hordeum vulgare*

IAA	Auxin
IPR	Isopentenyladenin riboside
K	Potassium
LC-MS/MS	Liquid chromatography-tandem mass spectrometry
LEA	Late embryogenesis abundant protein
Mo	molybdenum
N	Nitrogen
NAC	<u>N</u>AM, <u>A</u>TAF, and <u>C</u>UC transcription factor
NCED	9-*cis*-epoxycarotenoid dioxygenase
P	Phosphorus
Pap	Papain-like family of cysteine proteases
PCD	Programmed cell death
PCR	Polymerase chain reaction
PIP	Plasma membrane instrinsic protein
qRT- PCR	Quantitative real time polymerase chain reaction
RCA	Cortical aerenchyma formation
ROS	Reactive oxygen species
S	Sulfur
SA	Salicylic acid
SAG	Senescence associated gene
SE	Standard error
SLs	Strigolactones
TDC	Tryptophan decarboxylase
TFs	Transcription factors
TIP	Tonoplast intrinsic protein
tZR	Trans-zeatin riboside
WRKY	WRKY transcription factor
Zn	Zinc

Summary

Plant roots serve important functions in water and nutrient uptake, and in anchoring above-ground plant organs in the soil. In addition, roots take over an important part in the developmental program of plants by synthesizing phytohormones, which modulate shoot development and play key roles in biotic or abiotic stress responses. All these root functions are embedded within a certain lifespan of a given root, which is determined by the progress of root aging. On the one hand, root aging is an important agronomy trait, because it associates with root activities such as nutrient uptake. On the other hand, root aging also contributes to global carbon cycling, because turnover of aging roots results in carbon input from the biotic carbon pool into the soil carbon pool. Despite the importance of root aging (or senescence) in plant performance and ecological functions, the mechanisms determining and regulating root senescence have remained unknown. To better understand this developmental process, the present thesis monitored hydroponically-grown barley plants over a period of 53 days and investigated senescence processes in seminal roots at the morphological, physiological and molecular level.

In a first step, microscopic investigations in seminal roots captured the progression of cortical senescence and root browning, which have been previously described as phenotypical markers of root senescence. Both of these two morphological events were first observed at 39 days after germination, which temporally coincided with arrested root elongation and root mass at day 39-46.

The second part of the thesis took physiological measurements that were associated with phenotypical root senescence. Root activity, as determined by nitrate uptake capacity, declined remarkably after day 39. Such reduction of root activity did not result from depletion of assimilates. Protein degradation, as indicated by the upregulation of peptidases and accumulation of urea and certain amino acids, suggested protein catabolism allowing roots to re-utilize nitrogenous sources. In addition, among 13 quantified elements, especially phosphorus (P) and zinc (Zn) contents in seminal roots declined after day 39, suggesting remobilization to shoots. These observations reinforced the idea that the biological processes captured in seminal roots resembled those observed during leaf senescence and thus are under control of a developmental program. Remarkably, a prominent and sharp abscisic

acid (ABA) peak appeared at day 39, which is proposed as a trigger for root senescence, since ABA is known to accelerate senescence processes also in leaves. To identify molecular regulators of seminal root senescence, transcriptome profiling was conducted separately for the apical root zone (ARZ) and basal root zone (BRZ). Gene ontology analysis indicated an enrichment of genes involved in transcriptional or posttranslational regulation before day 39, which then switched over to genes participating in protein catabolism and in the synthesis of tryptamine and serotonin, which were previously shown to play a regulatory role in leaf senescence, and indeed accumulated also here in seminal roots. Moreover, from day 39 on transcripts related to redox processes accumulated strongly, indicative for enhanced oxidative stress responses. In parallel, transcripts became enriched, which are involved in cytokinin degradation and ABA biosynthesis and which act as transcriptional regulators. Among the latter were several transcription factors from the NAC-, WRKY- and AP2-type families that may represent promising candidates for regulating seminal root senescence.

The present study represents the first comprehensive study on root senescence. It identified promising candidates for root senescence at the morphological (degradation of cortical cells), physiological (tryptamine, serotonin) and at the molecular level (ROS-related genes and transcription factors) that appear to act in a temporally coordinated manner. Based on these observations, it is concluded that the degenerative process in aging seminal roots underlie a genetically determined program that can be assigned to root senescence.

Zusammenfassung

Pflanzenwurzeln erfüllen wichtige Funktionen bei der Wasser- und Nährstoffaufnahme und bei der Verankerung oberirdischer Pflanzenorgane im Boden. Darüber hinaus übernehmen Wurzeln eine wichtige Rolle im Entwicklungsprogramm von Pflanzen, indem sie Phytohormone synthetisieren, die die Entwicklung von Trieben modulieren und eine Schlüsselrolle bei biotischen oder abiotischen Stressreaktionen spielen. Alle diese Wurzelfunktionen sind innerhalb einer bestimmten Lebensdauer einer gegebenen Wurzel eingebettet, die durch den Fortschritt der Wurzelalterung bestimmt sind. Auf der einen Seite ist die Wurzelalterung ein wichtiges agronomisches Merkmal, weil sie sich mit Wurzelaktivitäten wie der Nährstoffaufnahme in Verbindung setzen lässt. Auf der anderen Seite trägt die Wurzelalterung auch zum globalen Kohlenstoffkreislauf bei, da der Umsatz von alternden Wurzeln dazu führt, dass Kohlenstoff aus dem biotischen Kohlenstoffpool in den Kohlenstoffpool des Bodens eingespeist wird. Trotz der Bedeutung der Wurzelseneszenz bei der Pflanzenleistung und den ökologischen Funktionen sind die Mechanismen, die die Wurzelalterung bestimmen und regulieren, unbekannt. Um diesen Entwicklungsprozess besser zu verstehen, wurden in der vorliegenden Arbeit über einen Zeitraum von 53 Tagen hydroponisch gewachsene Gerstenpflanzen untersucht und Seneszenzprozesse in Samenwurzeln auf morphologischer, physiologischer und molekularer Ebene untersucht.

In einem ersten Schritt wurden mit Hilfe mikroskopischer Untersuchungen an Samenwurzeln das Fortschreiten von kortikaler Seneszenz und Wurzelbräunung ermittelt, die zuvor als phänotypische Marker der Wurzelseneszenz beschrieben wurden. Beide morphologischen Ereignisse wurden zuerst 39 Tage nach der Keimung beobachtet, was zeitlich mit der festgestellten Wurzelverlängerung und der Wurzelmasse am Tag 39-46 zusammenfiel.

Im zweiten Teil der Arbeit wurden physiologische Messungen vorgenommen, die mit einer phänotypischen Wurzelalterung assoziiert waren. Die Wurzelaktivität, bestimmt durch die Nitrataufnahmekapazität, ist nach Tag 39 merklich zurückgegangen. Eine solche Verringerung der Wurzelaktivität resultierte nicht aus der Erschöpfung von Assimilaten. Der durch die Hochregulierung von Peptidasen und die Akkumulation von Harnstoff und bestimmten Aminosäuren angezeigte Proteinabbau, lässt auf einen Proteinkatabolismus schließen, der es den Wurzeln erlaubt, stickstoffhaltige

Quellen wiederzuverwenden. Außerdem sanken unter 13 quantifizierten Elementen, insbesondere der Phosphor (P) - und Zink (Zn) -Gehalt in Samenwurzeln nach Tag 39, was die Remobilisierung dieser Elemente in die Triebe nahe legt. Diese Beobachtungen unterstützen die Hypothese, dass die biologischen Prozesse, die in Samenwurzeln nachgewiesen wurden, denen ähnelten, die während der Blattseneszenz beobachtet wurden, und somit unter der Kontrolle eines Entwicklungsprogramms stehen. Bemerkenswerterweise erschien am Tag 39 ein prominenter und scharfer Abscisinsäure-Peak (ABA), der als Auslöser für die Wurzelalterung vorgeschlagen wird, da bekannt ist, dass ABA Seneszenzprozesse auch in Blättern beschleunigt.

Um molekulare Regulatoren der Samenwurzel-Seneszenz zu identifizieren, wurde das Transkriptom-Profiling getrennt für die apikale Wurzelzone (ARZ) und die Basalwurzelzone (BRZ) durchgeführt. Die Analyse zeigte eine Anreicherung von Genen, die am Tag 39 in die transkriptionelle oder posttranslationale Regulation involviert waren, die im Folgenden auf Gene übergingen, die am Proteinkatabolismus und an der Synthese von Tryptamin und Serotonin beteiligt sind. Für diese Gene wurde gezeigt, dass sie eine Rolle bei der Blattseneszenz spielen

Darüber hinaus gab es ab dem Tag 39 eine starke Akkumulation von Transkripten, die sich auf Redoxprozesse beziehen lassen, was auf verstärkte oxidative Stressantworten hindeutet. Parallel dazu wurden Transkripte angereichert, die am Cytokininabbau und der ABA-Biosynthese beteiligt sind und als Transkriptionsregulatoren wirken. Unter den letzteren waren mehrere Transkriptionsfaktoren aus den Familien der NAC-, WRKY- und AP2-Typen, die vielversprechende Kandidaten für die Regulierung der Samenwurzel-Seneszenz darstellen könnten.

Die vorliegende Studie stellt die erste umfassende Studie zur Wurzelalterung dar und identifizierte vielversprechende Kandidaten für die Wurzelseneszenz auf der morphologischen (Abbau von kortikalen Zellen), metabolischen (Tryptamin, Serotonin) und der molekularen Ebene (ROS-verwandte Gene und Transkriptionsfaktoren), die zeitlich koordiniert zu wirken scheinen. Auf der Grundlage dieser Beobachtungen wird der Schluss gezogen, dass der degenerative Prozess in alternden Samenwurzeln einem genetisch determinierten Programm unterliegt, das der Wurzel-Seneszenz zugeordnet werden kann.

1 Introduction

1.1 Definitions of aging, senescence and programmed cell death

The term "senescence" derives from latin "senescere", which describes the final stage during aging of a cell, a tissue or an organism (Thomas, 2013). It is defined as a highly controlled sequence of biochemical and physiological degenerative processes, whereby nutrients are recycled from older organs to mostly younger tissues of the plant before cell death sets in (Thomas and Stoddart, 1980). This degenerative process is reversible as long as plant organs stay physiologically active, for instance leaves start yellowing due to chlorophyll degradation but re-green upon external or internal stimuli, such as nitrogen (N) supplementation or cytokinin (CK) production, respectively (Thomas et al., 2003). At the tissue level, senescence usually ends up with cell death (Pegadaraju et al., 2005). Therefore, senescence partially overlaps with programmed cell death (PCD), which refers to a cell biological process in which cells promote their own death through the activation of self-destruction systems (Can and Amasino, 1997). It has been even proposed that senescence qualifies as a *bone fide* occurrence of PCD (Noodén et al., 1997). Compared to senescence, aging describes a time-dependent process from germination of a plant or the initiation of an organ until a certain developmental stage or its death (Gerbner et al., 1980). In the present study, aging is used whenever the biological process can't be well assigned to senescence or PCD.

To properly differentiate between senescence, aging and PCD, the core concepts are revisited for some of their characteristics. First, reversibility of senescence is widely observed after endogenous cytokinin production or exogenous cytokinin application, after nitrogen resupply or after removal of sink organs (Crafts-Brandner and Egli, 1987; Gan and Amasino, 1995; Gupta et al., 2000; Schildhauer et al., 2008). In contrast, PCD typically occurs in individual cells after damage, under extreme stress, such as pathogen attack, or it is associated with pollen incompatibility, aleurone death in barley, or formation of tracheary and sieve tube elements (Beers, 1997; Reape et al., 2008). During the present study, no report could be found that shows reversibility of PCD. Furthermore, nutrient remobilization has not been reported in the context of PCD. By contrast, nutrient remobilization has been defined as the major physiological purpose of plant senescence to enhance the utilization of endogenous resources (Fischer and Gan, 2007).

Nevertheless, senescence and PCD are related in a temporal manner, since the initial phase of degradation processes, esp. including those of chlorophyll, is reversible and considered as senescence, while the second, irreversible phase terminates with PCD (Thomas et al., 2003). Physiological and molecular evidence agrees with such definitions, since DNA laddering, a hallmark of PCD, can only be detected at very late stages while chlorophyll degradation is initiated long before (Delorme et al., 2000). In the present study, PCD is regarded only as the very final stage of tissue senescence, while aging is used to describe the recorded, age-dependent events as long as they cannot be properly assigned to senescence or PCD.

1.2 Leaf senescence in plants

Leaf senescence is a highly regulated and organized developmental process during which macromolecules of the mature green leaf tissue are remobilized for further use by the plant (Zentgraf et al., 2010). Leaf senescence is a genetically controlled biological process, since at least more than 800 genes are up-regulated during leaf senescence (Gepstein et al., 2003; Guo et al., 2004; Buchanan-Wollaston et al., 2005). These genes are named senescence-associated genes (SAGs).

Leaf senescence can be described by several highly robust markers that can be examined at different levels. At the phenotypic level, senescence expresses in leaf yellowing due to a decline of the chlorophyll concentration, which serves as a widely used physiological marker. Leaf senescence can also be visualized by an increase of trypan blue- or Evans blue-stained leaf areas, which is indicative for the disintegration of plasma membranes leading to an uncontrolled efflux or cellular metabolites and constituents (Kim et al., 2009; Zhou et al., 2011). Another prominent marker for leaf senescence is the breakdown of rubisco, because rubisco is the most abundant N-containing protein in C_3 plants and thus a major N source in leaves for re-translocation of N to sink organs (Kokubun et al., 2002; Bohner et al., 2015). Exogenous application of serotonin and melatonin, which are well known as a pineal hormones in mammals, delayed leaf senescence possibly by reducing the endogenous abscisic acid (ABA) level and increasing endogenous cytokinin (CK) levels (Kang et al., 2009; Wang et al., 2013; Zhang et al., 2017). Overexpression tryptophan decarboxylase, the gene encoding the rate-limiting enzyme for the biosynthesis of serotonin and melatonin, increased the concentrations of serotonin

and melatonin, which subsequently delayed leaf senescence (Kang et al., 2009; Byeon et al., 2014). Another report showed that overexpression of tryptophan decarboxylase in rice resulted in the accumulation of serotonin, stunted growth and low fertility (Kanjanaphachoat et al., 2012). By what mode of action tryptophan decarboxylase regulates plant growth and senescence is still not clear.

At the molecular level, the cysteine protease gene *AtSAG12* is most widely used as transcriptional marker, as its expression is tightly induced by leaf senescence at a relatively late developmental stage but not by other external factors that promote leaf senescence, such as dark or ethylene treatment (Noh and Amasino, 1999). Expression analyses of orthologous genes to *AtSAG12* in other species, including soybean, oilseed rape or creeping bentgrass, confirmed a similar transcriptional regulation as in Arabidopsis (Noh and Amasino, 1999; Otegui et al., 2005; Xu et al., 2008).

The progression of leaf senescence is affected by various internal and external factors (Figure 1.1). Cytokinin and ethylene are among the best documented endogenous factors delaying or accelerating leaf senescence, respectively. In general, the concentration of leaf cytokinins drops before the onset of senescence (Noodén et al., 1990). An increase in leaf cytokinins, either brought about by applying cytokinins to the shoot (Richmond and Lang, 1957; Nooden et al., 1979) or by genetically modulating cytokinins biosynthesis, e.g. via expression of an isopentenyl transferase gene under control of a *SAG12* promoter (Gan and Amasino, 1995; Ori et al., 1999), delays leaf senescence. Ethylene can induce leaf senescence, however, only during a certain phase of leaf development (Grbić and Bleecker, 1995; Jing et al., 2002). In Arabidopsis, induction of leaf senescence by ethylene involves upregulation of the gene ETHYLENE INSENSITIVE2 (EIN2), which is a central signaling component required for all ethylene responses. EIN2 elevates its downstream target ETHYLENE INSENSITIVE3 (EIN3), and EIN3 induces via miR164 repression *ORE1/NAC2* (Oh et al., 1997; Li et al., 2013). Another phytohormone promoting leaf senescence is ABA. Its level increases in senescing leaves and several SAGs, including NAC transcription factors, were induced by exogenous ABA application (Weaver et al., 1998; Christiansen et al., 2011). However, the role of ABA in leaf senescence is not as well established as that of CK or ethylene. Among the external factors, nutrient supply plays a major role. In particular nitrogen withdrawal from the medium accelerates leaf senescence (Egli et al., 1978), and as long as leaves are

only chlorotic, senescence can be reversed via nitrogen resupply (Schildhauer et al., 2008). Another prominent external factor that induces leaf senescence is drought, which usually decreases yield and diminishes seed set and seed filling (Munné-Bosch et al., 2001; Brevedan and Egli, 2003). Delaying leaf senescence by expression of an isopentenyltransferase gene driven by a stress- and maturation-induced promoter resulted in remarkable drought tolerance in tobacco (Rivero et al., 2007).
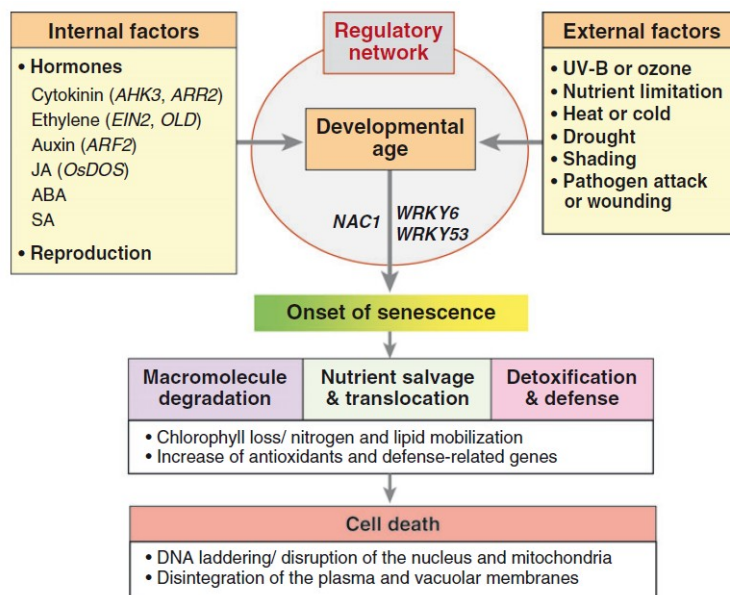
Figure 1.1 Model of the regulatory network leading to leaf senescence and cell death in plant leaves. Scheme taken from (Lim et al., 2007).

The regulatory network for leaf senescence is highly complex, since it is controlled by many factors and at multiple layers, including epigenetic, transcriptional as well as post-translational regulation. Among the major transcriptional regulators, individual members of the WRKY-, AP2-, NAC- and C2H2-type transcription factor (TF) families have been shown to regulate leaf senescence (Lim et al., 2007; Woo et al., 2013). For example, overexpression of *WRKY53* accelerated leaf senescence, while its suppression by RNAi or the gene knockout delayed leaf senescence. The putative target genes of *WRKY53* include several other WRKYs and other SAGs (Miao et al., 2004). Another well investigated leaf senescence regulator in Arabidopsis is *ORE1* (*ANAC092*), which controls the expression of at least 170 genes, and 48% of them

are known as SAGs (Balazadeh et al., 2010). Both *WRKY53* and *ORE1* have been described as early regulators of leaf senescence.

When internal and external factors are integrated into the regulatory network of leaf senescence, downstream processes including the breakdown of macromolecules and remobilization of nutrients are initiated, which are displayed by the decline of chlorophyll concentration and the degradation of rubisco for the relocation of N (Figure 1.1). This process also involves autophagy since several autophagy-related genes, including *AtAPG9* and *AtATG18a,* take part in the regulatory network of leaf senescence (Hanaoka et al., 2002; Xiong et al., 2005).

1.3 Plant roots and their turnover

Plant roots serve important functions in water and nutrient uptake, and in anchoring above-ground plant organs in the soil (Marschner, 2011). In addition, roots take over an important part in the developmental program of plants by synthesizing phytohormones including cytokinins (CKs), abscisic acid (ABA) and strigolactones (SLs), which modulate shoot development and play key roles in biotic or abiotic stress responses (Cornish and Zeevaart, 1985; Lachno and Baker, 1986; Letham, 1994; Dun et al., 2009). Despite of their importance, plant roots have not received much attention in crop breeding programs so far. Therefore, improving grain yield and quality by focusing on targeted breeding of root traits has been highlighted as "the second green revolution" in the 21st century (Lynch, 2007).

To better understand physiological processes and the molecular regulation underlying important root functions, numerous scientific achievements have been made in recent decades, such as uncovering genes involved in root gravitropism, drought tolerance, lateral root initiation or root-microbe interactions and their contribution to plant performance (Morita, 2010; Lavenus et al., 2013; Uga et al., 2013; Poole, 2017). Compared to the significant advance made in the understanding of such root-mediated plant traits, root aging and the determination of the lifespan of a root have remained poorly characterized. Elucidating the process of root aging and its determinants is not only important for breeding more efficient crop varieties, but also for providing a new ecological perspective on global carbon fixation. Plant roots make a large contribution to the pool of soil organic carbon (C) by releasing exudates or abandoning root tissue during root turnover (Gill and Jackson, 2000; Badri and Vivanco, 2009). A more than 10 years' experiment with maize estimated that at least

18% of root-bound C were finally transformed into soil organic C, while in case of C from the stalk residues it was only about 10% (Barber, 1979). At the global scale, plant roots are a major factor allocating C from the biotic pool to the soil pool, which contains 3 times more C than the biotic pool or the atmospheric pool (Lal, 2004). Therefore, root turnover and root aging are crucial processes in global C allocation to soils. In agricultural plant production systems, a better understanding of root aging is also required to economize fertilizer inputs, because a longer lifespan of roots allows maintaining a high level of nutrient uptake especially after flowering when root activity usually drops (Eshel and Beeckman, 2013). Hence, breeding cultivars with high vigor at late developmental stages and enhanced root activity during grain filling has become one of the breeding goals for rice in China (Cheng et al., 2004). In recent years, research related to root aging has received more attention, which is indicated by an increased number of publications addressing the turnover, lifespan, dynamics or aging of roots. However, definitions and mechanisms describing the biological events leading to root aging or senescence as a developmentally regulated process, which may be linked with nutrient remobilization or other beneficial metabolic processes supporting the development and maturation of seeds still remain unclear.

1.4 Cereal root types differ in anatomy and physiology

With regard to their development, roots are categorized into embryonic and postembryonic roots. Embryonic roots are formed originally from the embryo and are defined in graminaceous species as seminal roots, while postembryonic roots emerge after germination and include nodal roots. In maize, embryonic roots include one central primary root and a variable number of seminal roots, while postembryonic roots consist of nodal or crown roots and a few whorls of shoot-borne, so-called brace roots (Hochholdinger et al., 2004; Hochholdinger and Tuberosa, 2009; York and Lynch, 2015). Most other graminaceous species, such as wheat or barley, do not form a primary root but rather several seminal roots of similar age and emergence. In contrast, the root system of dicotyledonous plant species is relatively simple, since it is built from one primary root with continuously emerging lateral roots, which are postembryonic roots (Figure 1.2).
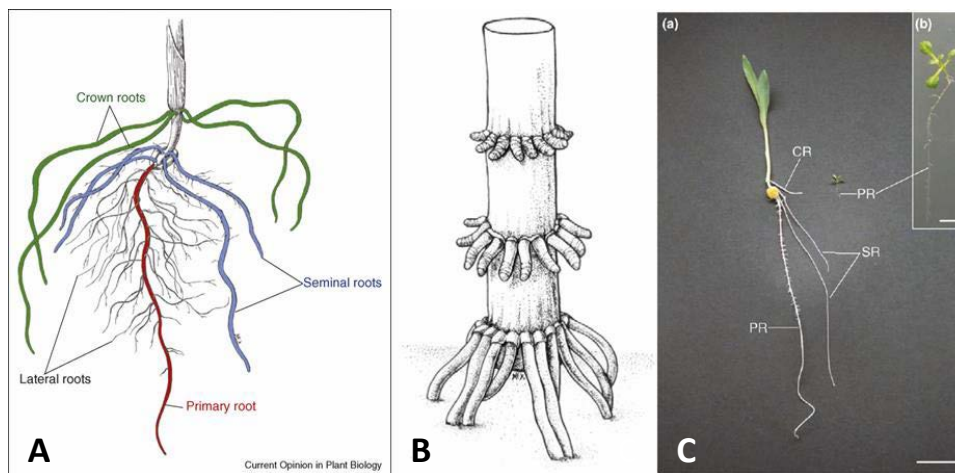
Figure 1.2 Root types of monocots and dicots. (A) The root system of maize includes one primary root (PR), several seminal roots (SR) and several whorls of crown roots (CR). (B) Example of different whorls of stem-borne roots in maize. (C) A comparison of the root system between maize and *Arabidopsis*. Pictures are taken from (Hochholdinger et al., 2004; Hochholdinger and Zimmermann, 2008; Hochholdinger and Tuberosa, 2009).

Even within the same root type, roots consist of tissues of different root age, which is a consequence of the developmental gradient established along a root axis. Taking postembryonic, nodal roots from barley as an example, the first nodal root initiates early during the juvenile growth phase. This process is followed by continuous emergence of nodal roots from newly established tillers. Finally, the gradually increasing nodal root system consists of roots that vary in their length from a few centimeters to more than 1 meter (Figure 1.3A). Inspecting a single root over its lifespan shows that an age gradient exists in longitudinal direction due to continuous cell division and elongation at the apex (Figure 1.3B). Age-dependent root gradients become more complex as soon as lateral roots of higher orders start emerging. Taken together, a root system consists of several age-dependent gradients along individual roots of different types and orders, which makes it difficult to investigate root aging processes in whole root systems.
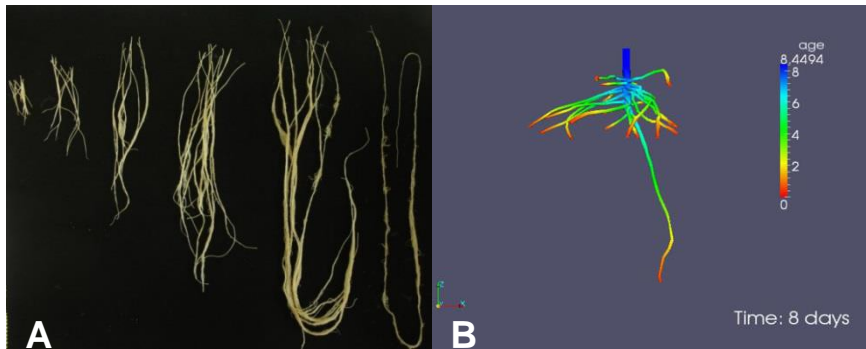
Figure 1.3 Root developmental stages and age-related gradient within a root type. (A) Nodal root system from a single barley plant at the age of 46 days. The nodal root system has been divided into 6 groups according to their developmental stage. (B) Tissue age distribution along the axes of primary and lateral roots of *Vicia faba* 8 days after planting. Pictures A and B have been taken from the present study and (Vetterlein and Doussan, 2016), respectively.

Differences between seminal and nodal roots become also evident at the anatomical level. In maize, the proportion of xylem vessels relative to the total stele area is significantly higher in seminal roots than in primary or crown roots, and the proportion of the stele area relative to the total root area is significantly higher in the crown roots (Figure 1.4A). In barley, seminal roots possess a thickened stele with a single large axile vessel and 6-8 xylem groups all bounded by a thick-walled endodermis, while neither the endodermis nor the stelar tissues are thickened in nodal roots which harbor 12-16 xylem groups (Figure 1.4B). These diverse root anatomies imply that different root types might differ in root functions.
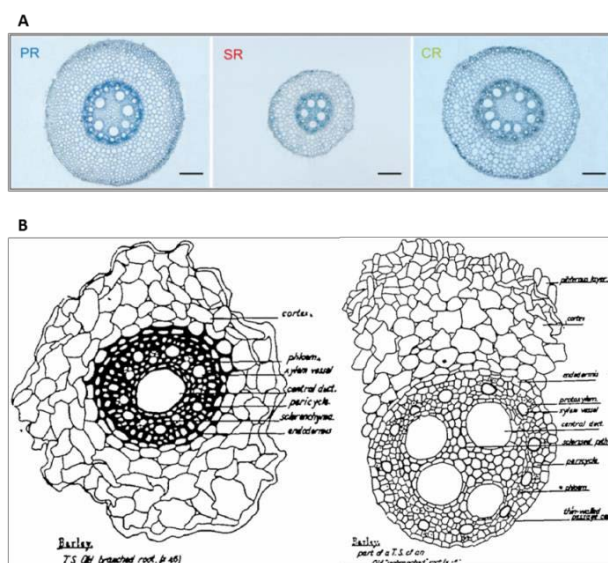
Figure 1.4 Anatomy of different root types in cereals. (A) Transverse sections of the proximal parts of 20 mm long roots of different root types in maize: primary root (PR), seminal root (SR) and crown root (CR). Scale bars = 200 μm. (B) Schematic comparison of transverse sections of a seminal root (left) and nodal root (right) in barley. Pictures have been taken from (Jackson, 1922; Tai et al., 2015).

Not only root anatomy but also physiological and molecular properties differ among root types of the same species (Valenzuela-Estrada et al., 2008; Lynch, 2013). For instance, root developmental programs differ between root types. A transcriptome study in rice revealed a significant enrichment of expressed genes associated with phytohormones and secondary cell wall metabolism in crown roots relative to seminal roots (Gutjahr et al., 2015). Under local supply of nitrate to maize, transcriptome studies revealed that pericycle cells of crown roots displayed the largest number of significant changes in gene expression when compared with other root types. This was interpreted as a prerequisite for the exceptionally large architectural plasticity of crown roots (Yu et al., 2016). Moreover, nutrient and water uptake capacities differ among root types. Based on the determination of nitrate uptake kinetics in maize, it has been shown that crown roots have a greater maximum influx rate, while seminal roots have a higher substrate affinity (York et al., 2016). In hydroponically-grown barley, hydraulic conductivity of cortical cells in the transition zone was significantly higher in nodal roots compared to seminal roots, which coincided with higher expression of *PIP2-* and *TIP*-type aquaporin genes involved in water transport. These results implied that nodal roots might be more efficient in water uptake than seminal roots (Knipfer et al., 2011).

In view of these important anatomical and physiological differences among root types, it is important to note that the investigation of root aging processes requires targeting of individual and defined root types whenever precise characterization is wanted.

1.5 Root aging in dependence of shoot development and source-sink relations

In ecological and agronomic studies, root dynamics is a widely used term to describe root growth processes over time, and in many cases, root dynamics has been used to assign root longevity or even senescence. By employing mini-rhizotrons, root dynamics has been expressed in terms of the formation of total root area (cm^2 m^{-2}), total root length (m m^{-2}) or root density (number of roots m^{-2}) over the lifespan of a plant. In case of wheat, barley or maize, all these dynamic root parameters increased as long as the plants were in their juvenile growth phase (Heeraman et al., 1993; Asseng et al., 1998; Liedgens et al., 2000). The time point of declining root dynamics was closely associated with flowering time, i.e. the transition of plants from vegetative to generative growth (Gregory et al., 1978; Merrill et al., 1996; Pietola and Alakukku, 2005; Pietola, 2005; Zhang et al., 2009; Kato and Okami, 2010). As shown in rice,

not only phenotypic parameters, but also physiological parameters such as root oxidation activity (Zhang et al., 2009) or root cytokinin concentrations (Yang et al., 2002) declined after heading. Moreover, estimating root N uptake capacity by a mathematical modeling approach suggested its decline when flowering starts (Guilbaud et al., 2015). The coincidence between flowering and the decline of root dynamics is best explained by altered source-sink relationships, since the formation of seeds creates a sink for assimilates, which outcompetes roots and decreases their provision with assimilates. The shortage of assimilates may induce a regulatory switch in roots that turns on a senescence program and decreases root dynamics.

Compared with studies integrating over the whole root system, split-root studies provide another perspective, which uncouples the link between flowering time and root dynamics. Growing roots of wheat or barley in a split hydroponic culture showed that water uptake capacity of seminal roots increased until day 40, before a sharp decrease set in (Krassovsky, 1926). When primary roots of maize were grown in sand and separately guided into a cylinder containing a ^{33}P-labeled phosphorus source, the shoot ^{33}P content reached its maximum at day 40, followed by stagnant values thereafter, which indicated that P uptake capacity of the primary root was almost completely lost after day 40 (Fusseder, 1987). By employing triphenyl-tetrazolium chloride reduction as a parameter to represent root activity in age-classified grape roots, it has been found that root activity decreased constantly from the 1st until the 6th week (Comas et al., 2000). As plants remained in their vegetative growth phase in the above-mentioned time frame, it appears that flowering was not the driving force for root degradation processes in these cases.

Noteworthy, mini-rhizotron-based approaches poorly differentiate between different root types, especially in case of graminaceous species, and risk to disregard that individual root types have distinct root ages and physiological properties (Zobel, 1992). Therefore, focusing on one specific root type is important when aging processes are to be monitored over the lifespan of a plant.

1.6 The current state of phenotypic, physiological and molecular studies provides an incomplete view of root aging

Anatomical studies have indicated that root aging frequently starts with the degradation of cortical cell layers. This so-called cortical senescence is considered a phenotypic or morphological event of root senescence, because it represents tissue

degradation, or even cell death, and leads to the final stage of the lifespan of a root. Cortical senescence was first identified in wheat and barley about half a century ago (Holden, 1975). In this study, dyes, such as acridine orange, were employed to stain nuclei and thereby to discriminate living, i.e. stained from dead cells. Surprisingly, cortical cell death set in already one week after germination, raising the question whether this reflects a purely developmentally regulated process. Although these observations were confirmed in wheat, barley, oat, rye and maize, their interpretation in the sense of a developmentally regulated program remained open (Deacon and Mitchell, 1985; KIRK and Deacon, 1986; Fusseder, 1987; Liljeroth, 1995). A more detailed study on cross sections from five weeks-old wheat roots revealed that degradation started in outer cortical cells, followed by those in the middle and by inner cortical cells. Moreover, this radial gradient progressed shoot-ward along the root axis (Bingham, 2007).

Cortical senescence can be induced by distinct external factors. For instance, hypoxia or waterlogging induce ethylene biosynthesis in roots, which induces cell death in cortical cells and causes cortical senescence (Justin and Armstrong, 1991; He et al., 1996). This is believed to be an adaptive process for better facilitating oxygen diffusion in roots under hypoxia (Armstrong, 1980). Nutritional factors, like low nitrogen or phosphorus provision, also induce cortical senescence (Drew et al., 1989; Fan et al., 2003), which suggests that cortical senescence is subject to regulation by internal and external stimuli. Reactive oxygen species (ROS) are believed to be a trigger of cortical senescence (Bouranis et al., 2003; Yamauchi et al., 2011). Apart from ROS, the characterization of molecular processes triggering cortical senescence is still poor. Transcriptome analysis revealed that 223 genes significantly changed their expression levels after inducing cortical senescence in primary roots of maize by ethylene. In this study, genes involved in ethylene signaling, cell wall modification and proteolysis were highlighted (Takahashi et al., 2015).

Compared to cortical senescence, root browning is another phenotypic marker that may indicate root senescence, since newly formed roots are white but turn brownish when they age. This phenotypic change is widely used in ecological studies when root turnover is investigated (Heeraman et al., 1993; Comas et al., 2000; Hishi and Takeda, 2005; Konôpka et al., 2006). In *Eucalyptus pilularis* and *Pinus banksiana*, root browning was associated with condensed tannin accumulation in cortical cell walls and decaying epidermis and cortex, leaving a dead, tannin-filled sheath

surrounding an intact and living stele (McKenzie and Peterson, 1995). In a physiological investigation, brown roots showed lower respiration rates and lower nitrate uptake capacities compared to white roots (Baldi et al., 2010). These studies indicated that root browning is correlated with declining physiological root functions. It is noteworthy that root aging is not the only factor that causes root browning, other factors such as low soil water content, metal toxicity or high soil temperature also enhanced root browning (Rogers, 1940; Bartsch, 1987; Rahman et al., 2005). So far, a comprehensive understanding of root aging is still lacking. Neither root cortical senescence nor root browning has been causally linked to root aging.

At the physiological level, nutrient uptake capacity has been widely utilized as a marker for root aging or senescence, but most results are difficult to interpret in the context of root aging processes. Actually, most of these uptake studies were conducted over a period of 1-3 hours with detached short root segments, instead of examining intact roots over a short time period, which is a standard when determining uptake capacities (Bouma et al., 2001; Volder et al., 2005). Biosynthesis of phenols might be another physiological marker for root aging, since soluble phenol concentrations significantly increased with increasing root order (Adams and Eissenstat, 2015). To date, robust physiological markers of root aging or senescence haven't been identified.

At the molecular level, a cysteine protease of red clover, *Tp-cp8*, was found to be up-regulated in roots under both, root aging and stress conditions, such as defoliation or shading (Webb et al., 2010). Overexpression of cytokinin oxidase genes in Arabidopsis, leading to cytokinin deficiency in roots, increased primary root length, lateral root number and the number of dividing cells in the apical root zone (Werner et al., 2003). Interestingly, cytokinin-depleted barley lines displayed less root browning than wild-type roots at later developmental stages, which may be indicative for delayed root senescence (Mrízová et al., 2013). However, to what extent cytokinin depletion may affect other root senescence markers has not been investigated yet.

1.7 Aim of the thesis

As described above, it still remains open how to define root senescence and how to set it apart from root aging. In particular the following questions remain to be addressed: i) How to dissect senescence-related processes in complex root systems, which consist of diverse root types? ii) How do root senescence-related processes

develop in relation to leaf senescence? iii) Can physiological and molecular markers be identified that describe root senescence? iv) What are the molecular determinants that regulate root senescence?

The goal of the present thesis was to characterize root aging processes at the morphological, physiological and molecular level and to examine their nature and progression in the context of organ senescence. For this purpose, a hydroponic culture system was used for the cultivation of barley plants to facilitate the access to defined root types. In order to reduce the complexity of the investigated root system, seminal roots instead of the whole root system were chosen as target organs. Over a period of 53 days, roots samples were taken weekly and independently from apical and basal root zones for the examination of tissue age- and plant age-related markers. The timeline of the present study was based on the appearance of cortical senescence and root browning, since these two phenomena were most evident and typical for degenerative processes in roots. These two processes were recorded together with other parameters, such as root biomass and total root length (chapter 3.1). Within the time frame of these degenerative processes, an uptake experiment with ^{15}N-labeled nitrate was conducted to describe root activity (chapter 3.2). To address the question to what extent these root aging processes depend on shoot development and assimilate delivery, chlorophyll concentrations were determined in individual leaves together with shoot meristem development and related to sugar concentrations of seminal roots (chapter 3.1, chapter 3.2).

Two fundamental differences that distinguish senescence and root aging are reversibility and nutrient remobilization (see above). The present study could not investigate the reversibility of root senescence due to limited knowledge of which internal or external factors may determine root senescence. Therefore, root samples were profiled for phytohormones, which may regulate root senescence as they do in leaf senescence. In addition, nutrient remobilization was also investigated in order to differentiate senescence and aging.

In chapter 3.3 of this thesis, plant age-dependent changes in the root transcriptome were recorded. GO term analysis was used to identify major processes characterizing distinct root developmental phases, and the expression pattern of putative marker genes was verified by qRT-PCR. On the basis of transcriptome studies, putative senescence-related metabolites were determined by MS-based analysis (chapter 3.4).

Chapter 4 of this thesis discusses all major results and findings in the context of previous work related to root aging or root senescence-related processes. This chapter integrates over the most relevant data to discern whether the recorded data reflect a genetically determined developmental process, which may even involve nutrient remobilization. The discussion further extends into the plant nutritional and agronomic dimension of root senescence.

2 Materials and methods

2.1 Plant culture and sampling

Barley (golden promise) seeds were germinated on wet filter paper for 5 days under dark condition at 4°C. Then germinated seeds were cultured on the soft plastic needles with half-strength nutrient solution which is in absence of iron for 7 days. Plants were finally grown in the full nutrient solution (2 mM $Ca(NO_3)_2$, 0.5 mM K_2SO_4, 0.5 mM $MgSO_4$, 0.1 mM KH_2PO_4, 0.1 m $MKCl$, 1 µM H_3BO_3, 2.5 µM $MnSO_4$, 0.5 µM $ZnSO_4$, 0.2 µM $CuSO_4$, 0.01 µM $(NH_4)_6Mo_7O_{24}$ and 0.1 mM Fe-EDTA) under long day condition (16 h light/ 8 h dark, light intensity 250 µmol m^{-2} sec^{-1}; 20°C/ 18°C light/dark, 70% humidity) and nutrient solutions were renewed every 3 days.

In order to distinguish organ age- and plant age-dependent markers, barley seminal roots were harvested as two fractions: the apical root zone (ARZ), which contains the tissue between root cap and the 1st 1mm lateral root, and, the basal root zone (BRZ), which consists of the remaining part after ARZ removal of the seminal roots. Ideally, the newly generated ARZ should not hold organ age-dependent but only plant age-dependent information. This is due to the logic that new ARZ has the same organ age, thus organ age-dependent information should be the equal between new ARZs, and the gradual altered expressions of genes between ARZs are suspected to correlate with plant age since it's accordingly increasing.

Experimental materials were collected weekly, i.e. at 18, 25, 32, 39, 46 and 53 days after germination: individual leaves of the main tiller were harvested and frozen in liquid nitrogen; the root system was first washed by 1mM $CaSO_4$ for 1 min and quickly wiped by paper tissue, then the apical root zone (ARZ), basal root zone (BRZ), whole seminal roots (non-fractionated) as well as the whole nodal roots were separately harvested and frozen in liquid nitrogen. For microarray and hormone quantification, ARZ and BRZ were separately analyzed. For all the physiological analysis, non-fractionated seminal roots were analyzed.

2.2 Total seminal root length and root mass quantification

At each harvest, 15 plants were taken for the total seminal root length measurement. Individual seminal root length from each plant was measured by ruler, sum data of individual seminal root length within each plant was taken as one biological replica of

total seminal root length. After seminal root length measurement, seminal roots, nodal roots and the whole shoots were dried in 65°C for 5 days and weighted to get their dry mass.

2.3 Staining and light microscopy

Root apical zone observation: fresh sampled seminal root tips were checked under VHX-5000 digital microscopy (Keyence Corporation) weekly.

Anatomical examination: Barley seminal roots were incubated with 0.25 % (w/v) Evans blue aqueous solution for 15 min at room temperature under vacuum condition. Stained roots were washed three times (10 min each) with distilled water on the shaker and then 4 different segments along with seminal roots with the length of 0.5 - 1 cm were collected. These 4 different segments are defined as: 5 cm under the hypocotyl, 20 cm under the hypocotyl, the position of the first 1 mm lateral root emerged and root meristem, respectively. All these segments were embedded in 4% agar and sliced by vibratome (Carl Zeiss) and photographed by light microscopy (Carl Zeiss).

2.4 ^{15}N uptake performance for seminal root

Nitrogen influx was examined every 7 days. The whole root system (including seminal and nodal roots) was washed in 1mM $CaSO_4$ solution for 1 min, seminal roots were spatially separated from nodal roots and then incubated for 20 min in full nutrient solution containing 0.5 mM $^{15}NO_3$ (98% ^{15}N), nodal roots were also incubated for 20 min but with another pot containing non-labeled N full nutrient solution. After rinsing the seminal and nodal roots in 1mM $CaSO_4$ for 1 min separately, plants were separated into seminal root, nodal roots and the whole shoot. All these organs were freeze-dried and subjected to ^{15}N determination by isotope ratio mass spectrometry (NU Instruments, http://www.nu-ins.com).

2.5 Chlorophyll concentration measurement

Chlorophyll was extracted and quantified as described *(Porra et al., 1989)*. 1.8 ml dimethylformamide (DMF) was added to 10 - 25 mg grinded leaf samples and incubated at 4°C for 1 day. Absorbance at 647nm and 664nm were collected by

spectrophotometer. Chlorophyll concentration was calculated by both chlorophyll a and b (µg mg^{-1}): 1.8*(7.04*Abs664 + 20.27*Abs647)/ FW.

2.6 Elemental analysis

For element analysis, grinded plant tissues were dried at 65°C for 5 days. About 2 mg dry materials were subjected to ICP-MS analysis.
Total nitrogen was quantified by EA-MS.

2.7 Sugar and amino acids analysis

Soluble sugars were determined according to the literature (Hajirezaei et al., 2000; Ahkami et al., 2009). Briefly, 50 mg frozen root material was homogenized in liquid nitrogen, dissolved in 0.75 ml of 80% (v/v) ethanol and incubated at 80°C for 60 min. Crude extracts were centrifuged at 14,000 rpm at 4ºC for 5 min and the upper phase was concentrated in a speed vacuum concentrator (Christ, RVC 2-33 IR, Germany) at 45°C for 180 min. The pellet was re-suspended in 0.3 ml HPLC-grade water and shaken for 15 min at 4°C for the measurement.

For the measurement of free amino acids, the same extracts as used for sugar analysis were used. To detect primary and secondary amino acids, a fluorescing reagent AQC (6-aminoquinolyl-N-hydroxysuccinimidylcarbamate) was used. ACQ was dissolved in 3 mg ml-1 of acetonitrile and incubated at 55°C for 10 min. Ten µl of sugar extracts were derivatized in a cocktail containing ´10 µl of the fluorescing reagent ACQ, 80 µl of a 0.2 M boric acid buffer (pH 8.8) in a final volume of 100 µl. The solution was incubated at 55°C for 10 min. Separation of soluble amino acids was performed on a newly developed UPLC-based method using Ultra pressure reversed phase chromatography (Acquity H-Class, Waters GmbH, Germany). UPLC system consisted of a quaternary solvent manager, a sample manager-FTN, a column manager and a fluorescent detector (PDA eλ Detector). The separation was carried out on a C18 reversed phase column (ACCQ Tag Ultra C18, 1.7 µm, 2.1x100 mm) with a flow rate of 0.7 ml per min and duration of 10.2 min. The column was heated at 50°C during the whole run. The detection wavelengths were 266 nm for excitation and 473 nm as emission. The gradient was accomplished with four solutions prepared from two different buffers purchased from Waters GmbH (eluent A concentrate and eluent B for amino acid analysis, Waters GmbH Germany). Eluent A

was pure concentrate, eluent B was a mixture of 90 % LCMS water (The Geyer GmbH, Germany) and 10 % eluent B concentrate, eluent C was pure concentrate (eluent B for amino acid analysis) and eluent D was LCMS water (The Geyer GmbH, Germany). The column was equilibrated with eluent A (10 %) and eluent C (90 %) for at least 30 minutes. The gradient was produced as follow: 0 min 10% A and 90 %C / 0.29 min 9.9 % A and 90.1 % C / 5.49 min 9 % A, 80 % B and 11 % C / 7.1 min 8 % A, 15.6 % B, 57.9 % C and 18.5 % D / 7.3 min8 % A, 15.6 % B, 57.9 % C and 18.5 % D / 7.69 % 7.8 % A, 70.9 % C and 21.3 % D / 7.99 min 4 % A, 36.3 % C and 59.7 % D / 8.68 min 10 %A, 90 % C / 10.2 min 10 % A and 90 % C.

2.8 Urea quantification

About 5mg milled freeze-dried sample are mixed with 350 µl 10 mM formic acid together with 2 small metal beans. Shaking the mixture overhead in 4℃ for 10 min followed by 13200 rpm centrifuge at 4°C for 15 min. Supernatant is transferred to a

new 1.5 ml Eppi then keep in -20℃ for at least 2 hours in order to make sugars down. For analysis, 50 µl room temperature warmed extracts is transferred into a new 1.5 ml Eppi then mixed with 1000µl Color development reagent. The new mix is incubated at 99°C for 15 min, shaking 750 rpm. Samples are immediately incubated on ice for 5 min then keep in dark at room temperature until measurement. The absorption is determined at 540nm with the Photometer. Standard curve by using pure urea with different dilutions are conducted with samples in parallel.

Buffer preparation:
Stock acid reagent: (stored in dark at 4 °C, storable for up to ½ year)
0.25 g ferric chloride hexahydrate ($FeCl_3.6H_2O$ MW=270.30g/mol)
7.5 ml MQ water
5.0 ml ortho-phosphoric acid (H_3PO_4 MW=98g/mol)

Mixed acid reagent: (stored in dark at 4 °C, storable for up to ½ year)
40 ml MQ water
10 ml concentrated H_2SO_4 (MW=98.08g/mol)
30 µl **Stock acid reagent**

Stock color reagent A: (stored in dark at 4 °C, storable for up to ½ year)

200 mg diacetylmonoxime (toxic, $C_4H_7NO_2$, MW=101.1g/mol)

10 ml MQ water

Stock color reagent B: (stored in dark at 4 °C, storable for up to ½ year)

50 mg thiosemicarbazide (toxic, CH_5N_3S, MW=91.14g/mol)

10 ml MQ water

Mixed color reagent: (stored in dark at 4 °C, storable for up to ½ year)

3.5 ml Stock color reagent A

3.5 ml Stock color reagent B

43.0 ml MQ water

Color development reagent: (always prepare fresh up to ½ day before you start,

this reagent should also keep in dark and on ice when you are using)

1: 1: 1 =MQ water: Mixed color reagent: Mixed acid reagent (v: v: v)

2.9 Catalase activity measurement

Catalase activity measurement is based on oxygen electrode method with the machine from Hansatech Instruments. Briefly, 200 µL 4°C pre-cooled PBS solution added 0.6 g grinded fresh samples, then add 200 µL 400 µL pre-cooled PBS solution 4°C, 1.6 g for each tube. After shake the mixture at 1400 for 20 min. Centrifuge, 4 °C, 10000 g for 15 min. Transfer the supernatant into a new tube. Set up the oxygen electrode by proper calibration as described by the handbook. Transferring 2 ml 50 mmol/L H_2O_2 to the oxygen electrode chamber followed by adding 40 µL extracted solution. Close the chamber and start recording data, the measurement should at least lasts for 2 min. Choosing the O_2 production curve between 0 min – 2 min to get total amount of O_2. Catalase Activity = (200µL / 40µL) x Oxygen / 2 min / FW

2.10 Phytohormone measurements

Methods for phytohormone quantification is describe as literatures (Kojima et al., 2009; Kermode, 2011). In brief, 10-30 mg freeze dried samples were extracted by 1 x 1 ml 0.5 % FA in H2O/MeOH 30/70 (4 °C) add 2 steel ball´s, vortex 30 sec. Add 15

min ultrasonic bath (4 °C). The mixtures were shaking overhead for 1h (4 °C) followed by centrifuge 10 min 4 °C 14.000 rpm, transfer supernatant to a new 2 ml Eppi. Repeat the extraction and combine the supernatants and evaporate the MeOH with vacuum centrifuge ca. 20 - 30 min = 0.6 ml left in the Eppi. Extract again by 1 x 1 ml 0.5 % FA in H2O (4 °C), vortex 30 sec. Add 15 min ultrasonic bath (4 °C). Extract with overhead shaking for 1h (4 °C) then centrifuge 10 min 4 °C 14.000 rpm, transfer supernatant and combine in the 2 ml Eppi. Add internal standard in 200 µl MeOH and evaporate MeOH with vacuum centrifuge ca. 15 min = 1,6 ml left in the Eppi. The extracted solutions then subjected for sample cleaning. Cleaned samples were then subjected to UPLC-MS analysis for hormone quantification.

2.11 Tryptophan, tryptamine and serotonin measurements

Extraction and analysis of tryptophan, tryptamine and serotonin was described in literatures but with some modifications (Cao et al., 2006; Kang et al., 2009). Root samples were grinded in liquid nitrogen. About 50-70 mg fresh sample was extracted with 300 µl 100% methanol. Solutions were centrifuged and supernatants were evaporated with vacuum centrifuge. Resolve the dried material by adding 60 µl 25% methanol. Quantify metabolites by subjecting the samples for UPLC-MS analysis.

2.12 Microarray analysis

About 100 mg fresh root samples (both apical root zone and basal root zone) of all 6 time points (day 18, 25, 32, 39, 46, 53) were subjected to RNA extraction, each time point had 3 biological replications. RNA was extracted using a Plant Mini RNA kit (Qiagen, Hilden, Germany) following the manufacturer's protocol. RNA was quantified using the NanoDrop ND-1000 (Peqlab, Erlangen, Germany) and the quality of extracted RNA was verified with a Bioanalyzer 2100 (Agilent Technologies, Santa Clara, CA, USA). RNA was labeled through the application of a low-input QuickAmp Labeling kit (Agilent Technologies). The labeled cRNA samples were subsequently purified using RNeasy Mini Spin columns (Qiagen), and 600 ng of Cy 3-labeled, amplified cRNA were hybridized, following the manufacturer's protocol, to a custom-synthesized 60k Barley Microarray (Agilent Technologies). The quantified feature text file was first subjected for quality checks using the Agilent QC chart tool and the resulting data were analyzed using Gene Spring 12.0 software (Agilent

Technologies). After quantile normalizing and baseline transformation to median of all samples, the probe sets (genes) were filtered by coefficient of variation < 50%, followed by moderated unpaired t-tests and Benjamini-Hochberg corrections. Probe sets that passed the P-value cut-off of ≤0.05 were defined as significant expressed genes.

Within the GO analysis, redundant GO terms are widely exist because transcripts are multifunctional. These redundant GO terms could be eventually narrow down to more specific biological processes without significantly reduced gene numbers. Therefore, to simplify these redundant GO terms and display more specified biological process, the lowest hierarchy GO terms of individual branch were chosen.

2.13 Quantitative RT-PCR

The methodology of qPCR is performed as described (Schmittgen and Livak, 2008). List of primer sequences for RT-PCR:

	Primer Forward	Primer Reverse
HvUBC	TCTGCTTTCAATCTGCTCGC	CTCCGTATCATCCCATGGCA
HvNAC005	CCATGTGAACAGCAGCGGCAAC	CCGACGTTGAGGCTGGTGAATC
HvNAC027	ACGGCTACGTGAACCACGACAC	CAAGCTGCCGCTGGATCTCTTC
HvPap-14	TACGCCTTCCAGTACATCGC	CGTCCTCATACCCGTCGATG
HvPap-15	TGATGAACGCTGTGGCAAAC	TACATGGCCCGTTGTAGATTCC
HvPap-17	AGCTGCGTGTGCATTTATCATG	GCGGTGAAATATGCAACCCA
HvNCED1	CCAGCACTAATCGATTCC	GAGAGTGGTGATGAGTAA
HvNCED2	CATGGAAAGAGGAAGTTG	GAAGCAAGTGTGAGCTAAC

2.14 Phylogenetic analyses

Amino acid sequence alignments were performed using the ClustalW module in the MEGA (Molecular Evolutionary Genetics Analysis) 6.0 program (Tamura et al., 2013). Neighbor-joining trees and bootstrap analyses were also conducted using MEGA 6.0, and the following parameters were selected: model, p-distance; bootstrap, 1000 replicates; and gap/missing data, pairwise deletion. NCBI accession numbers of individual proteins are listed within the phylogenetic tree.

3 Results

3.1 Phenotypical characterization of seminal root aging

3.1.1 ley plant development and seminal root growth

To monitor the onset and progression of the aging process in roots over time, barley plants were cultivated hydroponically for about 2 months. Seminal roots were spatially separated from later emerging nodal roots, and shoots, seminal and nodal roots were harvested at days 18, 25, 32, 39, 46 and 53. Tillering started approx. at day 25 (Figure 3.1). At day 53 plants were at growth stage 36 (GS36) and had developed 6 visible nodes (Figure 3.1). A timely start of plant sampling was required to catch early senescence processes in roots, as from day 25 on the first leaf of the main tiller became chlorotic (Figure 3.2A). The seminal roots proliferated until day 39 but then turned brown, indicating the appearance of root browning, a root senescence marker that formerly used in literatures (see introduction 1.6). In contrast, nodal roots started to develop from day 18 on and strongly proliferated until day 46. Then, also nodal roots turned brown while their biomass was still increasing until day 53 (Figure 3.1, Figure 3.2B).

According to their development individual leaves of the main tiller gradually turned yellow over time (Figure 3.2A). At the whole-main-tiller level, chlorophyll degradation proceeded in a stepwise manner starting for leaf 1 being completely chlorotic at day 32, while every subsequent leaf became fully chlorotic approx. one week later. Thus, at final harvest, four leaves of the main tiller were completely chlorotic (Figure 3.2A), while the whole shoot phenotype that was dominated by the leaves of younger tillers still appeared to be green (Figure 3.1).

From day 18 on, biomass of nodal roots increased exponentially over time, suggesting this trend continued also after day 53 (Figure 3.2B). In contrast, seminal root biomass increased linearly between day 18 and day 46 and then levelled off, while seminal root elongation begun to stagnate on day 39 (Figure 3.2C). A closer look at the apical zone of the seminal roots revealed that after day 32 some of the seminal root tips degraded – similar to the phenotype shown in Figure 3.3. On day 39, almost 20% of the seminal root tips were degraded and this value increased up to 80% at the last harvest (Figure 3.2D). At the whole plant level, root-to-shoot biomass ratio showed a gradual decrease until day 39, followed by a slight increase afterwards, which suggested that up to day 39 plants invested more assimilates in tiller formation

while after day 39 the root-to-shoot biomass ratio slightly increased due to the exponential growth of nodal roots (Figure 3.2E). Taken together, these data indicate that seminal root development underwent a transition around day 39, when they started turning brown, did not continue elongating and degradation of apical zone set in.

Figure 3.1 Visual development of shoots, seminal and nodal roots from day 18 to day 53 after germination. The root system has been separated into seminal (left) and nodal roots (right). Inserts show node elongation of the main tiller at day 46 and day 53. Each image represents one representative plant.

(A)

Leaf 11
Leaf 10
Leaf 9
Leaf 8
Leaf 7
Leaf 6
Leaf 5
Leaf 4
Leaf 3
Leaf 2
Leaf 1

1.8 1.4 1.0 0.6 (µg mg⁻¹ FW)
2.0 1.6 1.2 0.8 0.4

18 25 32 39 46 53
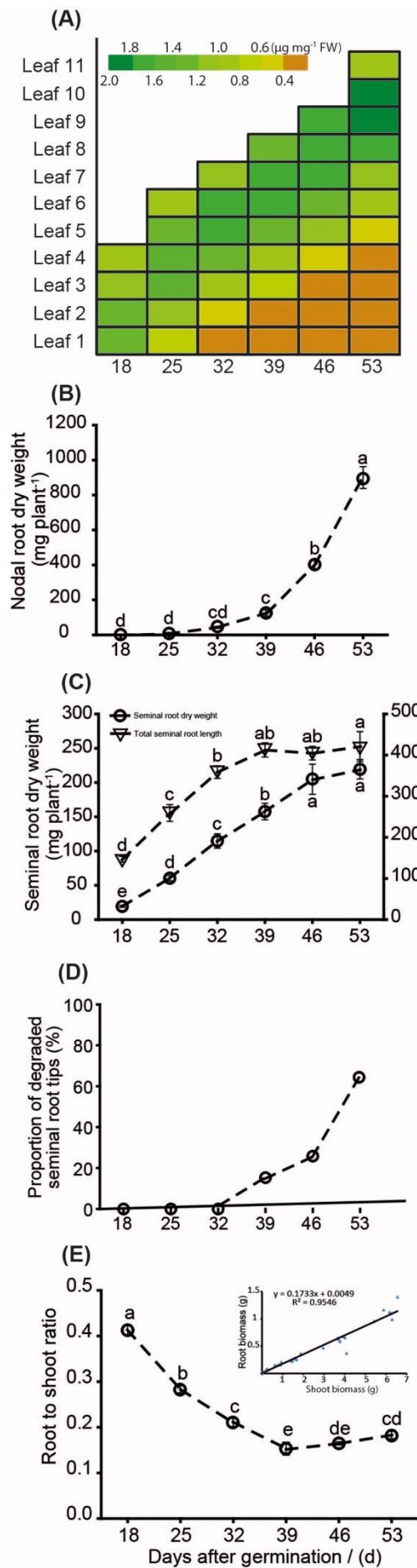
Figure 3.2 Quantitative analysis for barley shoot and root development from day 18 to day 53 after germination. (A) Chlorophyll concentrations of individual leaves of the main tiller. (B) Dry mass of the nodal root system. (C) Dry mass of the seminal root system and the total seminal root length. (D) Proportion of degraded apical zone of seminal roots. (E) Dry mass based root to shoot ratio. Error bars indicate mean values ± SE. For graph (A) - (D), n=5. For graph (E), n=15. Different letters indicate significant differences according to LSD, p<0.05.

3.1.2 eminal root structure and anatomy over time

To investigate whether macroscopic or cell structural changes were responsible for the arrested elongation and root tip decay of seminal roots, barley seminal roots were subjected to light microscopy. As a reference for shoot development, spike development of the main tiller was inspected in parallel.

At day 25, spike of the main tillers had entered the double rage stage. With regard to the apical root zone, the diameter of root tips appeared to increase between day 18/25 and day 32. Root tips were smooth and whitish before day 32 but turned brown with dark spots on the surface afterwards. Finally, the outer cell layers were degrading so that only the stele with the vascular system remained (Figure 3.3).

More detailed changes in tissue and cell structure were examined in radial root sections that were taken at four positions along the seminal root axis: i) 5 cm below the hypocotyl, ii) 20 cm below the hypocotyl, iii) at the position where the first lateral root had emerged to a maximum length of 1 mm, and iv) at the apical meristem. Evans blue staining indicated that already on day 18, epidermal cells in the most basal root section were partially leaky (Figure 3.4). Epidermal cell decay proceeded acropetally and on day 39 epidermal cell death had reached the root tips. In contrast, radial sections at the other three positions showed intact tissue structures at the first three time points (Figure 3.4). On day 39, epidermal, exodermal and cortical cells were partially degraded at the position in the basal root zone. Degradation of the other root cells proceeded acropetally and reached the apical zone (Figure 3.4). Taken together, this structural analysis indicated that epidermal cells partially lost integrity quite early during root development, whereas disintegration of the root tissue was mainly caused by the loss of cortical cells.

Figure 3.3 Developmental stages of the apical shoot meristem and the seminal root tip at harvested time points. Shoot meristems from the main tiller were photographed. 100x and 200x indicates microscopic magnification.
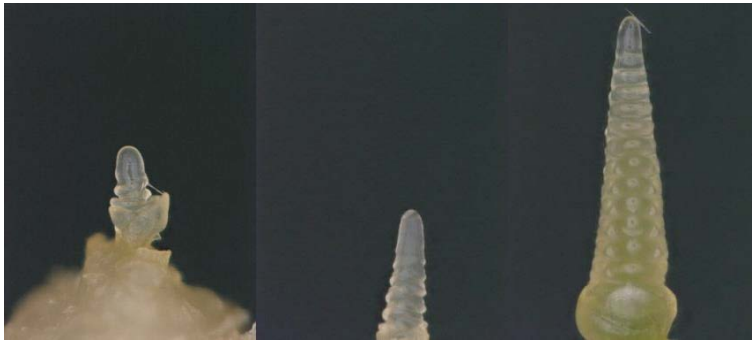
Day 18 200x	Day 25 200x	Day 32 200x
Day 18 100x	Day 25 100x	Day 32 100x
Day 39 100x	Day 46 100x	Day 53 50x
Day 39 100x	Day 46 100x	Day 53 100x
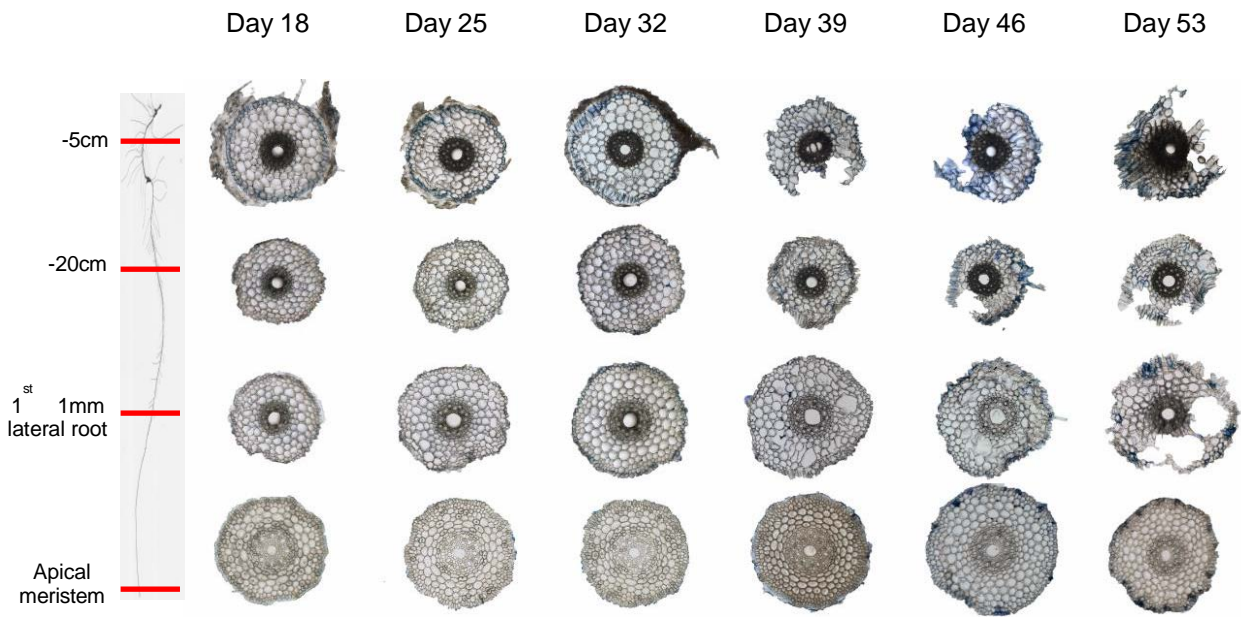
Figure 3.4 Structural changes in seminal roots over time. Seminal roots of hydroponically-grown barley plants were stained with Evan's blue. Roots were sectioned at four positions: i) 5 cm below the hypocotyl, ii) 20 cm below the hypocotyl, iii) at the position where the first lateral root had emerged to a maximum length of 1 mm, and iv) at the apical meristem. Each image shows a representative sample.

3.2 Physiological characterization of seminal root aging in barley

3.2.1 acterization of seminal root activity during aging

Nitrogen uptake capacity was chosen as an indicator of root activity, because nutrient uptake is one of the fundamental functions of roots that require a proper physiological status. In a set of separate plants, in which seminal roots were spatially separated from nodal roots, seminal roots were exposed for a period of 20 min to ^{15}N-labelled nitrate solution with the same concentrations of all other elements. Between day 18 and day 39 nitrate uptake capacity was constantly at approx. 3 µmol nitrate g^{-1} DW min^{-1} , before a significant drop set in after day 39 (Figure 3.5A). Likewise, ^{15}N translocation was almost stable or increasing until day 39, before it also decreased after day 39 (Figure 3.5B). Obviously, this drop in ^{15}N translocation was a direct consequence of the change in nitrate uptake capacity. These observations indicated that the physiological activity of barley seminal roots significantly dropped after day 39.
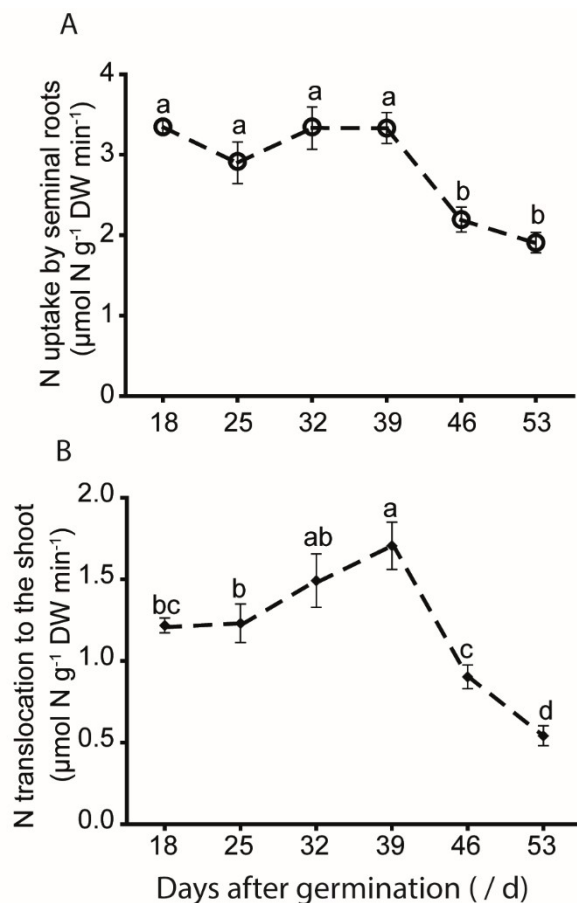
Figure 3.5 Plant age-dependent nitrate uptake capacity of seminal roots and root-to-shoot translocation of nitrogen. 1 mM K-^{15}NO$_3$ was supplied as the N source for the 20 min uptake experiment and the concentrations of all the other elements were maintained as non-labelled hydroponic solution. This uptake experiment was only done for barley seminal roots based on spatially separated root types. (A) nitrogen uptake capacity of barley seminal root during aging. (B) nitrogen translocation of barley seminal root during aging. At day 18, n = 5. From day 25 to day 53, n = 6. Error bars indicate mean values ± SE. Different letters indicate significant differences according to LSD test (p<0.05).

3.2.2 lant age-dependent changes in sugar levels of seminal roots

To address the question whether the drop of root activity was a consequence of energy depletion in seminal roots, sugar levels of seminal roots were analyzed because they represent the major assimilates required to produce ATP and redox equivalents and to sustain root activity. Glucose and fructose concentrations followed a highly similar pattern over time that was characterized by a sharp initial decline from day 18 to day 25 before values became stable at an approx. 2 fold lower level (Figure 3.6).
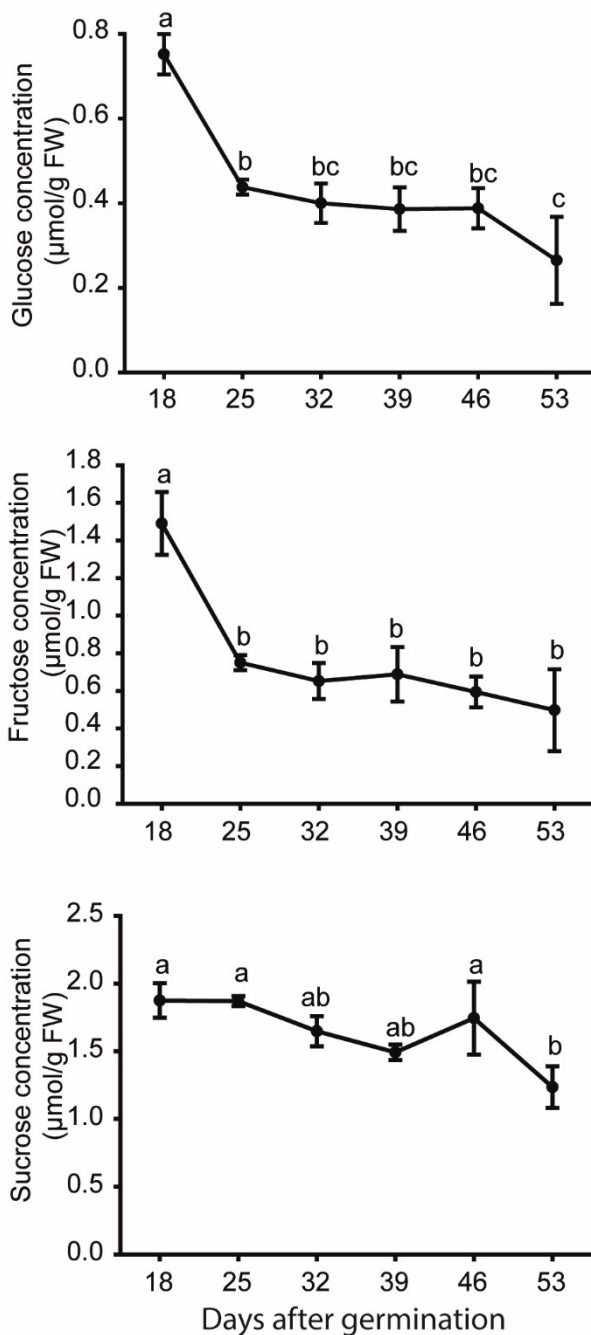
Figure 3.6 Sugar profiles of barley seminal roots over time. Seminal roots and leaves were harvested weekly from day 18 until day 53, when the main tiller had 4 chlorotic leaves (Figure 1A). n = 5. Error bars indicate mean values ± SE. Different letters indicate significant differences according to LSD test ($p < 0.05$).

In contrast, sucrose concentrations, which were similar to the sum of glucose and fructose together, remained relatively stable throughout the whole growth period, before a slight decrease was recorded at day 53 (Figure 3.6). Considering that these changes in sugar levels were highly distinct from root growth and root activity, which showed a transition point at day 39 (Figure 3.2, Figure 3.3), this analysis implied that seminal roots were not depleted of energy until the final harvest and that energy depletion was not the cause for the decreasing root activity.

3.2.3 Plant age-dependent changes in catalase activity of seminal roots

Since the timeline based sugar concentrations of the seminal roots implied that energy depletion was not the reason for the decreasing root activity, hydrogen peroxide (H_2O_2) was proposed as a cause since it was widely identified to play important role in triggering leaf senescence and casing cell death in varies organs (Van Breusegem and Dat, 2006; Bieker et al., 2012; Lee et al., 2012). The methodology of H_2O_2 quantification has not been established in the lab, therefore, catalase activity was taken as an indicator of H_2O_2 stress since the rise of catalase activity went along with rising H_2O_2 levels, because catalase is required for the detoxification of H_2O_2 (Djanaguiraman et al., 2009; Mhamdi et al., 2010). During early seminal root development, catalase activity was at a low level of approx. 4 nmol O_2 ml^{-1} mg^{-1} FW. However, after day 39 catalase activity steeply increased and eventually reached to 16 nmol O_2 ml^{-1} mg^{-1} FW, which was almost 4 times more (Figure 3.7). Considering that catalase activity mostly reflects hydrogen peroxide (H_2O_2) level, it was expected that also H_2O_2 concentration increased after day 39. This data indicated barely seminal roots might face oxidative stress at late stages which might subsequently reduce root activity such as ^{15}N uptake capacity.
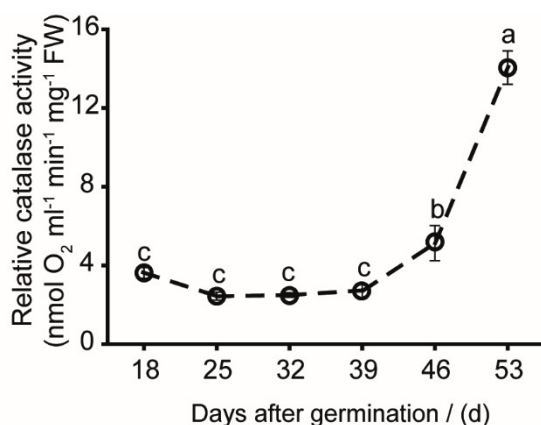
Figure 3.7 The catalase activity of seminal roots over time. Catalase activity was referred to the O_2 emission from H_2O_2 solution based on oxygen electrode method. Seminal roots and leaves were harvested weekly from day 18 until day 53, when the main tiller had 4 chlorotic leaves (Figure 1A). n = 5. Error bars indicate mean values ± SE. Different letters indicate significant differences according to LSD test (p<0.05).

3.2.4 Plant age-dependent profiles of mineral nutrient in seminal roots of barley

During leaf senescence, elements like nitrogen (N), potassium (K), phosphorus (P), sulfur (S), molybdate (Mo), copper (Cu) and zinc (Zn) are remobilized from old leaves to developing organs that act as a sink (Himelblau and Amasino, 2001). To investigate whether roots undergo a similar process during root aging, seminal roots of barley were subjected to EA-MS (for N) and IPC-MS (for the other elements) analysis. While nutrient concentrations in roots and shoots provided information on the nutritional status of the respective organs, seminal root contents additionally inform about the nutrient pool size in the seminal roots.

Nitrogen concentration in seminal root dry matter remained highly constant at 5% and dropped only slightly to 4.7% on day 53 (Appendix 1). Thus, as evident from seminal root, N content in seminal roots increased with the increase of root biomass (Figure 3.2C, Appendix 1). Many other essential elements such as S, Cu as well as Mo which are reported to be remobilized during leaf senescence didn't show the decrease of their pools during root aging, indicating that their nutritional status in seminal roots remained largely unaffected by plant age (Appendix 1). In contrast, P concentration of the seminal roots decreased gradually from day 18 onwards. However, root P content still increased until day 39 due to the increase of root biomass, but then gradually dropped although seminal root biomass was still increasing (Figure 3.2C, Figure 3.8A, Figure 3.8B). Within the whole experimental procedure, P concentrations of both roots and shoots were above the critical level that was recorded as 4 mg g^{-1} dry weight in barley (Reuter, 1997), which indicated P supply of the hydroponic solution is sufficient and the drop of root P pool was not likely due to deficiency (Appendix 1). Thus, the decrease of P pool may be indicative for P remobilization out of the seminal root P pool that set in at day 39. Among all the other nutrients, only Zn showed a highly similar pattern as P which indicated the possible remobilization of Zn during root aging too (Appendix 1, Figure 3.8C, 3.8D). K content showed a slightly similar pattern as P and Zn, but it was decreased at day 46 compare with day 39 of P and Zn (Appendix 1). Considering K is a highly movable element in plant tissue which is easily leaches from tissues, especially in aging tissues since cells lose their integrity (Tukey Jr, 1970; Orlando Filho, 1985), and the tissue degradation did observed in larger extent after day 46 (Figure 3.4), such late stage reduction of K pool was considered as the leakage to surround environment.

To summarize, physiological data indicated P and Zn but not other measured elements were remobilized during root aging.
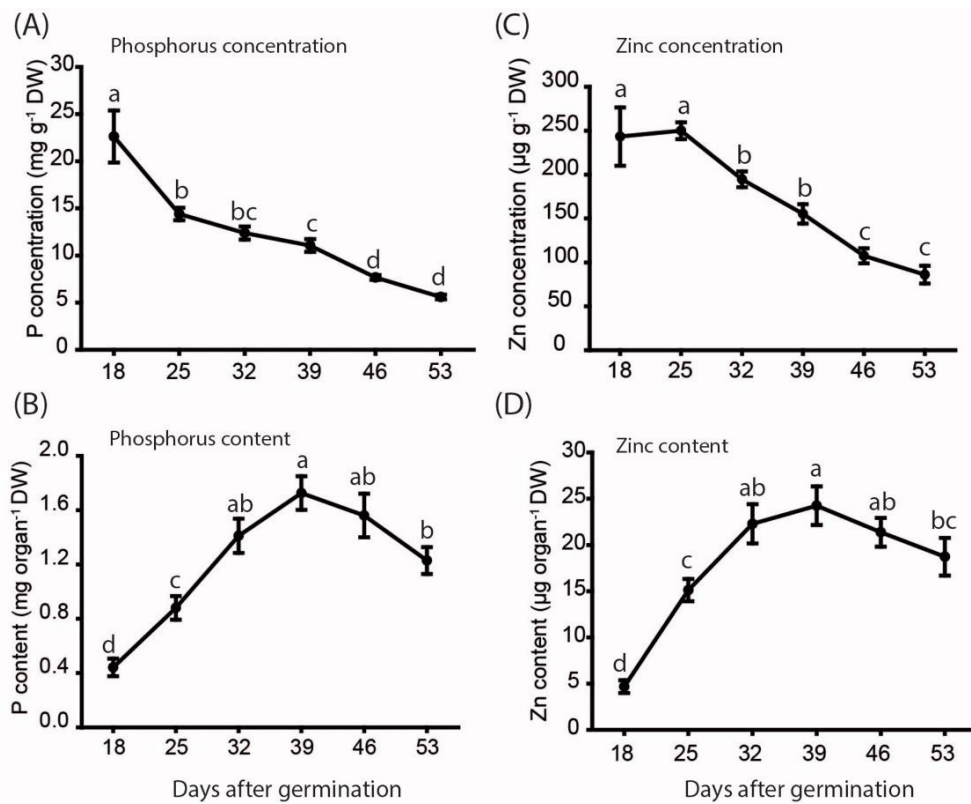
Figure 3.8 Plant age-dependent changes of phosphorus and zinc. The concentrations and contents of nitrogen (A-B) and Zn (C-D) of the seminal roots, respectively. Seminal roots and leaves were harvested weekly from day 18 until day 53, when the main tiller had 4 chlorotic leaves (Figure 3.2A). At day 18, n = 5, from day 25 to day 53, n = 6. Error bars indicate mean values ± SE. Different letters indicate significant differences according to LSD test (p<0.05).

3.2.5 Plant age-dependent profiles of urea and amino acids in seminal roots of barley

In Arabidopsis, urea has been characterized as an early metabolic marker for leaf senescence (Bohner et al., 2015). Urea derives either from root uptake or from protein and DNA degradation (Zonia et al., 1995; Kojima et al., 2006; Witte, 2011). In the present experiment, urea concentrations in seminal roots increased by a factor of 3 between day 18 and day 39, and then remained a rather constant level of 16-17 µmol g^{-1} DW (Figure 3.9). For comparison, urea concentration of leaf number 1-6 of Arabidopsis rose from 7 to 17 µmol g-1 DW during leaf senescence (Bohner et al., 2015). These two datasets generated from two aging organs, Arabidopsis leaves and barley seminal roots, showed similar pattern and even similar absolute values during organ aging. Due to the absence of urea from the hydroponic solution (see materials

and methods), the increase of urea in seminal roots was most likely indicative for enhanced protein and/or DNA degradation during later stages of root development.
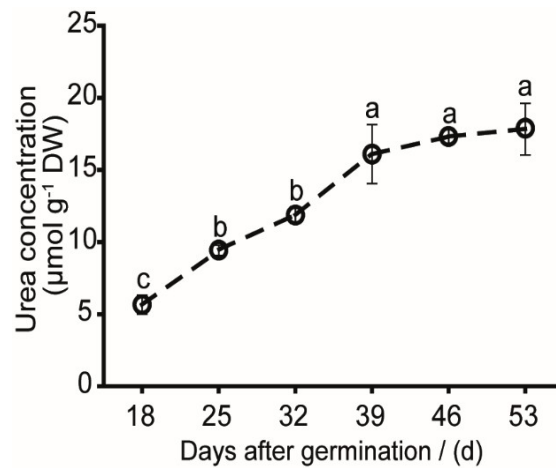
Figure 3.9 Plant age-dependent changes in urea concentrations in seminal roots of barley. Seminal roots and leaves of hydroponically-grown plants were harvested weekly from day 18 until day 53, when the main tiller had 4 chlorotic leaves (Figure 3.2A). n=5. Error bars indicate mean values ± SE. Different letters indicate significant differences according to LSD test (p<0.05).

To further verify the possibility of protein degradation, barley seminal root samples were subjected to amino acids analysis. At least some amino acids have also been characterized as degradation forms of N-rich macromolecules that are remobilized during leaf senescence (Guiboileau et al., 2010). Here, the identified amino acids were classified into 3 different groups due to their pattern changes within the time course. The first group included cysteine, lysine, tyrosine, arginine, glycine and phenylalanine. Concentrations of all of these amino acids increased, and most of them increased after day 39 (Figure 3.10). Within this group, lysine, tyrosine and phenylalanine showed similar patterns as found in leaf senescence of Arabidopsis, while arginine and glycine displayed different patterns between root and shoot since their concentrations decreased during leaf senescence (Bohner et al., 2015). The second group contains another six amino acids including proline, GABA, serine, aspartic acid, glutamic acid and asparagine were decreasing during seminal root aging, and in general, mainly dropped after day 39 (Figure 3.11). The concentrations of serine, aspartic acid, glutamic acid and asparagine displayed similar patterns as observed in leaf senescence of Arabidopsis. In contrast, proline and GABA were slightly increased in leaf senescence but downregulated in root aging (Bohner et al.,

2015). The amino acids of the third group showed very slight changes during root aging, these are: histidine, glutamine, isoleucine, valine, threonine, leucine and alanine (Figure 3.12). Interestingly, histidine, isoleucine, valine, threonine and leucine were accumulated during leaf senescence of Arabidopsis, while the concentrations of glutamine and alanine were decreased in leaf senescence (Bohner et al., 2015).

Taken together, concentrations of most amino acids showed the transitioning at day 39 (either decrease or increase), and those elevated amino acids might indicate the start of protein degradation. Many amino acids showed different patterns between leaf senescence and root aging, indicated the degeneration process might be different between these two processes.
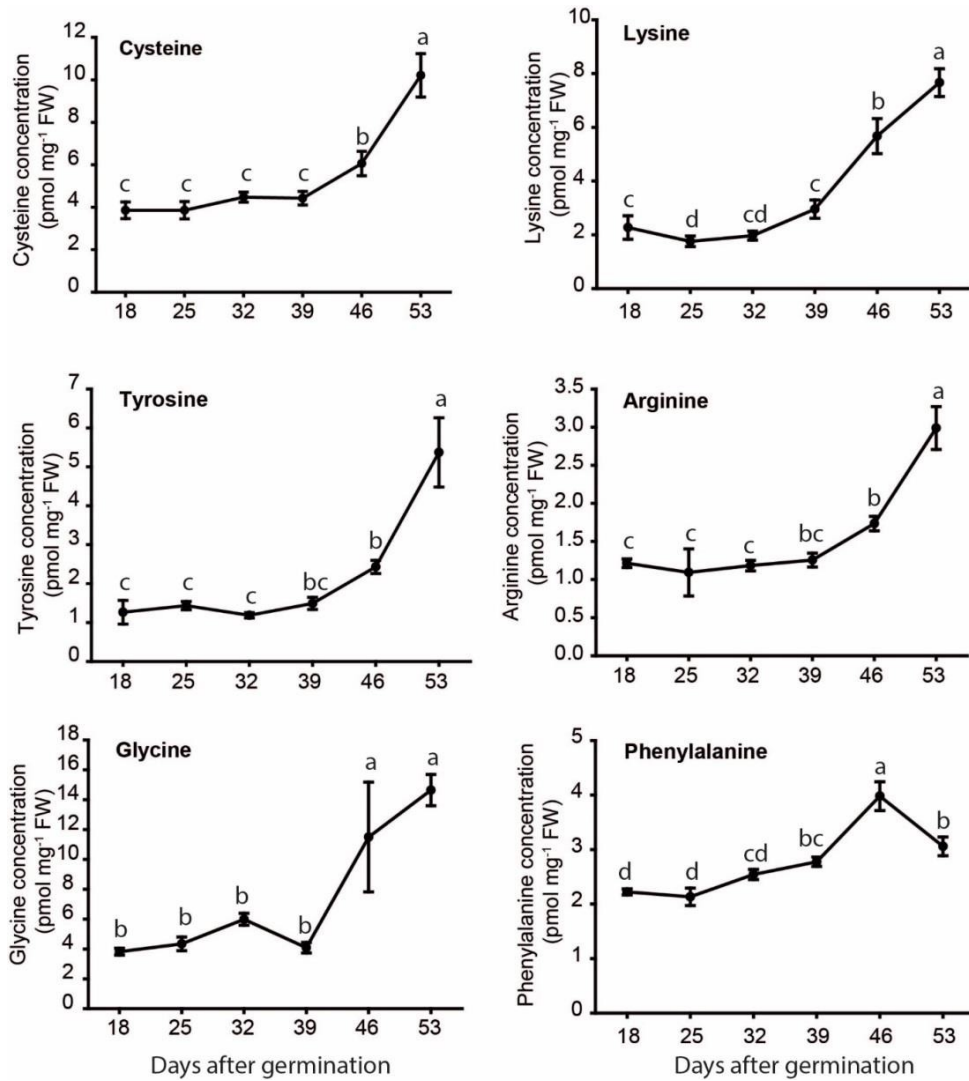
Figure 3.10 The profiles of up regulated amino acids of barley seminal roots over time. Seminal roots and leaves of hydroponically-grown plants were harvested weekly from day 18 until day 53, when the main tiller had 4 chlorotic leaves (Figure 3.2A). n=5. Error bars indicate mean values ± SE. Different letters indicate significant differences according to LSD test (p<0.05).
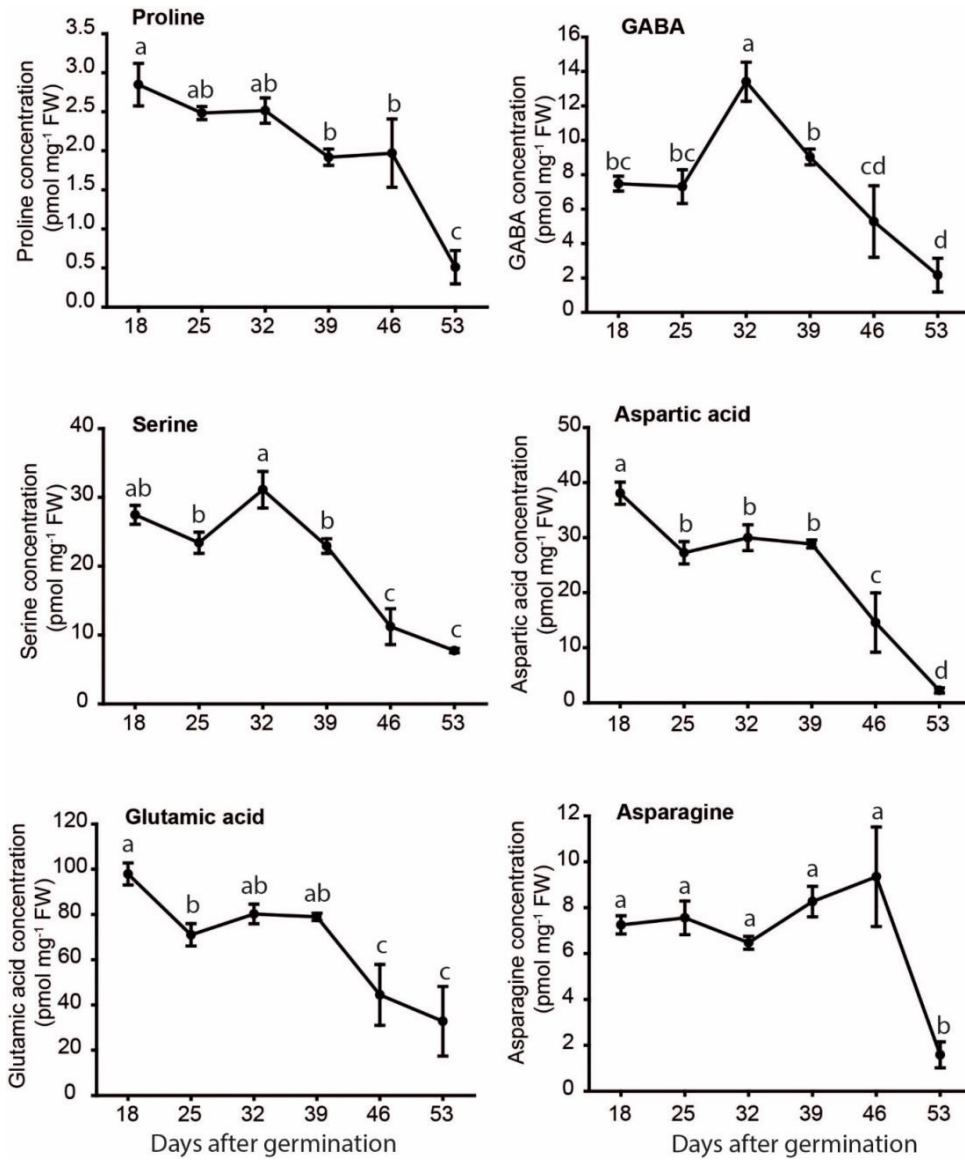
Figure 3.11 The profiles of down regulated amino acids of barley seminal roots over time. Seminal roots and leaves of hydroponically-grown plants were harvested weekly from day 18 until day 53, when the main tiller had 4 chlorotic leaves (Figure 3.2A). n=5. Error bars indicate mean values ± SE. Different letters indicate significant differences according to LSD test ($p < 0.05$).
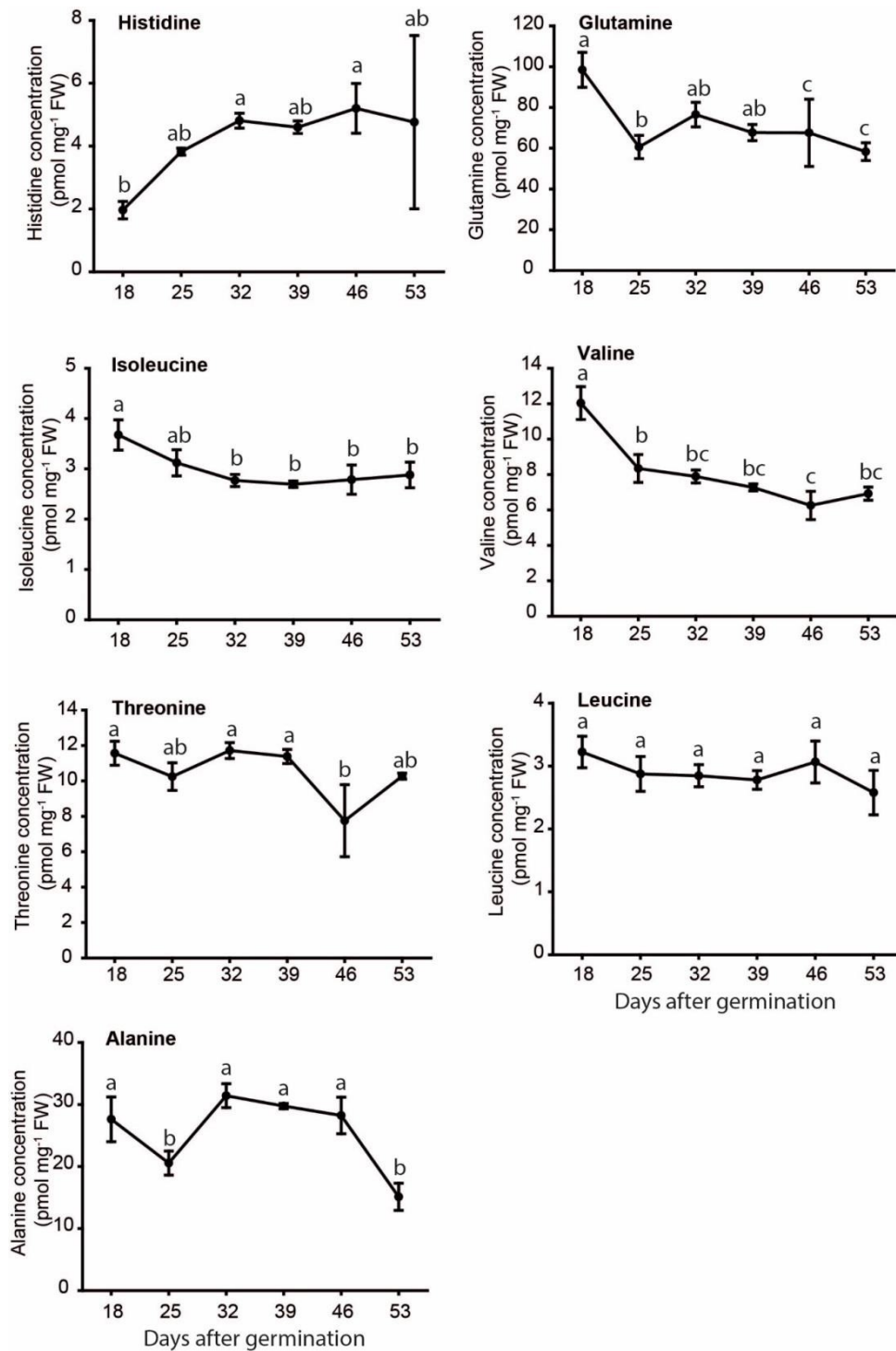
Figure 3.12 The other amino acids' profiles of barley seminal roots over time. Seminal roots and leaves of hydroponically-grown plants were harvested weekly from day 18 until day 53, when the main tiller had 4 chlorotic leaves (Figure 3.2A). n=5. Error bars indicate mean values ± SE. Different letters indicate significant differences according to LSD test ($p<0.05$).

3.2.6 Plant age-dependent profiles of major phytohormones in seminal roots

To investigate possible roles of phytohormones in the regulation of seminal root aging especially whether there could be a plant age-dependent regulation, seminal roots were separated from nodal roots and divided into two fractions: an apical root zone (ARZ), consisting of root tissue between root cap and the 1st 1mm lateral root, and a basal root zone (BRZ), consisting of all the rest part of the seminal roots including all the lateral roots. Both fractions were then subjected to the analysis of phytohormones by UPLC-MS/MS.

Salicylic acid (SA) has been described as a positive regulator of leaf senescence, since it accumulates during leaf senescence and mutant plants such as npr1 and pad4 defective in SA-signaling reduced the expression of *SAG12* as well as delayed leaf senescence (Morris et al., 2000). From day 18 to day 53, SA concentration increased by more than 3 times in both ARZ and BRZ (Figure 3.13A, 3.13B). This steady but slight/moderate increase in SA levels has been observed also in Arabidopsis and appears to be related to root aging (Morris et al., 2000). In comparison, auxin (IAA) was demonstrated as a negative regulator of leaf senescence, since elevated endogenous IAA by overexpression *YUCCA6* which is a rate-limiting enzyme for IAA biosynthesis, displayed prolonged leaf longevity and decreased the expression of several *SAG* genes including *SAG12*, *NAC1* and *NAC6* (Kim et al., 2011). In ARZ, IAA concentration increased from day 18 to day 32 by a factor of 2 and decreased from day 39 on to the initial level. The same age-dependent pattern was also observed in basal root fractions, even though with less pronounced changes (Figure 3.13C, 3.13D). The IAA pattern of root aging is in agreement with the finding in *Coleus* leaf senescence since IAA was also declined with increasing leaf age (Dela Fuente and Leopold, 1968). Among all hormones, cytokinins (CKs) have the strongest effect on retardation of leaf senescence (Gan, 2008). Three ribosylated forms were detected in the root fractions: trans-zeatin-riboside (tZR), which is the transport form of the most active cytokinins, cis-zeatin-riboside (cZR) and isopentenyladenin-riboside (iPR), which both represent transport forms or precursors of less active cytokinins (Heyl et al., 2006). Non-ribosylated active CKs were apparently below the detection limits. In general, cytokinin concentrations were much higher in the ARZ than in the BRZ (Figure 3.13E, 3.13F), which related to the fact that root apical meristem is a major tissue of CKs biosynthesis. In the ARZ, iPR and tZR were at a constant level between day 18 and

day 39, before their levels dropped drastically after day 39 down to 5-10-fold lower levels. A similar pattern was also observed in the basal root parts, but again, these changes were less pronounced (Figure 3.13E, 3.13F). Remarkably, also cZR showed here an initial increase just before day 39. This may be indicative for the conversion of cytokinins biosynthesis from the highly active tZR to the leass active form cZR. Among all measured phytohormones, ABA levels showed the most pronounced changes during the growth period. In both root fractions, ABA concentrations remained at a stable low level from day 18 – 32, but then showed a sudden increase at day 39 by a factor of 7-10. At day 46 and 53 ABA levels had returned to initial levels. (Figure 3.13G, 3.13H). Taken together, in particular cytokinins and ABA, and to a weaker extent auxin, displayed a transition-like pattern at day 39, which indicated a plant- or root age-dependent change in hormonal signaling.
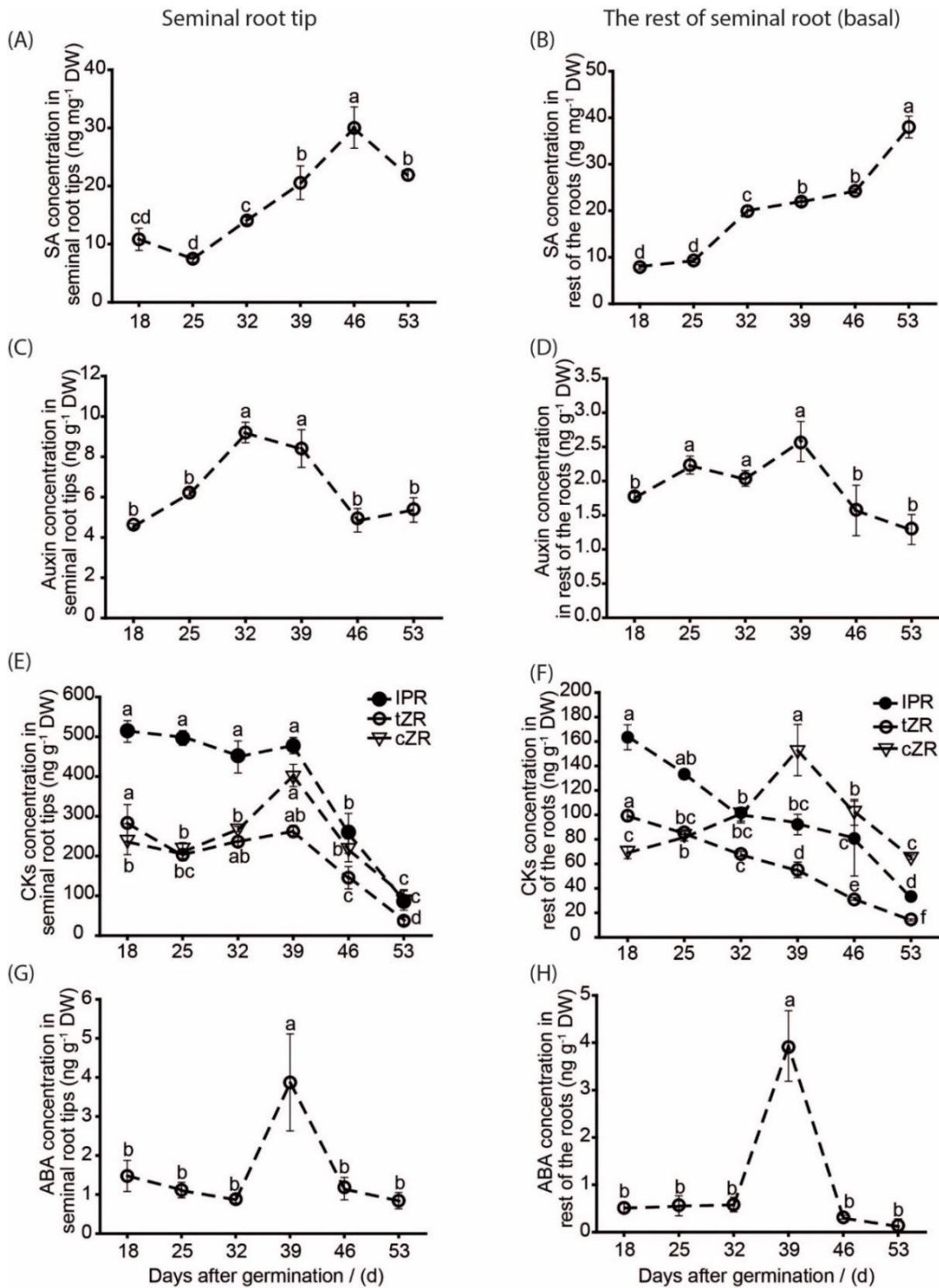
Figure 3.13 The hormone profiles of apical root zone (ARZ) and basal root zone (BRZ) over time. Seminal roots and leaves of hydroponically-grown plants were harvested weekly from day 18 until day 53, when the main tiller had 4 chlorotic leaves (Figure 3.2A). (A) and (B): salicylic acid profiles in both root fractions overtime. (C) and (D): auxin profiles in both root fractions overtime. (E) and (F): cytokinins profiles in both fractions over time. (G) and (H): abscisic acid profiles in both fractions overtime. Error bars indicate mean values ± SE. Different letters indicate significant differences according to LSD test (p<0.05). n=5.

3.3 Plant age-dependent transcriptome analysis of seminal roots in barley

3.3.1 -supervised clustering of gene expression data

To investigate root aging at the transcriptome level, root segments were taken from the apical root zone (ARZ) and from the basal root zone (BRZ) at different time points, i.e. 18, 25, 32, 39, 46 and 53 days after germination. Extracted RNA was reversed to cDNA then subjected to transcriptome analysis using a custom-made 60K barley microarray. The expression values of individual genes at day 18 were taken as references for calculating changes in gene expressions at later time points. Genes with adjusted p-values < 0.05 were defined as significantly up- or downregulated and expression levels were displayed by their log_2-fold change (log_2FC). To obtain an overview on gene expression changes, non-supervised clustering analysis was conducted for both root fractions.

In total, 26617 genes in ARZ and 22486 genes in BRZ were significantly changed at least at one time point within the time course. In the ARZ, the two largest groups contained 10792 or 9433 transcripts that continuously decreased (cluster 1) or increased (cluster 2), respectively. Interestingly, the majority of genes in these two groups showed most obvious changes at or after day 39 (Figure 3.14). The third and fourth largest group of ARZ genes displayed a transition pattern with a transient decrease (cluster 3) or transient increase (cluster 4) at day 39 or 32 and contained 3663 or 2565 genes, respectively (Figure 3.14). Most transcripts of cluster 4 showed a sharp increase by log_2FC of 2-7 at day 32. Majority of these transcripts maintained their expression at relatively high levels compared with day 18. 164 genes showed no prominent pattern was clustered as another cluster.

In the BRZ fraction, similar clusters were found compare with ARZ fraction. Continuously decreasing or increasing transcripts again formed the two largest clusters, with 7529 or 7380 transcripts, respectively. Compared with the corresponding two clusters in the ARZ, approx. 3000 transcripts less assembled in these two clusters of the BRZ were found (Figure 3.15). The third biggest cluster in the BRZ contained 4902 genes of sharp increasing transcripts at day 32 and thus contained almost the double number of transcripts than the corresponding cluster 4 in the ARZ. The cluster showed transient downregulation was again enriched in BRZ with 1667 genes, which contains about only 50% of the corresponding cluster in ARZ.

Interestingly, 1008 genes showed peaking pattern at day 39 were clustered as the last cluster (Figure 3.15).
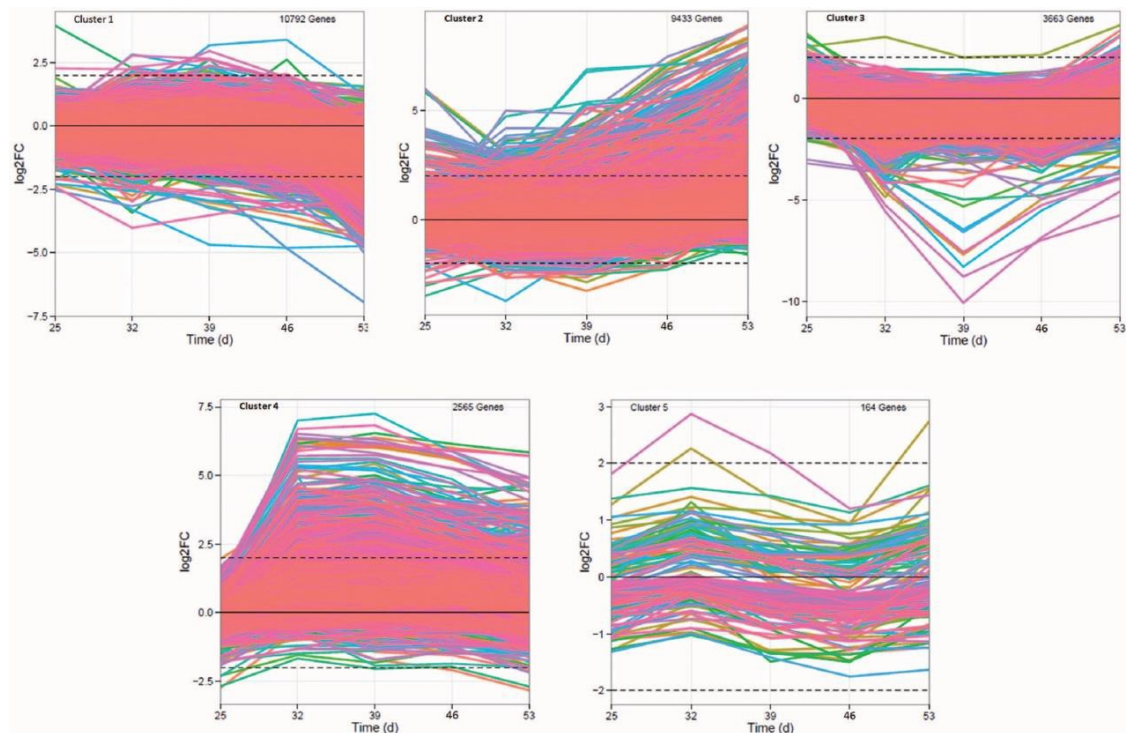
Figure 3.14 Non-supervised clustering for 26617 significant expressed genes during root aging in apical root zone (ARZ). Gene expression values at each time point represent the mean value of three biological replications.

Taken together, non-supervised clustering analysis identified that continuously up- or downregulated genes form the two largest clusters and thus represent the most abundant plant age-dependent patterns of gene expression in apical and basal root zones. In the ARZ, these clusters were followed by two similarly sized clusters of transiently down- or upregulated genes. By contrast, in the BRZ the transiently downregulated gene cluster was much smaller in favor of the transiently upregulated gene cluster. It was thus anticipated that especially the transiently regulated genes discriminate better between the biological processes involved in root ageing in these two types of root tissue.
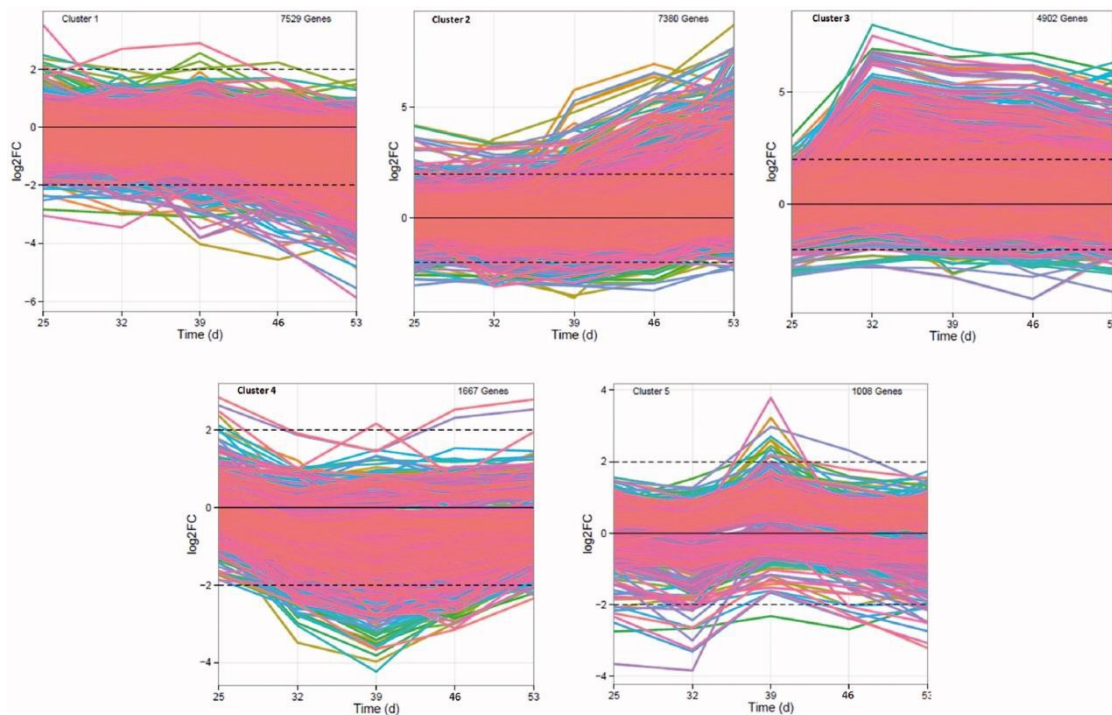
Figure 3.15 Non-supervised clustering for 22486 significant expressed genes during root aging in basal root zone (BRZ). Gene expression values at each time point represent the mean value of three biological replications.

3.3.2 Cluster based gene ontology analysis in the aging process of barley seminal roots

To describe functional processes encoded by the genes assembled in the individual clusters, gene ontology (GO) analysis was performed. GO terms with a p-value < 0.05 were defined as significantly enriched. Detailed GO terms are shown in Appendix 2.

In the ARZ, the cluster 1 which contained 10792 genes and identified as continuously downregulated cluster showed enrichment of 28 GO terms (Appendix 2.1). Within this downregulated cluster, the enriched "nucleobase biosynthetic process (GO: 0046112)" and "DNA replication initiation (GO: 0006270)" indicated the stagnant or slowdown of cell division/ metabolic activity over root aging. Other downregulated GO terms such as "cellulose biosynthetic process (GO: 0030244)", "cell wall biogenesis (GO: 0042546)" and "fatty acid biosynthetic process (GO: 0006633)" together implied the degeneration of cell components, since cellulose is one of the basic components of cell wall and plant membrane lipids are primarily composed by fatty acids (Millar et al., 2000; Pérez et al., 2002). The GO term "removal of superoxide radicals (GO:

0019430)" indicated the decline of the capability of the root tissue in removing superoxide radicals, which in another way means the increase of oxidase stress. Many other enriched GO terms in the cluster 1 of ARZ such as "L-serine biosynthetic process (GO: 0006564)" was indicative of the downregulation of the biosynthesis of serine, which indeed was the case since the concentration of serine was declined during root aging (Figure 3.11). The cluster 2 which has 9433 genes and identified as continuously upregulated cluster, contained 7 GO terms (Appendix 2.2). Within this cluster, the enriched "oxidation-reduction process (GO: 0055114)" was indicative of enhanced oxidation stress, especially at late stages of the root development since most of the genes in this cluster elevated their expressions after day 39. The GO term "regulation of transcription, DNA-templated (GO: 0006355)" implied this degenerative process involved the regulation at transcription level. Interestingly, "zinc II ion transmembrane transport (GO: 0071577)" was also enriched, indicated the zinc II ion is transported from one side of a membrane to the other. The cluster 3 with 3663 genes which showed a downregulation expression pattern at day 39 resulted with one GO enriched, "transmembrane transport (GO: 0055085)", which indicated the upregulation of solute transport during root aging (Appendix 2.3). The cluster 4 which was consisted of 2565 genes and showed obvious upregulation at day 32, enriched with "protein phosphorylation (GO: 0006468)", "phosphatidylserine biosynthetic process (GO: 0006659)" and "regulation of transcription, DNA-templated (GO: 0006355)", which implied the regulation at transcription and post-transcription levels (Appendix 2.4). In this cluster, the enrichment of "L-phenylalanine metabolic process (GO: 0006558)" correlated with the accumulation of phenylalanine (Figure 3.10). The smallest cluster contained 164 genes resulted with the enrichment of "glucosylceramide catabolic process (GO: 0006680)", which was indicative of glucosylceramide breakdown (Appendix 2.5).

In BRZ, some GO terms were identified again in the corresponding clusters as in ARZ. These GO terms include "cellulose biosynthetic process" (GO: 0030244) and "DNA replication initiation" (GO: 0006270) in the gradually decreased cluster (Appendix 2.6), "regulation of transcription, DNA-templated" (GO: 0006355), "zinc II ion transmembrane transport" (GO: 0071577) and "asparagine biosynthetic process" (GO: 0006529) of the gradually increased cluster (Appendix 2.7), "protein phosphorylation" (GO: 0006468) and "L-phenylalanine catabolic process" (GO: 0006559) in the day 32 transition cluster (Appendix 2.8). Also, some new GO terms

were enriched. For example, "lignin catabolic process (GO: 0046274)" was newly enriched in cluster 1in comparison of the cluster of ARZ, which indicated the accumulation of lignin during root aging (Appendix 2.6).

The cluster based GO enrichment displayed the degeneration-like process during root aging such as downregulation of cell division, cellulose biosynthetic process and fatty acid biosynthetic process. In parallel, the upregulation of transmembrane transport of Zn is indicative of remobilization of resources which is widely observed in leaf senescence. Even such cluster based GO analysis revealed some events shared by leaf senescence, it's necessary to keep it in mind that the genes belong to the same GO but have different expression patterns might be clustered into different clusters which lead to the possible fact that these GO terms couldn't be enriched. In another point, genes involve in the enriched GO are expected to be altered within the same timeframe. Therefore, time point based GO term analysis was also performed to provide an alternative point of view.

3.3.3 Time point based gene ontology analysis in the aging process of barley seminal roots

The alternative approach was chosen for GO term analysis by focusing on significantly expressed genes at each individual time point. For genes significantly expressed in the ARZ at day 25, no significant GO term was obtained, indicating that this tissue was still in a similar developmental or physiological stage as at day 18 (Figure 3.16). At day 32, the largest group of the enriched genes belonged to the GO term "regulation of transcription, DNA-templated" (217 genes) and "protein ubiquitination" (32 genes), which indicated substantial regulatory changes at the transcriptional and post-/translational levels (Figure 3.16). The third largest group, "L-phenylalanine metabolic process", enriched 11 out of 28 genes and coincided with elevated phenylalanine concentrations found at day 39 (Figure 3.10, Figure 3.16). The GO term "acetyl-CoA biosynthetic process from acetate" implied that fatty acid biosynthesis was altered at this time point, since acetyl-CoA is heavily involved in fatty acid synthesis in plastids. Interestingly, even after day 32, the GO term "Regulation of transcription, DNA-templated" was still overrepresented at day 39 or day 46 with 8 or 74 more genes, respectively, than at day 32, indicating that altered gene regulation became even more important after day 32. At day 39, the terms "Protein kinase C-activating G-protein coupled receptor signaling pathway", "defense

response to fungus" and "L-methionine salvage from methylthioadenosine" appeared, which implied a conversion of signaling and metabolic processes in the ARZ. At day 39, enrichment of 5 genes in the GO term "Defense response to fungus" may indicate that either roots were indeed exposed to fungal pathogens, which was not visually evident. Or, root degradation processes may have set in that resembled those observed in leaves, where genes belonging to fungal pathogen responses are also upregulated during senescence (Robatzek and Somssich, 2001; Xiao et al., 2004).

At days 46 and 53, transcripts from oxidation-related processes became most abundant in ARZ (Figure 3.16). Moreover, the category "oxidation-reduction process" almost doubled its number of significantly altered transcripts from day 46 to day 53, indicating that the ARZ was subjected to higher oxidative stress. The enrichment of genes belonging to the term "transport" at day 46 and "ATP hydrolysis coupled proton transport" at day 53 definitely indicated an enhanced need for inter- or intracellular compartmentalization processes including those involved in the remobilization of resources, such as assimilates and mineral elements. At day 46, this was accompanied by gene expression changes in the "pentose phosphate shunt", indicating that roots provided additional NADPH as intracellular energy carrier. Enriched "S-adenosylmethionine biosynthetic process" indicated the possible biosynthesis of polyamines and ethylene since an S-adenosylmethionine is an intermediate for these metabolites (Wi et al., 2006). Based on 5 out of 5 genes the GO term "sulfate reduction" was also overrepresented, which implied an enhanced need for the reduction of sulfate, maybe to deliver reduced sulfur to SAM biosynthesis. 146 out of 284 genes of the "ribose phosphate metabolic process" were significantly enriched at day 53, implying significant changes in chemical reactions or pathways involving ribose phosphate such as the synthesis or degradation of nucleotides and nucleic acids. The GO terms "nicotinamide nucleotide metabolic process", "electron transport chain", "pyruvate metabolic process" and "fructose 6-phosphate metabolic process" suggested biological changes in mitochondrial respiration, which is known to be upregulated during leaf senescence or other stress conditions (Ho et al., 2016; Kokáš et al., 2016). The GO term "negative regulation of transcription, DNA-templated" may be related to the degradation of DNA or nicotinamide nucleotides, as mentioned above, which in leaves serves for the recycling of organically-bound N. The enrichment of genes in "L-serine biosynthetic process" went along with the serine concentration profile that decreased at day 53 to

approx. 20% compared to day 18. Interestingly, genes involved in "photosynthesis, light reaction" were enriched with 9 out of 9 genes in this GO term. This may deserve more detailed investigation.

In the BRZ, GO term categories and dynamics were highly similar to those in the RAZ. Enrichment of genes from the GO term "response to water" may have been due to the fact that especially towards day 53 plant water consumption was so high that upper, i.e. basal root zones were no longer continuously submerged in nutrient solution and may then have experienced slight drought stress (Figure 3.17). Like in the RAZ, day 25 and 39 were characterized by GO terms, which reflect changes in transcriptional or post/translational regulation as well as signaling processes; these included "regulation of transcription, DNA-templated", "protein ubiquitination", "protein phosphorylation" and "protein kinase C-activating G-protein coupled receptor signaling pathway". The term "exocytosis" at day 32 might also indicate signal transduction events or reflect the need for protein export processes. Like in RAZ, "S-adenosylmethionine biosynthetic process" and "L-phenylalanine metabolic process" were also enriched at day 32. Notably, from day 46 to 53, the most dominant transcripts belonged to oxidation-reduction-related processes. The overrepresentation of the two terms "cell growth" (9 out of 11 transcripts) at day 46 and "microtubule-based process" (87 out of 184 transcripts) at day 53 may go back to tissue degradation, disorganization of cell structures and suspended root elongation, which were observed in this growth phase (Figure 3.2C, Figure 3.3, Figure 3.4).

Taken together, GO term analysis of altered transcripts in the ARZ and BRZ displayed a highly similar dynamic regulation of developmental and physiological processes. Most importantly, these processes indicated that seminal root aging in barley could be roughly divided into two distinct phases: i) day 18 – day 39, when major biological events build on an altered regulation at transcript and protein levels, and ii) day 46 – day 53, when major biological events were dominated by oxidation-reduction-related processes that are indicative for oxidative stress.

day 25	day 32	day 39	day 46	day 53	
No significant GO terms	GO:0006355 regulation of transcription, DNA-templated	GO:0006355 regulation of transcription, DNA-templated	GO:0055114 oxidation-reduction process	GO:0055114 oxidation-reduction process	GO:0006979 response to oxidative stress
	0.0000058	0.00027	0.0000011	0.00000023	0.00004
	217 / 1175	225 / 1175	503 / 2083	984 / 2083	129 / 234
	GO:0016567 protein ubiquitination	GO:0007205 protein kinase C-activating G-protein coupled receptor signaling pathway	GO:0006355 regulation of transcription, DNA-templated	GO:0019693 ribose phosphate metabolic process	GO:0046496 nicotinamide nucleotide metabolic process
	0.000038	0.00017	0.000043	0.00098	0.00061
	32 / 111	11 / 22	291 / 1175	146 / 284	95 / 174
	GO:0006558 L-phenylalanine metabolic process	GO:0050832 defense response to fungus	GO:0006810 transport	GO:0006090 pyruvate metabolic process	GO:0022900 electron transport chain
	0.00087	0.00047	0.00094	0.000046	0.00016
	11 / 28	5 / 6	447 / 1952	87 / 149	32 / 46
	GO:0019427 acetyl-CoA biosynthetic process from acetate	GO:0019509 L-methionine biosynthetic process from methylthioadenosine	GO:0006098 pentose-phosphate shunt	GO:0015991 ATP hydrolysis coupled proton transport	GO:0006556 S-adenosylmethionine biosynthetic process
	0.00089	0.0004	0.00024	0.00144	0.00021
	5 / 7	7 / 11	13 / 24	31 / 48	16 / 19
		GO:0006559 L-phenylalanine catabolic process	GO:0006556 S-adenosylmethionine biosynthetic process	GO:0045892 negative regulation of transcription, DNA-templated	GO:0006002 fructose 6-phosphate metabolic process
		0.00019	0.000056	0.00166	0.00043
		10 / 19	12 / 19	16 / 21	15 / 18
			GO:0019419 sulfate reduction	GO:0006564 L-serine biosynthetic process	GO:0019684 photosynthesis, light reaction
			0.00034	0.00108	0.00042
			5 / 5	12 / 14	9 / 9

Figure 3.16 Significantly overrepresented GO terms in the apical root zone (ARZ) during root aging. Seminal roots were harvested weekly from day 18 until day 53 and fractionated into ARZ and BRZ for microarray analysis. For each date, overrepresented GO terms are indicated in rectangles with GO term number, name, adjusted p-value and the number of transcripts that were significantly altered relative to the number of genes in this category.

day 25	day 32	day 39	day 46	day 53
GO:0009415 response to water 0.00000014 7 / 20	GO:0006468 protein phosphorylation 3.7E-26 419 / 1847	GO:0006468 protein phosphorylation 0.0000000076 379 / 1847	GO:0055114 oxidation-reduction process 0.00000064 568 / 2083	GO:0055114 oxidation-reduction process 0.000033 803 / 2083
GO:0046168 glycerol-3-phosphate catabolic process 0.000066 4 / 11	GO:0006355 regulation of transcription, DNA-templated 0.0000014 224 / 1175	GO:0006355 regulation of transcription, DNA-templated 0.00025 230 / 1175	GO:0006468 protein phosphorylation 0.00013 489 / 1847	GO:0006979 response to oxidative stress 0.000000012 123 / 234
	GO:0016567 protein ubiquitination 0.00032 30 / 111	GO:0016567 protein ubiquitination 0.00018 33 / 111	GO:0006979 response to oxidative stress 0.000000035 91 / 234	GO:0006260 DNA replication 0.00024 53 / 102
	GO:0007205 protein kinase C-activating G-protein coupled receptor signaling pathway 0.00000015 14 / 22	GO:0007205 protein kinase C-activating G-protein coupled receptor signaling pathway 0.000034 12 / 22	GO:0007205 protein kinase C-activating G-protein coupled receptor signaling pathway 0.0003 13 / 22	GO:0007017 microtubule-based process 0.00026 87 / 184
	GO:0006887 exocytosis 0.00011 18 / 50	GO:1901700 response to oxygen containing compound 0.00056 15 / 39	GO:0016049 cell growth 0.000064 9 / 11	GO:0006556 S-adenosylmethionine biosynthetic process 0.000013 16 / 19
	GO:0006559 L-phenylalanine catabolic process 0.000093 10 / 19	GO:0006556 S-adenosylmethionine biosynthetic process 0.000035 11 / 19	GO:0006556 S-adenosylmethionine biosynthetic process 0.000034 13 / 19	GO:0008299 isoprenoid biosynthetic process 0.00016 18 / 25
	GO:0048544 recognition of pollen 0.00088 24 / 87	GO:0010035 response to inorganic substance 0.00071 13 / 32		

Figure 3.17 Significantly overrepresented GO terms in the basal root zone (BRZ) during root aging. Seminal roots were harvested weekly from day 18 until day 53 and fractionated into ARZ and BRZ for microarray analysis. For each date, overrepresented GO terms are indicated in rectangles with GO term number, name, adjusted p-value and the number of transcripts that were significantly altered relative to the number of genes in this category.

3.3.4 Mapman-based gene expression analysis for the categories "transcription factor", "development" and "protein degradation"

As by GO term analysis, the major biological event in the first phase of root aging (day 18 – day 39) was an enhanced regulation at transcript and protein levels. To specify these regulation-related transcripts further, transcriptome data were processed by the Mapman software, which provides detailed information of individual regulation modules (Thimm et al., 2004).

At day 25, both root zones displayed only slight changes in the transcriptional regulation of transcription factors, when compared to day 18. However, from day 32 on the number of de-regulated transcription factors increased, and upregulation of transcription factors largely dominated over downregulation (Figure 3.18A). Notably, fold-change values altered more drastically in the BRZ, possibly because this fraction containing older root tissues responded earlier than the RAZ. When the module "transcription factor" was dissected into individual TF families, AP2-, WRKY- and NAC-type families turned out as most outstanding groups (Figure 3.18B). More detailed expression patterns and gene annotations of these three TF families are visualized in the heat map (Appendix 3).

Among these three families, NAC TFs are best understood in leaf senescence. In the barley NAC family, *HvNAC005* was found to be up-regulated in leaves by ABA treatment (Christiansen et al., 2011). Over-expression of *HvNAC005* resulted in precocious leaf senescence (Christiansen et al., 2016). A close homolog, *HvNAC027,* was also proposed as a potential leaf senescence regulator (Christiansen et al., 2011). The barley 60K microarray, which was used in this experiment, contained a probe for *HvNAC005* (probe name: CUST_3522_PI404877155) and revealed that *HvNAC005* was up-regulated after day 39 (Appendix 4). However, the microarray contained no probe for *HvNAC027*. To compare plant age-dependent regulation of *HvNAC005* and of *HvNAC027* in roots, specific primers were designed for these two barley genes. Transcript levels of *HvNAC005* increased continuously with the most prominent increase (> 2-fold change) starting at day 39 (Figure 3.19A). This result was similar to that found in the microarray analysis (Appendix 4). *HvNAC027* displayed a slightly distinct expression pattern with more gradual up-regulation in particular in the ARZ over time. Transcript levels of *HvNAC027* increased by more than 400 times at day 53 relative to day 18 (Figure 3.19B).
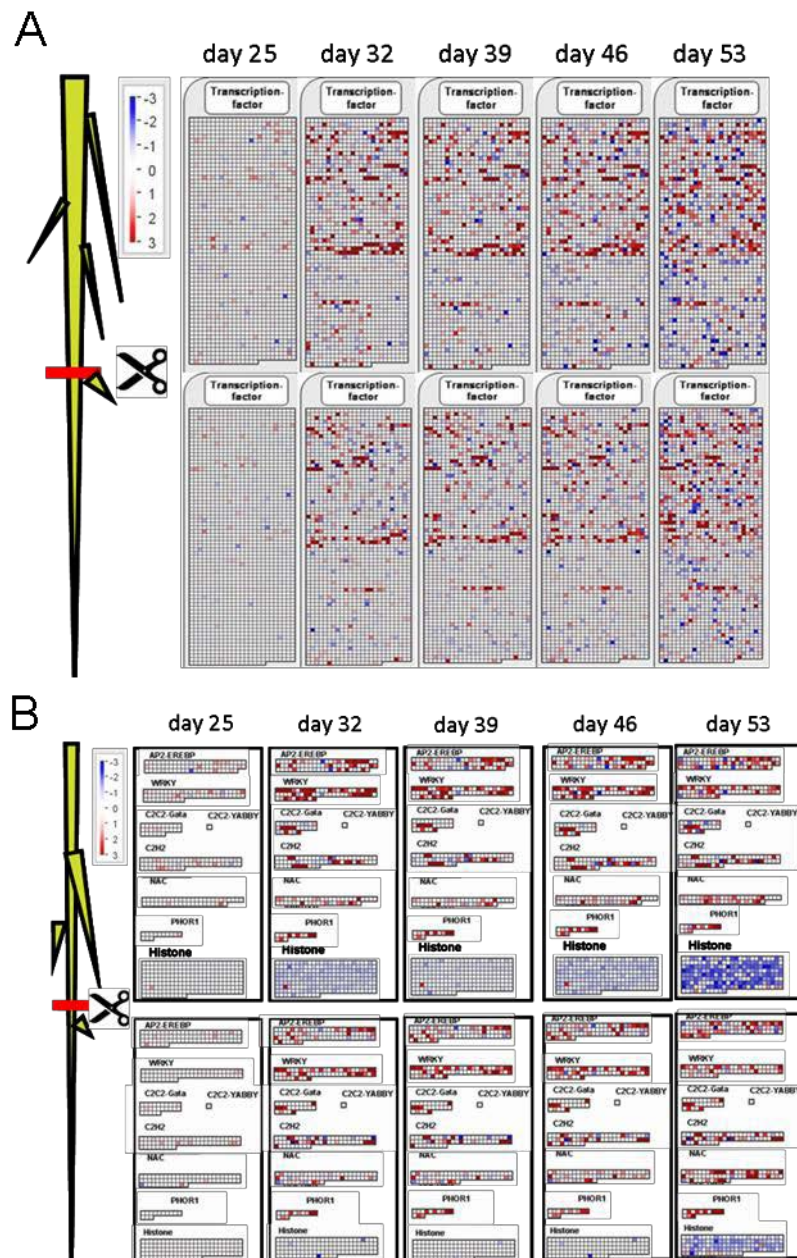
Figure 3.18 Mapman analysis of significantly altered transcription factors in the apical and basal root zones during root aging. Seminal roots were harvested weekly from day 18 until day 53 and fractionated into ARZ and BRZ for microarray analysis. Blue and red colored squares indicate fold-change values for down- and up-regulated genes, respectively. (A) Gene expression changes of all transcription factors over time. (B) Gene expression changes of members from individual transcription factors families over time.

Taken together, gene expression analysis of TFs indicated a transition point with mainly downregulated genes at day 32. This transition in TF regulation was highly prominent in the ARZ and to a lower extent in the BRZ.
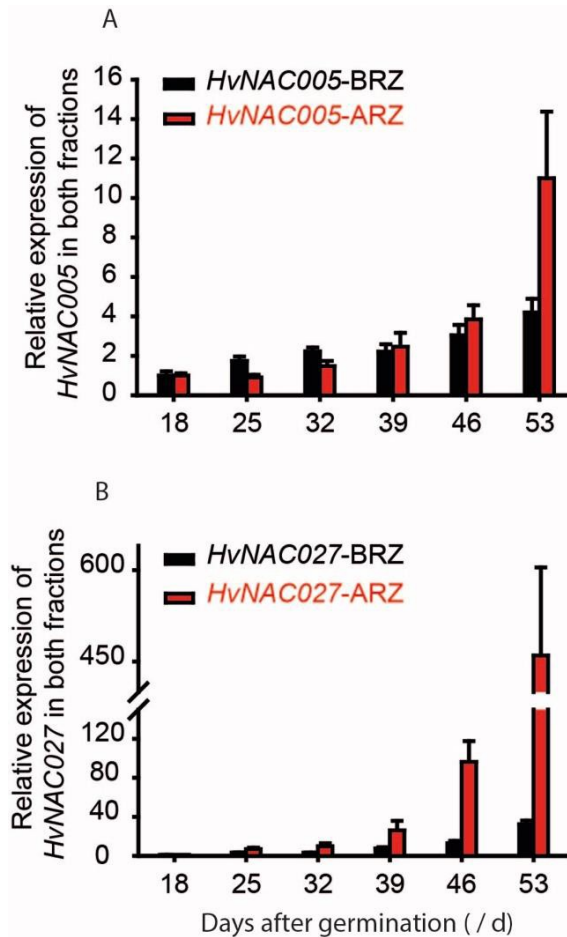
Figure 3.19 Relative expression levels of *HvNAC005* and *HvNAC027* in the apical and basal root zones during root ageing. Seminal roots were harvested weekly from day 18 until day 53 and fractionated into ARZ and BRZ for qPCR analysis. Expression values were normalized by using the *ubiquitin-C* gene as internal standard. Relative transcript levels of A, *HvNAC005* and B, *HvNAC027*. Error bars indicate mean values ± SE. n = 5.

To visualize the dynamics in root development at the molecular level, the gene expression module "cellular response" was analyzed in more detail. Genes belonging to the terms "cell division" and "cell cycle" showed largely constant mRNA levels in both root tissues from day 18 until day 46, while pronounced differences were most prominent in the last harvest. In contrast, the module "development" showed a steady

increase in the number of differentially expressed transcripts especially from day 32 on in both root tissues (Figure 3.20).

Figure 3.20 Mapman enrichment analysis for cell development in ARZ and BRZ over time. Seminal roots were harvested weekly from day 18 until day 53 and fractionated into RAZ and BSR for microarray analysis. Colors of blue and red indicated the degree of fold change for down and up-regulation respectively.

Gene expression changes in the module "protein degradation" was also visualized by Mapman, since protein degradation is a prominent process during leaf senescence (Yoshida, 2003) and, indeed, some amino acids accumulated also here at later stages of root development (Figure 3.10). A first obvious change in the expression of protein degradation-related transcripts was observed at day 32. The next most significant expression change happened at day 53 in either tissue (Figure 3.21). In general, these expression changes occurred earlier in the BRZ than in the ARZ, which implied that protein degradation set in earlier in the BRZ.

To gain more specified information about protein degradation, expression levels of three cysteine protease, *HvPap14*, *HvPap15* and *HvPap17*, were monitored via qPCR. Transcript levels of all three proteases became upregulated over time, especially at or after day 39. *HvPap14* displayed relatively slight changes, within

factor 2-5, compared with the other two cysteine proteases in either root fraction. *HvPap15* mRNA levels started increasing at day 32 in both tissues and became up-regulated by > 50 times during root aging. The cysteine protease *HvPap17*, a putative homologue of *AtSAG12* (Díaz-Mendoza et al., 2014)*,* was up regulated by > 1000 times in ARZ (Figure 3.22). Taken together, transcriptome and qPCR analysis indicated elevated protein degradation from day 32 on and maintained at a high level thereafter.

Figure 3.21 Mapman enrichment analysis for protein degradation in ARZ and BRZ over time. Seminal roots were harvested weekly from day 18 until day 53 and fractionated into ARZ and BRZ for microarray analysis. Blue or red color indicates degree of fold-changes for down- or up-regulated genes, respectively.
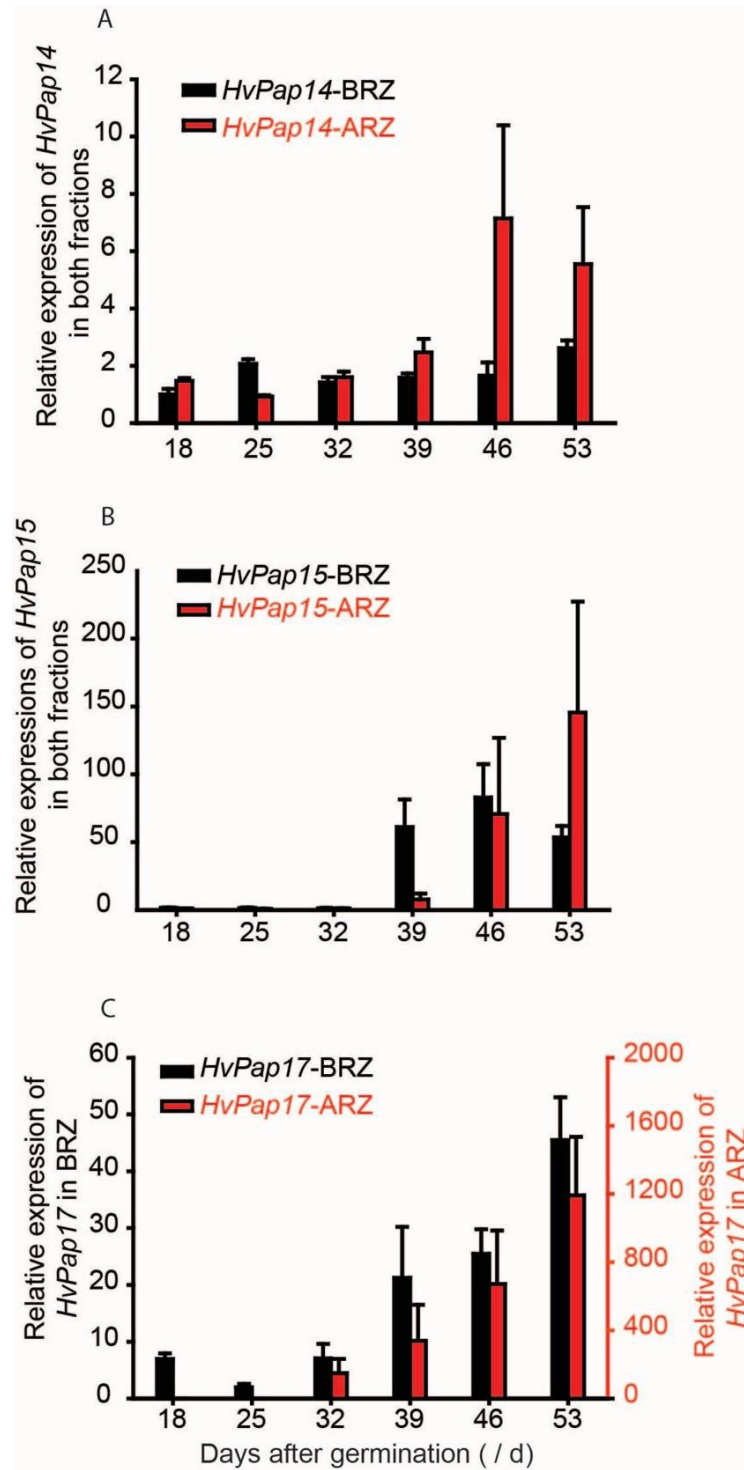
Figure 3.22 Relative expressions of *HvPap14*, *HvPap15* and *HvPap17* in ARZ and BRZ over time. Seminal roots were harvested weekly from day 18 until day 53 and fractionated into ARZ and BRZ for qPCR analysis. Expression values were normalized using the ubiquitin-C gene as internal standard. Bars indicate mean values ± SE. n = 5.

3.3.5 Expression analysis of hormone-related genes during root aging

To investigate changes in the regulation of phytohormone metabolism and homeostasis, hormone-related genes were extracted from the transcriptome dataset, clustered according to their expression profiles and displayed in the form of heat maps.

Regarding genes related to ABA metabolism, especially two transcripts became drastically upregulated at day 32 in the ARZ and BRZ and maintained expression at relatively high level thereafter (Figure 3.23): 9-cis-epoxycarotenoid dioxygenase 2 (*HvNCED2*, probe: CUST_12472_PI399408534), which encodes the enzyme catalyzing the rate-limiting step in ABA biosynthesis, and 9-cis-epoxycarotenoid dioxygenase-like gene, also named viviparous-14 protein (*VIP-14*, probe: CUST_17284_PI404877155).
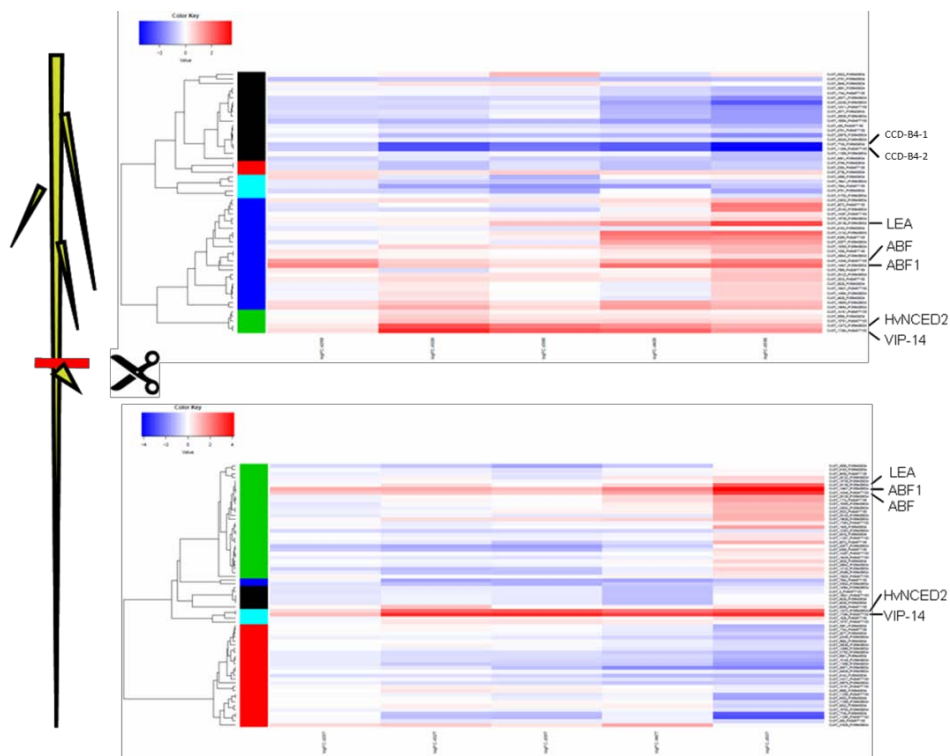
Figure 3.23 Heatmap visualization of expression levels of ABA-related genes during root aging. Seminal roots were harvested weekly from day 18 until day 53 and fractionated into apical and basal root zones for microarray analysis. Blue or red color indicates degree of fold-changes for down- or up-regulated genes, respectively. Expression values of *LEA*, *ABF*, *ABF1*, *HvNCED2* and *VIP-14* are indicated.

Moreover, another set of genes had elevated mRNA levels from day 18 on, including a homolog of the ABA response element-binding factor (*ABF*, probe: CUST_14346_PI404877155), the ABA response element binding factor 1 (*ABF1*,

probe: CUST_14847_PI399408534) and a gene encoding a late embryogenesis abundant protein (*LEA*, probe: CUST_25138_PI399408534). Proteins encoded by these three genes have been confirmed as ABA-induced proteins (Galau et al., 1986; Kobayashi et al., 2005). Furthermore, two genes became strongly downregulated in the ARZ from day 25 on, these were orthologues of 2 Triticum aestivum *CCD-B4* genes which named as *CCD-B4-1* (probe: CUST_7745_PI399408534) and *CCD-B4-2* (probe: CUST_11294_PI404877155). CCD genes, known as carotenoid cleavage dioxigenases, belong to NCED/CCD family, but are not considered to play important roles in ABA biosynthesis compare with AtNCED2, 3, 5, 6, and 9 in Arabidopsis (Lefebvre et al., 2006).

To verify the expression patterns of some of these ABA-related genes, specific primers were selected for *HvNCED* genes (Seiler et al., 2011). It is worth noting that there were two *HvNCED* genes (*HvNCED1* and *HvNCED2*) identified in barley according to the paper of Christiane Seiler, but only *HvNCED2* had a probe on the microarray (Seiler et al., 2011). qPCR analysis confirmed the result found in the microarray, in that *HvNCED1* and *HvNCED2* showed strong upregulation at day 32 in the ARZ and BRZ, and their expressions were maintained at high levels afterwards (Figure 3.24, Figure 3.25). Taken together, transcriptome data confirmed a strong up-regulation of ABA biosynthesis-related genes in both root tissues at day 32, which was accompanied by enhanced expression of ABA-induced genes.
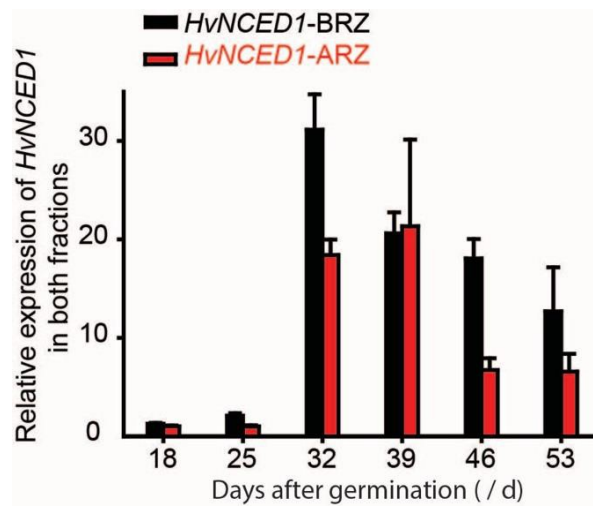
Figure 3.24 Relative expressions of *HvNCED1* in both fractions over time. Seminal roots were harvested weekly from day 18 until day 53 and fractionated into ARZ and BRZ for qPCR analysis. Expression values were normalized using the ubiquitin-C gene as internal standard. Error bars indicate mean values ± SE. n = 5.
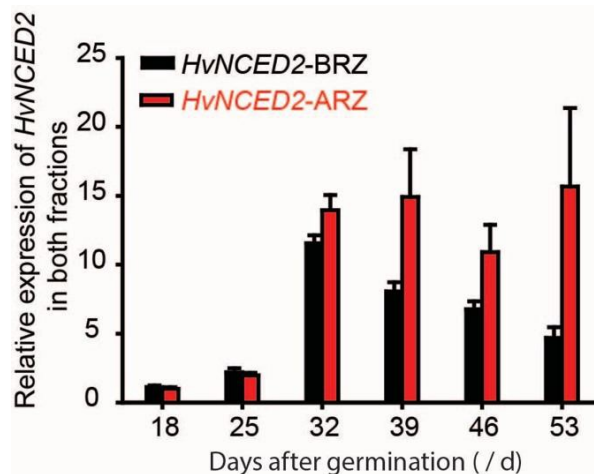
Figure 3.25 Relative expressions of *HvNCED2* in BRZ over time. Seminal roots were harvested weekly from day 18 until day 53 and fractionated into ARZ and BRZ for qPCR analysis. Expression values were normalized using the ubiquitin-C gene as internal standard. Error bars indicate mean values ± SE. n = 5.

The CK-related transcripts were roughly separated into two groups: downregulated and upregulated genes. In the down-regulated group, CK-type A response regulator 1-like gene (*CKAR-1*, probe: CUST_13498_PI399408534) was most prominent as mRNA levels decreased in both tissues, which suggested a possible decline in CK

signaling. Among the upregulated genes, a CK oxidase gene (*CKX*, probe: CUST_8238_PI404877155) and a CK dehydrogenase gene (*CKX2*, probe: CUST_11028_PI399408534) showed highly elevated transcript levels at day 32 which remained high thereafter (Figure 3.26). Expression changes in these three CK-related genes implied that CK concentrations might decrease from day 32 on.
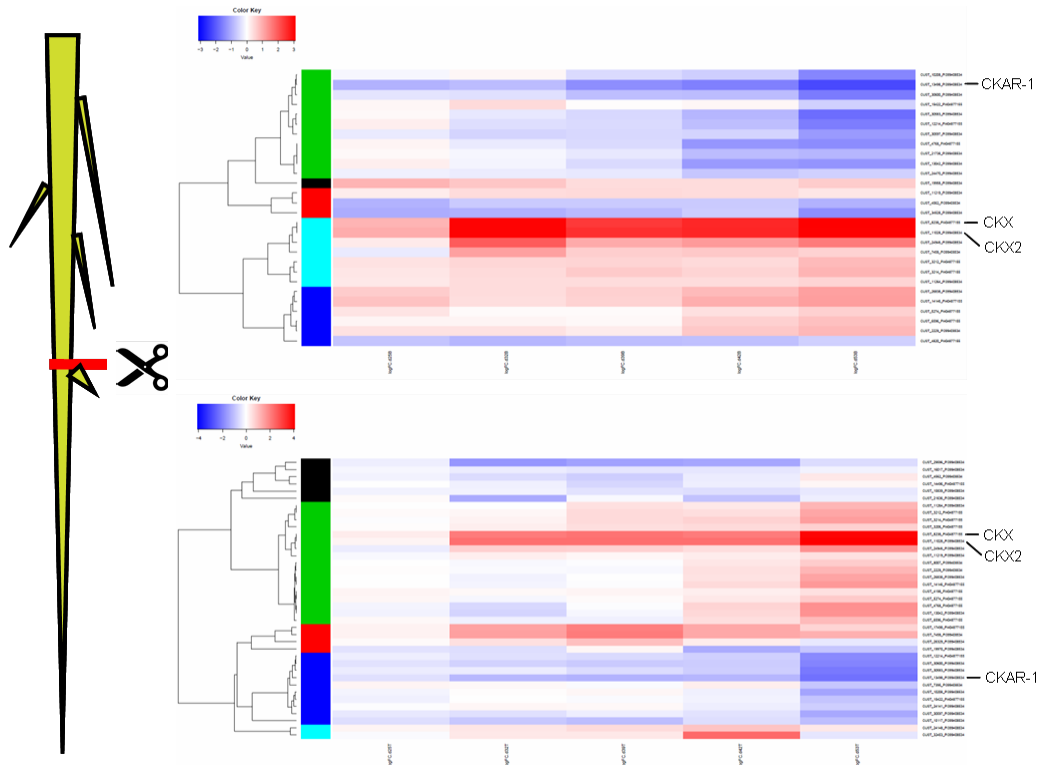
Figure 3.26 Enrichment analysis for CKs related transcripts in ARZ and BRZ over time. Seminal roots were harvested weekly from day 18 until day 53 and fractionated into ARZ and BRZ for microarray analysis. Colors of blue and red indicated the degree of fold change for down and up-regulation respectively. Expression values of *CKX*, *CKX2* and *CKAR-1* are indicated.

Expression analysis for ethylene-related genes yielded a large amount of transcripts that were up-regulated at day 32, including ethylene responsive transcription factor 6 (*ERTF6*, probe: CUST_8342_PI404877155) and ethylene responsive element binding factor 3 (*ERBF3*, probe: CUST_21373_PI399408534). Moreover, three homologs of 1-aminocyclopropane-1-carboxylate oxidase, encoding ACC oxidase catalyzing the last step in ethylene biosynthesis, were up-regulated at day 32 and kept high levels throughout (*ACCO1*, probe: CUST_8846_PI404877155; *ACCO2*, probe: CUST_18658_PI404877155; *ACCO3*, probe: CUST_32632_PI399408534). Interestingly, these 5 genes grouped in the same cluster in the ARZ and BRZ,

indicating their co-regulation over time (Figure 3.27). Oppositely, two probed showed but actually represented the same gene that strongly downregulated in ARZ: iron deficiency-specific clone 2 (*ISD2*, probe: CUST_742_PI399408534). *ISD2* resembles that of 2-oxoglutarate-dependent dioxygenase and induced under iron deficiency (Okumura et al., 1994). The reason of the downregulation of *ISD2* in ARZ needs more detailed study.

Taken together, evaluation of those genes that showed most dramatic changes during root aging indicated that ethylene biosynthesis was elevated from day 32 on.
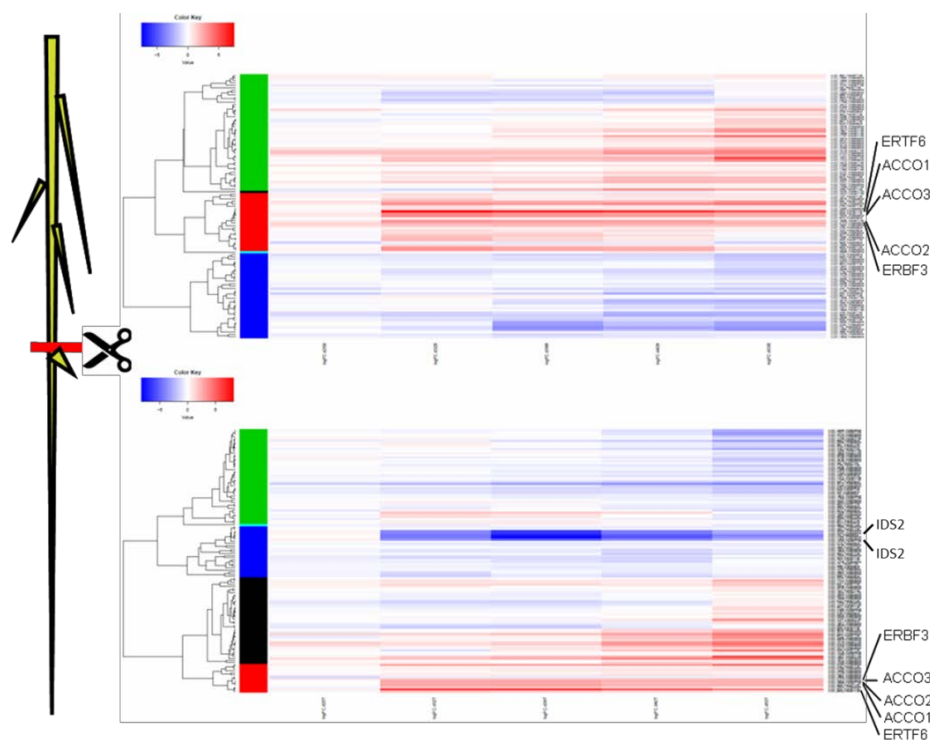
Figure 3.27 Enrichment analysis for ETH related transcripts in ARZ and BRZ over time. Seminal roots were harvested weekly from day 18 until day 53 and fractionated into ARZ and BRZ for microarray analysis. Colors of blue and red indicated the degree of fold change for down and up-regulation respectively. Expression values of *ERTF6*, *ERBF3*, *ACCO1*, *ACCO2* and *ACCO3* are indicated.

Among the GA-related genes, GA 2-oxidase is considered to play an important role in the regulation of plant growth through the reduction of endogenous levels of bioactive GAs (Sakamoto et al., 2001). Two genes encoding putative GA 2-oxidases showed outstanding upregulation in both root tissues from day 32 on: *GA2-O1*, probe:

CUST_757_PI404877155, and *GA2-O2*, probe: CUST_34128_PI399408534. Another GA 2-oxidase-like gene showed rather slight upregulation at day 39 followed by higher expression level afterwards (*GA2-O3*, probe: CUST_19936_PI399408534) (Figure 3.28). Taken together, in particular the two GA oxidase genes responded in a way that indicates that enhanced GA degradation set in at day 32.
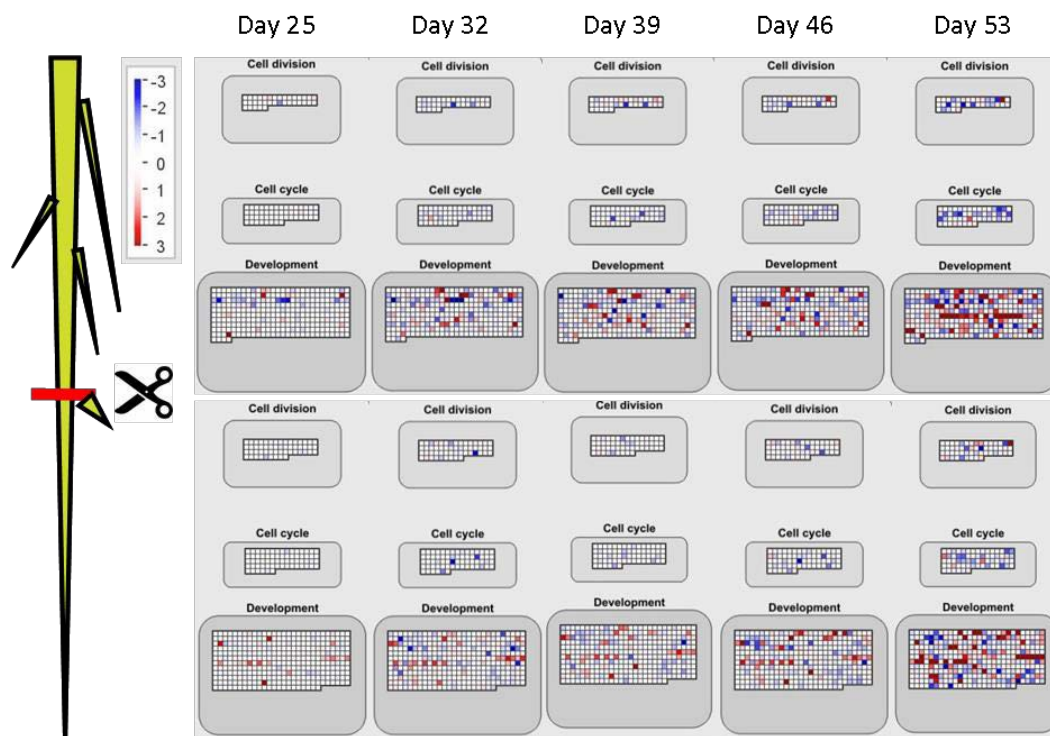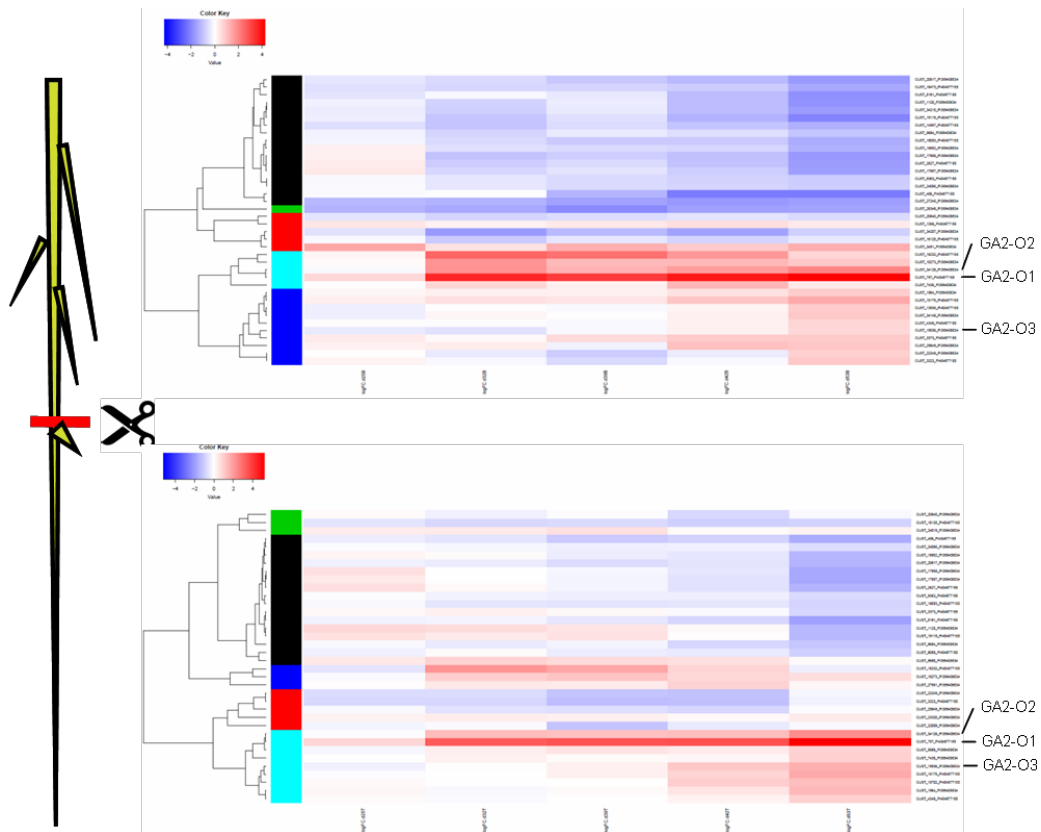

Figure 3.28 Enrichment analysis for GA related transcripts in ARZ and BRZ over time. Seminal roots were harvested weekly from day 18 until day 53 and fractionated into ARZ and BRZ for microarray analysis. Colors of blue and red indicated the degree of fold change for down and up-regulation respectively. Expression values of *GA2-O1*, *GA2-O2* and *GA2-O3* are indicated.
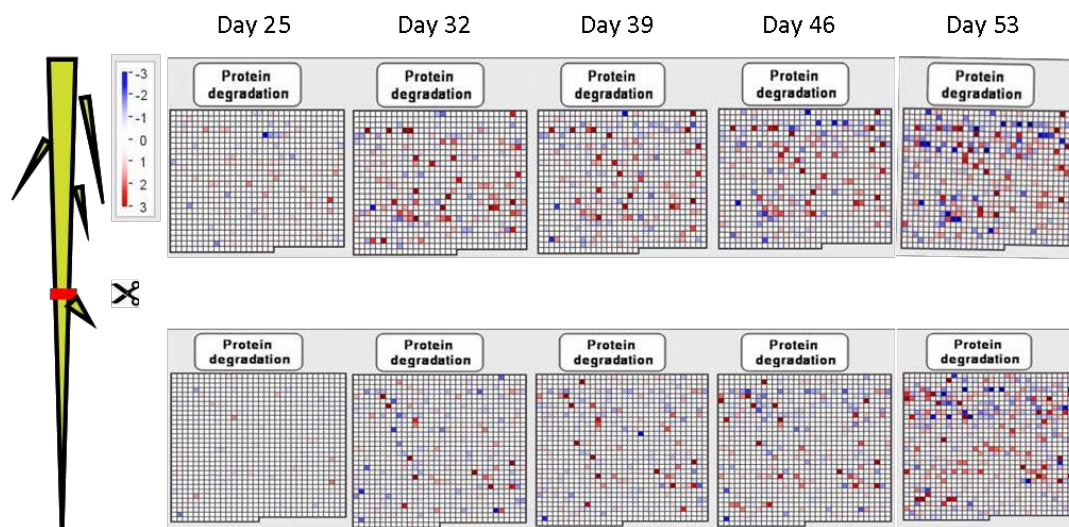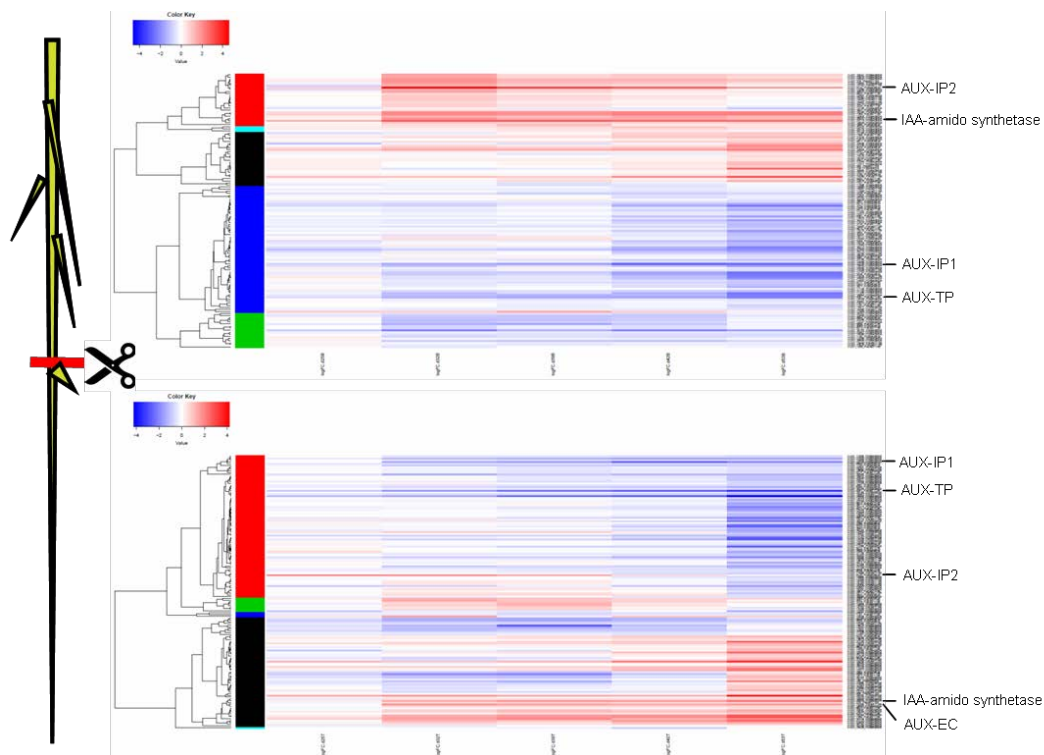
Figure 3.29 Enrichment analysis for auxin related transcripts in ARZ and BRZ over time. Seminal roots were harvested weekly from day 18 until day 53 and fractionated into ARZ and BRZ for microarray analysis. Colors of blue and red indicated the degree of fold change for down and up-regulation respectively. Expression values of *AUX-IP1*, *AUX-IP2*, *AUX-TP*, *AUX-EC* and *IAA-amido synthetase* are indicated.

Auxin-related genes were also divided into two groups according to their expression patterns: the first group displayed up regulation of mRNA levels at late stages, such as indole-3-acetic acid-amido synthetase gene (*IAA-amido synthetase*, probe: CUST_25920_PI399408534), which encodes an enzyme that conjugates auxin to amino acids to reduce the endogenous bioactive auxin level. One of the auxin efflux carrier proteins was also identified in this group, as it showed elevated expression from day 32 on (*AUX-EC*, probe: CUST_19209_PI404877155). The second group included genes with downregulated transcript levels at late stages, such as putative auxin transport protein (*AUX-TP*, probe: CUST_4361_PI404877155) and two auxin-induced protein-like genes (*AUX-IP1*, probe: CUST_22339_PI399408534; *AUX-IP2*, probe: CUST_8120_PI399408534). All these above-mentioned genes were identified in both, the ARZ and BRZ except for *AUX-EC*, which was only significantly expressed

in ARZ (Figure 3.29). This might indicate that *AUX-EC* is mainly functional in the apical root zone.

To gain an overview of the hormone metabolism, key genes involved in hormone biosynthesis/ degradation/ oxidation/ transport were annotated and grouped in Table 3.1. Age-dependent expression patterns of these genes are shown in Figure 3.30. For these genes, expression levels slightly changed at day 25 relative to day 18. However, these genes displayed a transition pattern at day 32, with a $\log_2$FC change from 2 to 7 (Figure 3.30). Notably, these altered gene expression levels were maintained from day 32 to day 53, supporting their involvement in the changes starting at day 32. As genes from different phytohormone classes shared this type of regulation, age-dependent changes in hormone regulation appeared to be coordinated.

Table 3.1 Identified genes involve in hormone biosynthesis, degradation, oxidation and transport

	ProbeName	Harvest assembly ID	Putative orthologous	FUNCAT
	CUST_12472_PI399408534	35_27680	9-cis-epoxycarotenoid dioxygenase 2 (barley)	hormone metabolism.abscisic acid.synthesis-degradation.
ABA	CUST_17284_PI404877155	HT11N18r_s_at	viviparous-14 protein (maize)	hormone metabolism.abscisic acid.synthesis-degradation.
	CUST_8238_PI404877155	Contig24300_at	cytokinin oxidase (rice)	hormone metabolism.cytokinin.synthesis-degradation
CK	CUST_11028_PI399408534	35_13504	cytokinin dehydrogenase (rice)	hormone metabolism.cytokinin.synthesis-degradation
	CUST_8342_PI404877155	Contig2471_at	ethylene responsive transcription factor 6 (wheat)	hormone metabolism.ethylene.signal transduction
	CUST_8846_PI404877155	Contig2642_at	1-aminocyclopropane-1-carboxylate oxidase (sorghum)	hormone metabolism.ethylene.synthesis-degradation
	CUST_18658_PI404877155	HVSMEm0001015r2_s_at	1-aminocyclopropane-1-carboxylate oxidase (sorghum)	hormone metabolism.ethylene.synthesis-degradation
	CUST_32632_PI399408534	35_573	1-aminocyclopropane-1-carboxylate oxidase (rice)	hormone metabolism.ethylene.synthesis-degradation
ETH	CUST_21373_PI399408534	35_17532	Ethylene responsive element binding factor 3 (rice)	hormone metabolism.ethylene.signal transduction
	CUST_757_PI404877155	Contig10718_at	GA 2-oxidase (rice)	hormone metabolism.gibberelin.synthesis-degradation.
GA	CUST_34128_PI399408534	35_10034	Gibberellin 2-oxidase (rice)	hormone metabolism.gibberelin.synthesis-degradation.
	CUST_8120_PI399408534	35_13621	auxin-induced protein (maize)	hormone metabolism.auxin.induced-regulated-responsive-activated
	CUST_4361_PI404877155	Contig15329_at	auxin transport protein (rice)	hormone metabolism.auxin.signal transduction
Auxin	CUST_28864_PI399408534	35_21797	auxin efflux carrier component 6 (rice)	hormone metabolism.auxin.signal transduction

	Putative orthologous	logFC d25	logFC d32	logFC d39	logFC d46	logFC d53
ABA	9-cis-epoxycarotenoid dioxygenase 2 (barley)	0.31	2.44	1.84	1.57	1.12
	viviparous-14 protein (maize)	0.49	2.99	2.32	2.16	1.48
CK	cytokinin oxidase (rice)	0.91	3.05	2.39	2.62	3.12
	cytokinin dehydrogenase (rice)	1.01	3.07	2.53	2.85	3.09
ETH	ethylene responsive transcription factor 6 (wheat)	0.31	7.52	6.45	6.09	5.14
	1-aminocyclopropane-1-carboxylate oxidase (sorghum)	0.71	3.50	3.09	2.87	2.35
	1-aminocyclopropane-1-carboxylate oxidase (sorghum)	0.69	3.34	2.97	2.85	1.93
	1-aminocyclopropane-1-carboxylate oxidase (rice)	0.67	3.61	3.09	2.91	2.32
	Ethylene responsive element binding factor 3 (rice)	1.18	2.46	2.45	2.50	2.27
GA	GA 2-oxidase (rice)	0.64	3.68	3.27	3.84	4.27
	Gibberellin 2-oxidase (rice)	-0.10	1.82	1.29	1.67	2.05
Auxin	auxin-induced protein (maize)	0.89	4.61	3.60	3.06	1.93
	auxin transport protein (rice)	-0.64	-1.34	-1.55	-1.59	-2.28
	auxin efflux carrier component 6 (rice)	-0.41	-1.15	-1.44	-1.23	-2.33

	Putative orthologous	logFC d25	logFC D32	logFC d39	logFC d46	logFC d53
ABA	9-cis-epoxycarotenoid dioxygenase 2 (barley)	0.61	2.46	2.67	2.19	2.51
	viviparous-14 protein (maize)	1.09	3.48	3.54	3.11	3.46
CK	cytokinin oxidase (rice)	0.30	2.12	2.22	2.09	3.99
	cytokinin dehydrogenase (rice)	0.19	2.30	2.29	2.30	4.11
ETH	ethylene responsive transcription factor 6 (wheat)	0.56	6.70	6.83	5.68	4.41
	1-aminocyclopropane-1-carboxylate oxidase (sorghum)	0.19	2.04	3.06	2.49	2.71
	1-aminocyclopropane-1-carboxylate oxidase (sorghum)	-0.01	2.76	2.72	2.24	2.29
	1-aminocyclopropane-1-carboxylate oxidase (rice)	0.05	2.84	2.93	2.40	2.48
	Ethylene responsive element binding factor 3 (rice)	0.94	2.12	2.05	2.11	2.31
GA	GA 2-oxidase (rice)	0.83	3.33	3.50	3.58	5.23
	Gibberellin 2-oxidase (rice)	-0.08	1.38	1.30	1.32	2.31
Auxin	auxin-induced protein (maize)	2.28	2.24	1.68	0.63	0.14
	auxin transport protein (rice)	-0.85	-1.63	-2.23	-2.51	-3.26
	auxin efflux carrier component 6 (rice)	-1.06	-1.44	-2.30	-2.53	-4.22

Figure 3.30 Heatmap visualization of expression levels of hormone-related genes during root aging. Seminal roots were harvested weekly from day 18 until day 53 and fractionated into apical and basal root zones for microarray analysis. Blue or red color indicates the degree of fold-changes for down- or up-regulated genes, respectively. Numbers in colored squares stand for the $\log_2$-fold change ($\log_2 FC$) values relative to day 18.

3.3.6 Expression analysis of element transporters during root aging

The expression levels of genes encoding transporters for essential mineral elements were monitored over time. Since boron (B) concentrations were relatively stable and root B contents didn't indicate that B was remobilized during root aging (Appendix 1), the expression levels of B transporters were taken as reference for the other elements. As P and Zn showed different time-dependent changes in root contents, and N remobilization was a prominent event during leaf senescence, focus was placed on these three elements.

During root aging, expression levels of B transporters were largely stable in both, the ARZ and BRZ (expression levels varied between -1 and 1 log$_2$FC), except for the last harvest when transcript levels of most B transporters went down (Figure 3.31). These expression data were in agreement with root B concentrations or contents, which implied that there was no B remobilization from roots to sink organs during seminal root aging. A comparable result was obtained for nitrate transporters in the BRZ, as most N transporters showed no significant change (-1 < log$_2$FC< 1) from day 18 to day 53 (Figure 3.32). By contrast, in the ARZ, there was a strong downregulation of most nitrate transporters already at day 25 (Figure 3.32). Two nitrate transporters made a clear-cut exception to the other nitrate transporters, as they displayed strong up-regulation of their mRNA levels at day 32 in both, the RAZ and BSR (probe: CUST_142347_PI403524517, CUST_166139_PI403524517). These two genes deserve more attention in future investigations. In summary, the prominent downregulation of most nitrate transporters in the ARZ compared to the BRZ may imply decreasing uptake activity in the apex of seminal roots.

ID	Putative orthologous	logFC d25	logFC d32	logFC d39	logFC d46	logFC d53
CUST_24668_PI403524517	NIP3-1(rice)	-1.09	-1.21	-0.15	-0.14	-0.27
CUST_57292_PI403524517	HvNIP2;1(barley)	-0.35	-0.40	-0.24	-1.05	-1.20
CUST_36094_PI403524517	boron transporter Bot1(barley)	1.10	0.96	0.70	0.91	-1.03
CUST_37284_PI403524517	boron transporter 4 (Brachypodium distachyon)	-0.31	-0.43	-0.53	-0.41	-0.99
CUST_6611_PI404877155	TaBOR11(wheat)	-0.41	-0.36	-0.03	-0.22	-0.30
CUST_72645_PI403524517	boron transporter (barley)	-0.35	-0.68	-0.59	-0.44	-2.21
CUST_98752_PI403524517	boron transporter (barley)	-0.44	-0.91	-0.90	-0.76	-1.43
CUST_98836_PI403524517	boron transporter (barley)	0.43	1.07	0.48	0.97	0.23

ID	Putative orthologous	logFC d25	logFC d32	logFC d39	logFC d46	logFC d53
CUST_24668_PI403524517	NIP3-1(rice)	-0.26	-0.41	-0.33	-0.33	0.52
CUST_57292_PI403524517	HvNIP2;1(barley)	-0.49	-0.65	-0.75	-0.80	-2.01
CUST_169334_PI403524517	TaBOR11(wheat)	-0.52	-0.53	-0.49	-0.49	-1.30
CUST_36094_PI403524517	boron transporter Bot1(barley)	0.77	0.94	0.51	1.04	0.29
CUST_37284_PI403524517	boron transporter 4 (Brachypodium distachyon)	-0.92	-0.51	-0.93	-0.69	-0.40
CUST_6611_PI404877155	TaBOR11(wheat)	-0.04	0.12	0.08	0.13	-0.34
CUST_72645_PI403524517	boron transporter (barley)	0.01	0.03	0.04	-0.33	-2.21
CUST_82593_PI403524517	TaBOR11(wheat)	0.07	0.10	0.23	0.15	-0.38
CUST_98752_PI403524517	boron transporter (barley)	-0.33	-0.74	-0.40	-0.76	-1.69

Figure 3.31 Expression analysis of genes encoding boron transporters during root aging. Seminal roots were harvested weekly from day 18 until day 53 and fractionated in apical and basal root zones for microarray analysis. Blue or red color indicates the degree of fold-changes for down- or up-regulated genes, respectively. Numbers in the colored squares stand for log$_2$-fold changes (log$_2$FC) relative to the expression levels at day 18.
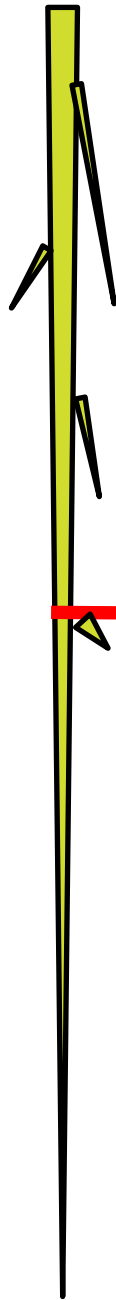
ID	Putative orthologous	logFC d25	logFC d32	logFC d39	logFC d46	logFC d53
CUST_39134_PI403524517	NRT1 (Brachypodium distachyon)	0.02	-0.41	-0.1	0.33	1.26
CUST_42914_PI403524517	Low affinity nitrate transporter NRT1.1 (wheat)	-0.02	-0.43	-1.41	-0.65	-0.65
CUST_47447_PI403524517	Nitrate transporter (Barley)	0.3	0.29	0.31	2.38	0.47
CUST_55631_PI403524517	NRT1 (Brachypodium distachyon)	-0.12	-0.15	0.05	-0.4	-0.77
CUST_57514_PI403524517	High affinity nitrate transporter (Barley)	0.14	0.29	0.13	0.58	0.72
CUST_60576_PI403524517	NRT1 (Setaria italica)	-0.37	-0.02	-0.43	-0.5	-0.71
CUST_62442_PI403524517	NRT1 (Brachypodium distachyon)	0.05	-0.04	0.08	0.36	0.76
CUST_87301_PI403524517	NRT1 (Brachypodium distachyon)	-0.08	-0.1	-0.4	-0.28	-0.9
CUST_98210_PI403524517	high affinity nitrate transporter (BCH3) (barley)	-0.1	-0.34	0.13	0.41	1.22
CUST_108819_PI403524517	Nitrate transporter (Barley)	-0.57	-0.07	0.79	0.34	-1
CUST_109249_PI403524517	Nitrate transporter (Barley)	-0.2	0.17	0.86	0.27	-0.96
CUST_11230_PI403524517	low affinity nitrate transporter (wheat)	0.09	0.33	-0.22	0.43	1.23
CUST_142347_PI403524517	NRT1 (rice)	0.95	3.5	2.52	2.35	1.8
CUST_155531_PI403524517	NRT1 (Brachypodium distachyon)	0.3	1.31	0.68	0.76	0.41
CUST_166139_PI403524517	NRT1 (Brachypodium distachyon)	0.8	3.19	2.71	2.27	1.45
CUST_167014_PI403524517	NRT1 (rice)	-0.37	-0.32	-0.51	-0.31	-0.12
CUST_171984_PI403524517	NRT1 (Brachypodium distachyon)	0.34	0.36	0.35	0.67	0.41
CUST_24_PI404877155	high affinity nitrate transporter (BCH3) (barley)	-0.08	-0.31	0.14	0.5	1.31
CUST_13663_PI404877155	NRT1 (Brachypodium distachyon)	-0.28	-0.21	0.08	-0.48	-0.97
CUST_13954_PI404877155	low affinity nitrate transporter (wheat)	0.09	0.19	-0.34	0.66	1.43
CUST_13958_PI404877155	Nitrate transporter 1.1 (barley)	-0.42	-0.18	-0.63	-0.03	0.75
CUST_13964_PI404877155	Nitrate transporter (Barley)	-0.35	-0.63	-0.41	-0.69	-0.02

ID	Putative orthologous	logFC d25	logFC d32	logFC d39	logFC d46	logFC d53
CUST_42914_PI403524517	Low affinity nitrate transporter NRT1.1 (wheat)	-0.76	-1.83	-1.06	-2.06	-0.78
CUST_57514_PI403524517	High affinity nitrate transporter (Barley)	-0.51	-0.68	-0.80	-0.19	0.72
CUST_57519_PI403524517	NAR2.1 (barley)	-1.15	-1.37	-1.78	-1.43	-0.32
CUST_60576_PI403524517	NRT1 (Setaria italica)	-0.50	-0.58	-0.75	-0.92	-1.14
CUST_62442_PI403524517	NRT1 (Brachypodium distachyon)	-0.22	-0.23	-0.08	0.46	1.67
CUST_80030_PI403524517	High affinity nitrate transporter NRT2.6 (barley)	-1.89	-1.39	-1.60	-1.44	1.00
CUST_84356_PI403524517	NRT1 (Brachypodium distachyon)	-0.94	-0.60	-0.95	-0.76	-1.37
CUST_84422_PI403524517	NRT1 (Brachypodium distachyon)	-0.59	-0.66	-0.72	-0.54	-0.58
CUST_86150_PI403524517	NAR2.2 (barley)	-0.82	-1.36	-1.47	-0.91	0.06
CUST_87301_PI403524517	NRT1 (Brachypodium distachyon)	-0.63	-0.88	-1.12	-0.95	-0.88
CUST_88500_PI403524517	NRT1 (Brachypodium distachyon)	-0.85	-0.91	-1.09	-0.83	-0.56
CUST_92213_PI403524517	high affinity nitrate transporter BCH2 (barley)	-2.68	-1.33	-0.83	0.13	2.65
CUST_98210_PI403524517	high affinity nitrate transporter (BCH3) (barley)	-2.35	-1.08	-1.45	-1.21	0.92
CUST_101810_PI403524517	NRT1 (Brachypodium distachyon)	-0.89	-0.91	-1.07	-0.81	-0.83
CUST_106544_PI403524517	NRT1 (Setaria italica)	-1.17	-0.91	-1.57	-1.00	-1.17
CUST_109249_PI403524517	Nitrate transporter (Barley)	-0.02	0.23	0.32	0.04	-1.22
CUST_11230_PI403524517	low affinity nitrate transporter (wheat)	-1.14	-1.64	-2.92	-1.61	-0.04
CUST_142347_PI403524517	NRT1 (rice)	-0.03	2.21	1.96	1.54	1.31
CUST_155774_PI403524517	NRT1 (Brachypodium distachyon)	0.21	0.11	0.32	0.06	0.72
CUST_166139_PI403524517	NRT1 (Brachypodium distachyon)	0.09	2.37	2.12	1.71	0.29
CUST_167014_PI403524517	NRT1 (rice)	-0.22	-0.48	-0.42	-0.70	-0.52
CUST_182360_PI403524517	High affinity nitrate transporter BCH1 (barley)	-3.03	-1.96	-2.19	-2.08	-0.98
CUST_24_PI404877155	high affinity nitrate transporter (BCH3) (barley)	-2.13	-1.27	-1.49	-1.22	0.86
CUST_5485_PI404877155	High affinity nitrate transporter NRT2.6 (barley)	-1.63	-1.29	-1.42	-1.18	1.22
CUST_5944_PI404877155	low affinity nitrate transporter (wheat)	-0.31	0.05	-0.37	-0.22	-0.81
CUST_8039_PI404877155	NRT1 (Brachypodium distachyon)	-0.74	-0.90	-0.93	-0.62	-0.64
CUST_8875_PI404877155	High affinity nitrate transporter BCH2 (barley)	-2.36	-1.56	-0.74	0.10	2.73
CUST_13954_PI404877155	low affinity nitrate transporter (wheat)	-1.25	-1.85	-2.86	-1.46	-0.03
CUST_13958_PI404877155	Nitrate transporter 1.1 (barley)	-0.46	-0.82	-0.89	-0.74	-0.33
CUST_13964_PI404877155	Nitrate transporter (Barley)	-0.82	-0.70	-0.64	-0.84	0.48
CUST_14142_PI404877155	NRT1 (Brachypodium distachyon)	-0.29	-0.29	-0.13	0.39	1.64
CUST_19730_PI404877155	High affinity nitrate transporter BCH1 (barley)	-3.49	-2.29	-2.51	-2.29	-1.09

Figure 3.32 Expression analysis of genes encoding nitrate transporters during root aging. Seminal roots were harvested weekly from day 18 until day 53 and fractionated in apical and basal root zones for microarray analysis. Blue or red color indicates the degree of fold-changes for down- or up-regulated genes, respectively. Numbers in the colored squares stand for $\log_2$-fold changes ($\log_2$FC) relative to the expression level at day 18.

Compare with B and N transporters, many P and Zn transporters showed up regulation within the time course, especially after day 39 (Figure 3.33, Figure 3.34). For these up-regulated P and Zn transporters, all of them displayed even higher expression levels at late stages. For the up-regulated Zn transporters, they mainly elevated their expression levels at day 39 in BRZ, which is one or two weeks earlier than their up-regulations in ARZ. Similar phenomenon could also be found for P transporters. Such event might due to the fact that BRZ contains older tissue and when senescence started the resources such as P and Zn should be remobilized earlier in BSR compare with the remobilization in ARZ. Taken together, the up regulation of these P and Zn transporters indicated P and Zn might be remobilized during root senescence.

ID	Putative orthologous	logFC d25	logFC d32	logFC d39	logFC d46	logFC d53
CUST_14119_PI404877155	phosphate transporter 6 (barley)	0.38	0.34	0.89	1.57	1.96
CUST_1895_PI403524517	Inorganic phosphate transporter 3 (Maize)	0.35	0.45	0.95	1.52	1.85
CUST_98566_PI403524517	Putative phosphate transporter (rice)	0.04	0.04	0.07	1.05	1.13
CUST_159057_PI403524517	Phosphate transporter 8 (Wheat)	-0.04	0.41	0.55	1.21	0.66
CUST_120876_PI403524517	Putative phosphate transporter (rice)	0.45	0.06	0.48	0.58	0.62
CUST_14044_PI404877155	Putative phosphate transporter (rice)	0.14	0.17	0.13	0.30	0.68
CUST_16409_PI403524517	Putative phosphate transporter (arabidopsis)	0.49	0.74	0.53	0.68	0.49

ID	Putative orthologous	logFC d25	logFC d32	logFC d39	logFC d46	logFC d53
CUST_111660_PI403524517	Phosphate transporter HvPT5 (barley)	0.20	0.55	1.24	0.71	1.57
CUST_14119_PI404877155	phosphate transporter 6 (barley)	0.48	0.19	1.02	0.86	1.62
CUST_1895_PI403524517	Inorganic phosphate transporter 3 (Maize)	0.46	0.49	0.94	0.86	1.67
CUST_14044_PI404877155	Putative phosphate transporter (rice)	-0.03	0.03	0.04	0.23	0.77
CUST_159057_PI403524517	Phosphate transporter 8 (Wheat)	-0.75	-1.39	-0.58	0.04	1.01
CUST_182070_PI403524517	Putative phosphate transporter (rice)	-0.86	-1.21	-1.36	-1.04	-0.68

Figure 3.33 Expression analysis of genes encoding phosphate transporters during root aging. Seminal roots were harvested weekly from day 18 until day 53 and fractionated in apical and basal root zones for microarray analysis. Blue or red color indicates the degree of fold-changes for down- or up-regulated genes, respectively. Numbers in the colored squares stand for $\log_2$-fold changes ($\log_2$FC) relative to the expression level at day 18.
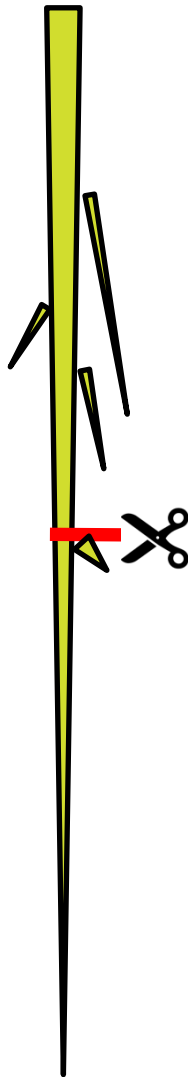
ID	Putative orthologous	logFC d25	logFC d32	logFC d39	logFC d46	logFC d53
CUST_133338_PI403524517	Putative Zinc transporter zupT (rice)	0.08	-0.22	-0.37	-0.62	-1.02
CUST_135639_PI403524517	Zinc transporter protein ZIP7 (barley)	-0.29	0.54	1.67	2.37	3.04
CUST_15193_PI403524517	Putative Zinc transporter zupT (rice)	0.22	-0.12	-0.47	-0.37	-0.45
CUST_1580_PI404877155	putative zinc transporter (rice)	0.56	1.39	1.17	1.58	2.07
CUST_161983_PI403524517	Zinc transporter protein ZIP7 (barley)	-0.41	0.07	0.57	1.05	1.95
CUST_16678_PI404877155	putative ZIP-like zinc transporter (rice)	-0.36	0.46	1.56	2.24	2.93
CUST_17560_PI404877155	zinc transporter (rice)	-0.25	-0.22	-0.40	-0.42	-0.48
CUST_19034_PI403524517	Putative zinc transporter (rice)	0.55	1.52	1.35	1.65	2.19
CUST_2038_PI404877155	zinc transporter (rice)	-0.03	-0.46	-0.56	-0.50	-0.82
CUST_23437_PI403524517	Putative ZIP-like zinc transporter (rice)	-0.32	0.16	0.93	1.50	1.59
CUST_26621_PI403524517	Putative zinc transporter (rice)	-0.05	0.17	0.92	1.57	2.58
CUST_38909_PI403524517	Zinc transporter ZIP (wheat)	-0.88	0.22	1.26	1.65	4.02
CUST_41397_PI403524517	Putative Zn transporter (barley)	-0.68	-0.46	-1.03	-0.79	-0.81
CUST_4960_PI404877155	putative zinc transporter ZIP1 (rice)	0.06	0.24	1.04	1.63	2.80
CUST_54200_PI403524517	Putative Zn transporter (barley)	-0.19	-0.28	-0.39	-0.32	-0.34
CUST_54205_PI403524517	Putative Zn transporter (barley)	0.08	-0.45	-0.54	-0.37	-0.73
CUST_78772_PI403524517	Zinc transporter ZIP (wheat)	-0.63	0.33	1.00	1.57	4.02
CUST_8777_PI404877155	zinc transporter ZIP3 (rice)	-1.20	0.18	1.06	1.58	3.95
CUST_89068_PI403524517	Putative zinc transporter OsZIP2	-1.10	0.25	2.56	3.70	4.23
CUST_91792_PI403524517	cadmium/zinc-transporting ATPase 3 (arabidopsis)	0.93	1.24	1.48	2.37	3.12
CUST_9569_PI403524517	cadmium/zinc-transporting ATPase 3 (arabidopsis)	0.48	0.29	0.35	0.80	1.25

ID	Putative orthologous	logFC d25	logFC d32	logFC d39	logFC d46	logFC d53
CUST_104816_PI403524517	Cadmium/zinc-transporting ATPase 4 (arabidopsis)	-0.44	-0.78	-1.01	-0.25	-0.30
CUST_115406_PI403524517	Zinc transporter (rice)	-0.35	-0.52	-0.63	-0.45	-0.28
CUST_127983_PI403524517	Putative Zinc transporter zupT (rice)	0.66	0.89	0.61	0.64	2.47
CUST_133338_PI403524517	Putative Zinc transporter zupT (rice)	-0.10	-0.12	-0.29	-0.68	-0.87
CUST_135639_PI403524517	Zinc transporter protein ZIP7 (barley)	-0.62	0.17	0.88	1.68	3.26
CUST_15193_PI403524517	Putative Zinc transporter zupT (rice)	-0.04	-0.27	-0.46	-0.42	-0.32
CUST_1580_PI404877155	putative zinc transporter (rice)	0.52	0.90	0.56	0.51	0.86
CUST_161983_PI403524517	Zinc transporter protein ZIP7 (barley)	-0.05	-0.13	0.20	0.54	1.85
CUST_16678_PI404877155	putative ZIP-like zinc transporter (rice)	-0.58	0.08	0.82	1.56	3.21
CUST_19034_PI403524517	Putative zinc transporter (rice)	0.54	0.99	0.82	0.55	0.91
CUST_23437_PI403524517	putative ZIP-like zinc transporter (rice)	-0.50	0.00	0.17	0.97	2.03
CUST_26621_PI403524517	Putative zinc transporter (rice)	0.32	0.59	0.50	0.17	1.27
CUST_38909_PI403524517	Zinc transporter ZIP (wheat)	-0.16	0.88	1.32	0.84	2.68
CUST_41397_PI403524517	Putative Zn transporter (barley)	-0.49	-1.00	-0.95	-0.65	-0.35
CUST_4960_PI404877155	putative zinc transporter ZIP1 (rice)	0.37	0.62	0.57	0.24	1.44
CUST_54205_PI403524517	Putative Zn transporter (barley)	-0.24	-0.48	-0.51	-0.19	0.25
CUST_78772_PI403524517	Zinc transporter ZIP (wheat)	-0.52	0.33	0.69	0.60	2.02
CUST_8777_PI404877155	zinc transporter ZIP3 (rice)	-0.43	0.86	0.88	0.78	2.65
CUST_89068_PI403524517	Putative zinc transporter OsZIP2	0.04	0.18	1.20	2.01	3.71
CUST_9569_PI403524517	cadmium/zinc-transporting ATPase 3 (arabidopsis)	-0.20	-0.17	-0.20	0.52	1.61
CUST_97069_PI403524517	Zinc transporter (rice)	-0.37	-0.44	-0.53	-0.34	-0.06

Figure 3.34 Expression analysis of genes encoding zinc transporters during root aging. Seminal roots were harvested weekly from day 18 until day 53 and fractionated in apical and basal root zones for microarray analysis. Blue or red color indicates the degree of fold-changes for down- or up-regulated genes, respectively. Numbers in the colored squares stand for $\log_2$-fold changes ($\log_2$FC) relative to the expression level at day 18.

3.4 Analysis of plant age-dependent marker, tryptophan decarboxylase, and the potential roles of its up- and downstream metabolites, typtophan, typtamine and serotonin in root aging

To identify plant age-dependent genes, ARZ was harvested weekly and samples were subjected to microarray based transcriptome analysis. The logic of identifying

plant age-dependent regulators was demonstrated previously (see materials and methods 2.1). The data of average seminal root length during root aging displayed a
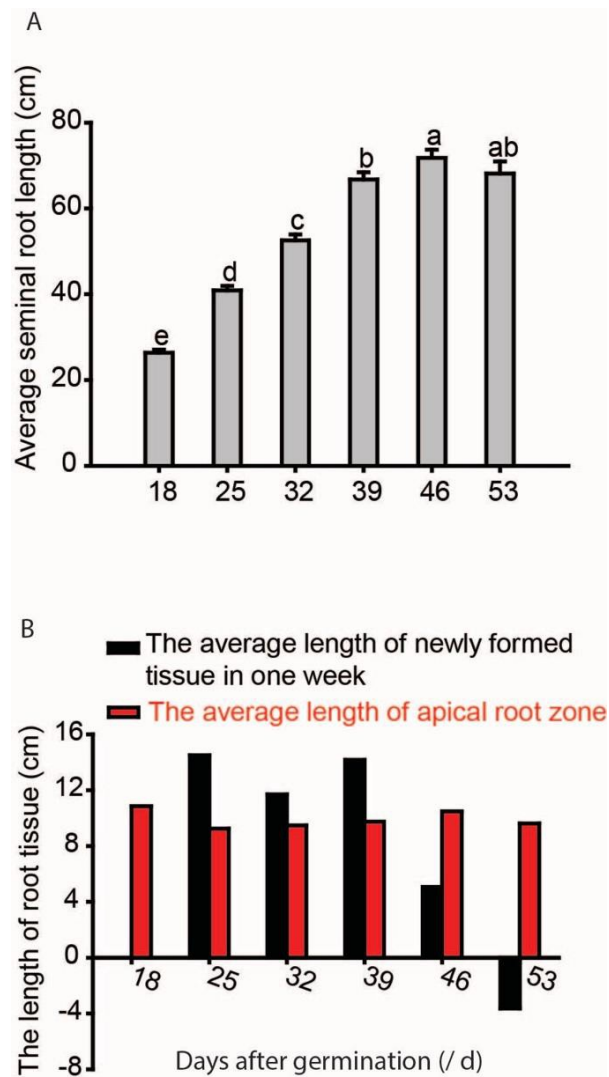
Figure 3.35 The elongation of seminal root. Seminal roots and leaves of hydroponically-grown plants were harvested weekly from day 18 until day 53, when the main tiller had 4 chlorotic leaves (Figure 3.2A). Average seminal root length were calculated as the mean value of total seminal root length (A) and average length of newly formed tissue was subtracted between two nearby average seminal root length (B). n=15.

linearly root elongation between day 18 and day 39 (Figure 3.35A). Moreover, the weekly generated new root segments were longer than the ARZ before day 39 indicating these ARZs were newly generated (Figure 3.35B). Therefore, genes displayed gradual up- or downregulation in ARZ before day 39 were assigned as plant age-dependent regulators.

By applying the criteria that plant age-dependent genes should be gradually up- or downregulated with factor 1 (log$_2$FC) from day 25 on until day 39 in ARZ, 20 genes fulfill the demands (Table 3.2). 7 genes belong to the group of gradually upregulated and the other 13 genes consist of the gradually downregulated group. The criteria then strengthened that among these 20 genes, they must showed up- or downregulation started from day 18, which finally fulfill the demand of the plant age-dependent genes. This sorting procedure resulted with 2 genes satisfied as plant age-dependent genes, which were tagged with the probe number CUST_108866_PI403524517 and CUST_40150_PI403524517, respectively (Table 3.2). CUST_108866_PI403524517 correspond to the Harvest assembly ID 35_30956, which showed 100% identity to a barley gene, HORVU7Hr1G010870 (IPK barley database number), and 89% identity to barley tryptophan decarboxylase gene (ID: AB162960.1). The other probe which showed gradually downregulated got no hint from NCBI (https://www.ncbi.nlm.nih.gov/) or IPK barley blast (http://webblast.ipk-gatersleben.de/barley_ibsc/). Therefore, further investigation was only focused on the upregulated gene, HORVU7Hr1G010870.

Table 3.2 Gradual up- or downregulated genes between day 25 and day 39 in ARZ. Seminal roots were harvested weekly from day 18 until day 53 and fractionated in apical and basal root zones for microarray analysis. Blue or red color indicates the degree of fold-changes for down- or up-regulated genes, respectively. Numbers in the colored squares stand for log$_2$-fold changes (log$_2$FC) relative to the expression level at day 18.

ID	Harvest assembly ID	logFC d25	logFC d32	logFC d39	logFC d42	logFC d53	Putative orthologous
CUST_7333_PI399408534	35_9403	0.64	1.76	2.96	1.91	1.13	
CUST_106809_PI403524517	35_30399	0.61	2.44	3.75	3.85	4.70	
CUST_108866_PI403524517	35_30956	1.41	2.42	3.59	3.33	4.36	Tryptophan decarboxylase (Barley)
CUST_23719_PI403524517	35_6893	0.25	1.60	3.10	3.87	5.35	
CUST_24817_PI403524517	35_7200	0.32	1.41	2.81	4.57	5.37	
CUST_32305_PI403524517	35_9315	-0.31	0.71	1.97	2.54	4.04	
CUST_18577_PI403524517	35_5369	3.96	2.28	1.23	0.81	0.55	
CUST_40150_PI403524517	35_11546	-1.65	-3.31	-4.69	-4.81	-4.74	No hint from NCBI and IPK blast
CUST_104835_PI403524517	35_29870	0.42	-1.13	-3.26	-1.60	1.20	
CUST_11585_PI403524517	35_3288	0.74	-4.62	-7.70	-4.97	-2.78	
CUST_14583_PI399408534	35_28026	0.51	-3.59	-5.33	-3.92	-2.57	
CUST_164994_PI403524517	35_45984	-0.57	-3.93	-4.99	-4.78	-3.69	
CUST_21693_PI399408534	35_13139	0.11	-4.29	-8.30	-5.53	-3.57	
CUST_22351_PI399408534	35_6218	0.34	-4.00	-6.46	-4.30	-2.85	
CUST_24800_PI403524517	35_7193	-0.17	-1.48	-2.74	-2.17	-1.19	
CUST_29092_PI399408534	35_29257	0.28	-3.90	-6.59	-4.26	-2.79	
CUST_37497_PI403524517	35_10800	-0.13	-1.95	-2.97	-2.72	-2.46	
CUST_67779_PI403524517	35_19363	0.30	-5.57	-10.07	-6.85	-4.60	
CUST_67783_PI403524517	35_19364	0.13	-5.26	-8.78	-6.98	-5.77	
CUST_742_PI399408534	35_26375	0.11	-4.41	-7.58	-5.27	-3.98	

Since the Harvest assembly ID, 35_30956, showed 100% identity to HORVU7Hr1G010870 gene, thus HORVU7Hr1G010870 was taken as the correspondent gene as identified by microarray. By a blast based on NCBI database, the translated amino acids sequence of the full CDS of HORVU7Hr1G010870 showed 100% query cover and 89% identity to two full CDS of barley tryptophan decarboxylase genes (Accession: AB162960.1, AB162961.1), which got the highest scores among all the named sequences. Therefore, HORVU7Hr1G010870 was identified as a tryptophan decarboxylase (TDC) gene in barley. This gene was named as *HvTDC* for short. To better visualize the evolution relationships between TDC genes among species, a phylogenetic analysis was performed across monocotyledonous and dicotyledonous plants.
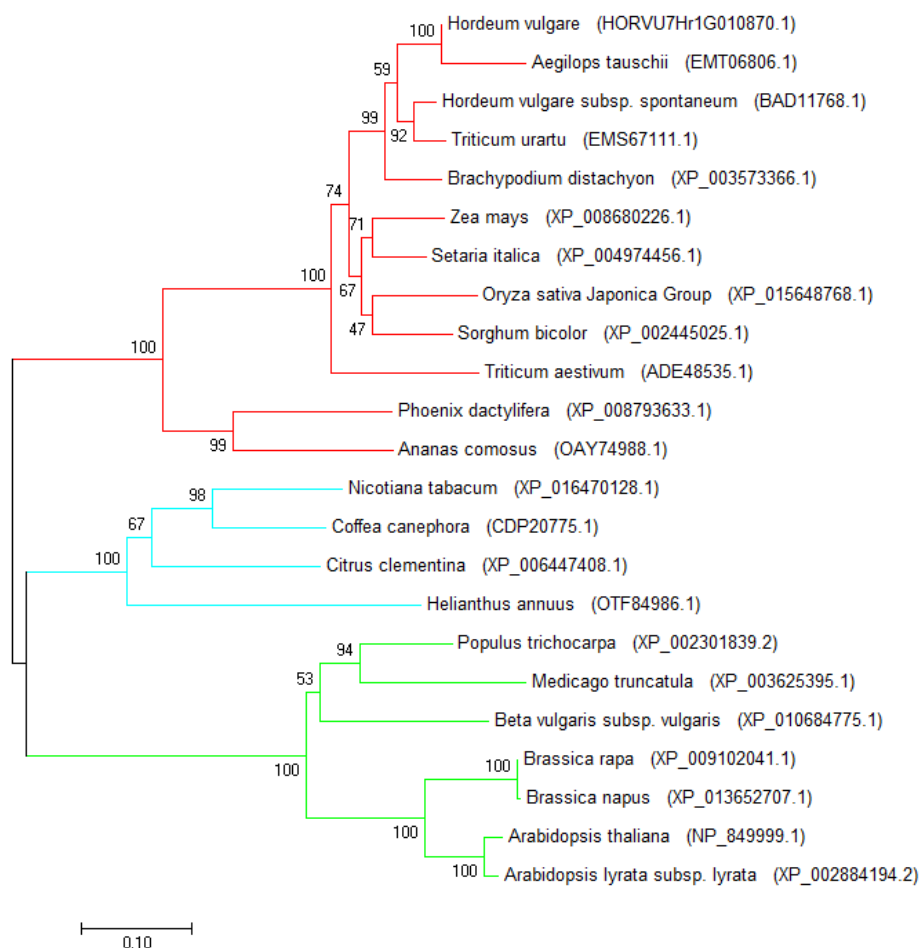
Figure 3.36 Phylogenetic tree of tryptophan decarboxylase across species. Different color indicated different sub-groups, numbers indicated the similarity between sequences.

Relationships among the target gene orthologue sets were examined in arbitrarily rooted neighbour-joining phylogenies of protein sequences. Comparison among sequences from monocot and dicot plants identified at least three separate clades of TDC genes. In this case, a likely barley TDC protein encoded by HORVU7Hr1G010870 and named as *HvTDC*, appeared as a close homologue to Aegilops tauschii aromatic-L-amino-acid decarboxylase protein which is a big enzyme family include TDC proteins (Figure 3.36). *HvTDC* had 89% sequence identity with the TDC gene of barley subspecies spontaneum. These phylogenetic relationships among different TDC genes across species provided the baseline information for their subsequent functional characterization.

In plants, tryptophan is first catalyzed into tryptamine by tryptophan decarboxylase (TDC), followed by the catalysis of tryptamine by tryptamine 5-hydroxylase (T5H) to synthesize serotonin (Schröder et al., 1999). TDC plays a rate-limiting role for serotonin biosynthesis. Exogenous application and transgenic approaches identified serotonin as a negative regulator in leaf senescence probably due to its ROS scavenging ability (Kang et al., 2009). To address the question whether serotonin was accumulated due to the gradual upregulation of *HvTDC*, serotonin as well as its precursors, tryptophan and tryptamine, were quantified by UPLC-MS/MS.

During root aging, tryptophan showed slight but significant increase from day 18 to day 39, followed by clear accumulation thereafter (Figure 3.37A). Similar pattern was also observed in tryptamine as it also displayed obvious elevation after day 39 (Figure 3.37B). However, serotonin behaved different compare with tryptophan and tryptamine, since it was under the detection limits at day 18 but further increased to approxi. 60 p mol g^{-1} FW at day 39. The concentration of serotonin was almost tripled at day 53 compare with day 39 (Figure 3.37C). The gradual accumulation of serotonin correlated with the gradually upregulation of *HvTDC* which indicated *HvTDC* and serotonin might involve in root aging process.
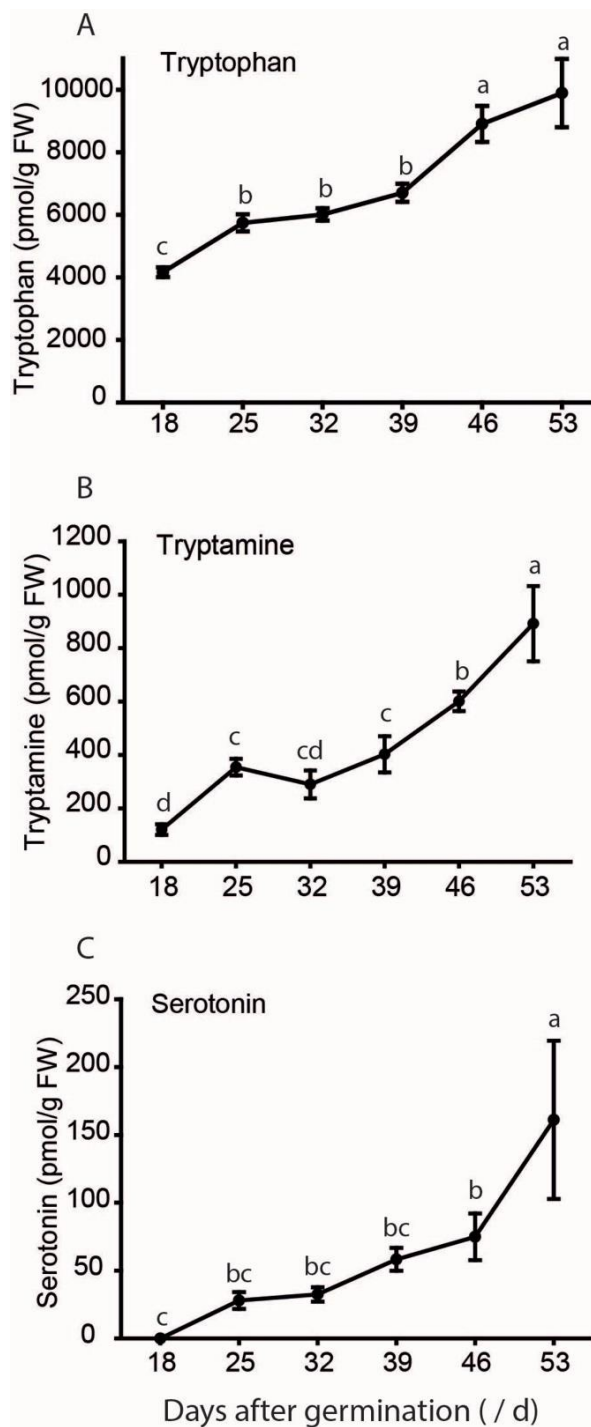
Figure 3.37 Plant age-dependent dynamics of tryptophan, tryptamine and serotonin. Seminal roots and leaves were harvested weekly from day 18 until day 53, when the main tiller had 4 chlorotic leaves (Figure 3.2A). (A) Tryptophan concentration in seminal roots during root aging. (B) Tryptamine concentration in seminal roots during root aging. (C) Serotonin concentration in seminal roots during root aging. n=5. Error bars indicate mean values ± SE. Different letters indicate significant differences according to LSD test ($p < 0.05$).

4 Discussion

4.1 Several phenotypic, physiological, and molecular processes during root aging are reminiscent of leaf senescence

In plant sciences, leaf senescence is an intensively studied topic (until 2017 > 20.000 papers published on this topic; acc. to google scholar). In contrast, root senescence has remained unknown despite its importance for plant performance and ecological functions. The present work set out to i) assign root degenerative process to either root aging or root senescence, ii) characterize degenerative processes in roots at the phenotypical, physiological and molecular level and iii) identify potential markers that regulate this processes.

In the present study, several lines of evidence indicated that plant age-dependent changes in recorded root parameters are reminiscent of those observed in senescing leaves:

i) After chloroplast degradation, the loss of plasma membrane integrity is often referred to as the initial phase of leaf senescence. Disintegration of the plasma membrane during leaf senescence has frequently been monitored by electrolyte leakage or histological staining procedures (Guo and Crawford, 2005; Kim et al., 2009; Coll et al., 2010). In the present study, microscopy of root tissues after Evans blue staining showed that from day 39 on, tissue degradation began in cortical and epidermal cells of basal root segments before it expanded along the seminal root axis (Figure 3.4). A possible physiological consequence of uncontrolled membrane permeability may be seen in the decline in root K concentrations, presuming that this loss reflected K leakage from outer root cells into the hydroponic medium (Appendix 1).

ii) Another typical physiological process during leaf senescence is protein degradation. Most prominently, rubisco is among the first proteins to be degraded during leaf senescence for nutrient recycling, mainly of N (Yoshida, 2003; Hörtensteiner, 2009). In particular cysteine proteases are strongly engaged in protein turnover (Bhalerao et al., 2003; Gepstein et al., 2003; Parrott et al., 2010). Many cysteine proteases showed remarkable up-regulation at both, transcript and protein activity levels, when leaf senescence set in (Wagstaff et al., 2002; Martínez et al., 2007). These cysteine proteases are highly relevant for the progression of tissue senescence, as shown by suppression of the cysteine protease gene *BoCP5* in

broccoli, which delayed senescence (Eason et al., 2005). In the present investigation, protein degradation became evident also in roots. Transcriptome studies showed that protein degradation-related transcripts, including those of several cysteine proteases, were highly upregulated (Figure 3.21, Figure 3.22). For instance, the barley cysteine protease *HvPap17*, a putative ortholog of *AtSAG12*, was upregulated by more than 1000 times. Such a remarkable upregulation was also observed for *AtSAG12* mRNA levels during leaf senescence (Bohner et al., 2015). At the physiological level, metabolites representing degradation forms of proteins and nucleic acids, such as urea, accumulated in senescing root tissue (Figure 3.9). Moreover, amino acids that typically accumulate in senescing leaves, such as lysine, tyrosine, phenylalanine or tryptophan (Bohner et al., 2015), also accumulated in a plant age-dependent manner in roots (Figure 3.10, Figure 3.37). Moreover, altered phenylalanine metabolic process was significantly enriched by GO term analysis in both ARZ and BRZ (Figure 3.16, Figure 3.17). Therefore, protein degradation was definitely a prominent process in roots during the time course of plant aging that went along with progressing leaf senescence (Figure 3.2A).

iii) Physiological responses to hydrogen peroxide accumulation and oxidative stress, such as the onset of catalase or peroxidase activities, as typically seen in senescing leaves (Zimmermann et al., 2006), were also observed in roots. Between day 39-46, seminal roots showed a strong increase in catalase activity (Figure 3.7), which was accompanied by an upregulation of genes belonging to the GO terms "oxidation-reduction process" and "response to oxidative stress", which refer to plant defense responses to oxidative stress (Figure 3.16, Figure 3.17).

Considering that loss of membrane integrity, protein degradation and oxidative stress responses all became most prominent from day 39 on, it appears that around day 39 there was a coordinated change in root processes at the tissue, enzymatic and gene expression level. Such a coordinated change at multiple levels is not expected, if roots just underwent aging. It is thus tempting to speculate that around day 39 plants initiated a developmental program in seminal roots that is reminiscent of leaf senescence.

4.2 Root senescence is unlikely under control of the shoot

A decline in root dynamics mostly occurs during plant transition from the vegetative to the generative phase. At flowering, source-sink relationships undergo a major change as newly forming seeds generate sink activity. This may lead to energy depletion in roots and concomitant decline in root activity (Comas et al., 2005). In the present study, the uptake capacity for ^{15}N-labeled nitrate was determined in intact seminal roots of barley over a period of 6 weeks. Setting off from a stable level from day 18 to 39, nitrate uptake capacity steadily declined thereafter (Figure 3.5A). Interestingly, the timeline of this decline is in strong agreement with another study conducted in hydroponically-grown barley, in which water uptake capacity of seminal roots declined after 40 days of growth (Krassovsky, 1926). Similarly, seminal roots of maize were also reported to be active in the uptake and translocation of ^{33}P-labelled phosphate up to a plant age of 30-40 days (Fusseder, 1987). These findings corroborate the conclusion that the embryonic root system in cereals is functionally important only during the early stages of plant development (Hochholdinger et al., 2004). An early loss of physiological activity in seminal roots became also evident from taking morphological root parameters, as total seminal root length was arrested from day 39 on (Figure 3.2C). However, this morphological and physiological transition at day 39 in seminal roots did not correlate with a developmental transition in the shoot, which most evidently begins at flowering. In fact, at day 39 developing barley spikes were just in the double-ridge stage, which is still far before flowering time and thus far ahead of creating an assimilate sink (Figure 3.3). These observations indicated that seminal root senescence was uncoupled from the development of the shoot apical meristem and in particular from flowering time.

Root activity relies on assimilate delivery from the shoot, because sugar catabolism provides the energy required to energize nutrient uptake processes (Radin et al., 1978; Eveland and Jackson, 2011). In wheat, leaf pruning, which generally reduces sugar delivery to roots, reduced root growth but did not affect the progression of root cortical senescence (Lascaris and Deacon, 1991). A similar observation was made by pruning the canopy of grape plants, indicating that suppressed assimilation capacity in shoots did not affect the lifespan of roots, which was described by the time from root emergence to the onset of root browning (Comas et al., 2000). These experiments indicated that senescence processes in roots may not directly depend

on assimilate delivery from shoots. In the present study, root senescence processes were monitored in parallel with root sugar concentrations, which did not coincide at a temporal scale. In fact, a decrease of glucose and fructose concentrations was observed already at day 25, while roots were still elongating for another two weeks (Figure 3.2C, Figure 3.6). Thus, neither sugar delivery from shoots nor sugar levels in seminal roots can justify the decrease in nitrate uptake capacity or root elongation.

A major difficulty when comparing senescence processes between leaves and roots is that only in leaf senescence a plant age- and a tissue age-dependent component can be clearly distinguished. As shown by chlorophyll analysis in individual leaves of different developmental stages, chlorophyll degradation in the first true leaf of the main tiller started at day 25 and was completed already one week later (Figure 3.2A). In the second leaf, chlorophyll degradation began one week later and in the next leaf another week later. This pattern of progressing leaf senescence along the main tiller axis did not show a particular change at day 39 or shortly before. It is therefore unlikely that photo-assimilate supply from leaves or any other leaf-related signal triggered the senescence processes observed in roots around day 39. However, this conclusion does not exclude a participation of shoot-derived compounds or signals in the onset of senescence-related processes in roots, considering that shoot signals may require achieving a critical concentration or exceeding a certain threshold to trigger defined root responses. Elucidating this question in future experiments will require manipulation of leaf senescence processes under parallel examination of the roots.

4.3 Cortical senescence and its putative role in nutrient remobilization

In cereals, root cortical senescence has been widely described as an adaptation to anoxic conditions in the soil. In compacted or water-saturated soils with poor aeration, graminaceous plants, such as maize, often degrade cortical root cells to form aerenchyma, which conducts air from the above-ground atmosphere into the root tissue to improve root respiratory processes. This morphological adaptation has been frequently reported in lowland rice growing under water-logged conditions (Parreno-de Guzman and Zamora, 2008). Surprisingly, root cortical aerenchyma formation (RCA) can also go along with a decrease root respiration and in root P and N concentrations (Saengwilai et al., 2014; Schneider et al., 2017). Under drought conditions, maize lines with high RCA formation showed better growth and higher

yield than lines with low RCA formation (Chimungu et al., 2015). Root modeling indicated that RCA could support growth under P deficiency by 70% in maize and by 14% in bean, primarily by reducing the P content of root tissue, and secondarily by reducing root respiration (Postma and Lynch, 2010; Lynch, 2011).

While the above-stated hypothesis regards root cortical senescence as an adaptive process to environmental stress conditions to reduce metabolic costs for the sake of energy efficiency and root foraging, other data suggest that root cortical senescence is a programmed developmental process. Approaches using ^{33}P and autoradiography showed that the cortical P content in maize roots increased until day 30 followed by a drop by more than 50% until day 40, while the shoot ^{33}P content increased remarkably after day 30. These data indicated that ^{33}P might be remobilized from the root cortex to the shoot (Kraus et al., 1987). In a screening of hundreds of maize genotypes, cortical senescence occurred at a root age of 30 to 40 days (Zhu et al., 2010; Burton et al., 2013). Thus, it is likely that cortical senescence and P remobilization might be part of a coordinated biological event. Interestingly, P deficiency can lead to earlier root cortical senescence in wheat, maize and common bean, which indicates that P remobilization might even be a major physiological function of root cortical senescence (He et al., 1992; Elliott et al., 1993; Fan et al., 2003).

Similar to P, the majority of root Zn is bound as Zn phytate and deposited primarily in the vacuoles of cortical root cells (Van Steveninck et al., 1993; Palmgren et al., 2008). In soybean plants, the concentration of Zn in roots was approximately 22 times greater than that in the shoots, which indicates the presence of a large reserve of Zn in the root tissue (Van Steveninck et al., 1993). At flowering, the root Zn content of wheat dramatically dropped by a factor of 5, which implied that Zn was remobilized from the root to other tissues (Pearson and Rengel, 1994). The present data also displayed a strong decrease in the contents of both, P and Zn, at day 39, which temporally coincided with the initiation of cortical senescence (Figure 3.4, Figure 3.8). Therefore, it is likely that root cortical senescence was prerequisite for the remobilization of cortical P and Zn also in barley.

Phosphorus and Zn remobilization during organ senescence are still poorly understood at the molecular level, except for some P transporters that contribute to P remobilization. For instance, in Arabidopsis *Pht1;5* has been identified as a positive regulator for P remobilization from senescing leaves to developing organs, since

corresponding knockout lines resulted in reduced P allocation, and overexpression lines accumulated two-fold more P in siliques than wild-type plants (Nagarajan et al., 2011). An upregulation of P transporters during senescence in above-ground plant tissues has been described also in *Petunia corolla*, where approx. 74% of the P was remobilized during senescence. This coincided with the upregulation of *PhPT1*, a high-affinity phosphate transporter. By contrast, in the ethylene-insensitive line *etr1-1* only 34% of the P was remobilized, coinciding with a delayed upregulation of *PhPT1* and a delayed onset of senescence (Chapin and Jones, 2009). The expression of P transporters was also upregulated when senescence started in rice flag leaves (Jeong et al., 2016). In cell cultures of wild-type rice, a putative P transporter was strongly upregulated when cells underwent programmed cell death following infection by *Acidovorax avenae*. There was no significant change in the expression of this transporter when programmed cell death was reduced by knock-down of *OsNAC4*, a NAC-type TF that regulates programmed cell death (Kaneda et al., 2009). This transgenic approach in rice indicated that P transport and associated with P remobilization was initiated before programmed cell death set in. In hydroponically-grown rice roots, when low P stress induced the expression of oxidative stress-related and protein degradation-related genes in roots, P transporters were upregulated in parallel (Li et al., 2010). Evidence for a parallel increase in the expression of Zn transporters in aging roots is still lacking. In the present study, P and Zn transporters were mainly upregulated at or after day 39, which provides evidence that these mineral elements were either subject to *de-novo* uptake by roots or remobilized, as for most of these transporters it is not clear whether they confer a cellular import of export function. However, the significant decrease in P and Zn contents and concomitant increase in P and Zn transporter expression (Figure 3.8, Figure 3.33, Figure 3.34) set in when most senescence-related processes began. Moreover, the time point at day 39 coincided also with the beginning of cortical senescence (Figure 3.4). Taken together, this temporal coincidence supports the view that cortical senescence might be directly associated with P and Zn remobilization.

The view that root cortical senescence is an adaptive trait allowing to reduce metabolic costs is based on the temporal coincidence of RCA formation with a reduction of root respiration, of root P concentrations (Fan et al., 2003), and the formation of a deeper root system (Saengwilai et al., 2014). However, it remains

open whether this is associated with reduced metabolic costs for the sake of continued, deeper rooting. Generally, the nutrient uptake capacity declines when the root system or root tissue becomes old (Ernst et al., 1989; Baldi et al., 2010). Unfortunately, no reports could be found on the dynamics of nutrient uptake capacities with respect to the lifespan of the whole root system. In the present split-root system, the nitrate uptake capacity could be determined only for seminal roots and showed that nitrate uptake was kept at a stable level until day 39, before a sharp decline set in (Figure 3.5A). This drop of nitrate uptake capacity coincided with the beginning of root cortical senescence (Figure 3.4). This observation supports the notion that cortical senescence reduces rather than improves physiological root performance. Moreover, when cortical senescence set in at day 39, total seminal root length and root biomass became arrested (Figure 3.2C). This observation disagrees with the above-mentioned hypothesis that root cortical senescence promotes root elongation for soil exploration, which is based on a functional-structural modelling approach (Schneider et al., 2017). Moreover, even after cortical senescence had set in at day 39, any change in "metabolic costs" did not become apparent, since sugar concentrations remained unaffected (Figure 3.6). It is thus concluded that root cortical senescence represents a process allowing to improve the utilization of endogenous nutrient resources in the root. In support of this notion, Lynch and coworkers recently employed their simulation approach to propose that root cortical senescence may also serve for nutrient remobilization (Schneider et al., 2017).

4.4 Putative regulatory factors of root senescence

Multiple developmental and environmental signals modulate the onset and progression of leaf senescence (Lim et al., 2003). Dissecting the impact of individual genes being up- or downregulated during leaf senescence resulted in the identification of several transcription factors (TFs), especially from the NAC- and WRKY-type families, which represent major regulators of leaf senescence (Woo et al., 2013). The Arabidopsis gene *ORE1* is a NAC-type transcription factor acting as positive regulator of leaf senescence (Kim et al., 2009). Expression of *ORE1* is induced during leaf aging in an ethylene-dependent manner. *ORE1* controls the expression of at least 170 genes, of which 78 genes are known SAGs (Balazadeh et al., 2010). Overexpression of another NAC-type TF, *NAP* (*ANAC029*), triggers precocious senescence in young leaves, whereas the corresponding knockout line

exhibited retarded leaf senescence (Guo and Gan, 2006). *NAP* regulates leaf senescence partially through its direct binding to the promoter of *SAG113*, a negative regulator of the ABA pathway inhibiting stomatal closure, which in turn triggers leaf senescence (Zhang and Gan, 2012). Also the Arabidopsis *WRKY53* gene has a positive role in leaf senescence by targeting various SAGs, such as *WRKY30*, which has been suggested to be involved in ROS signaling (Miao et al., 2004; Scarpeci et al., 2013). Moreover, *WRKY22*, another downstream target of *WRKY53*, is a positive regulator of dark-induced leaf senescence (Zhou et al., 2011).

Very recently, a study demonstrated that overexpression of *OsNAC2* dramatically accelerated leaf senescence, whereas its knockdown lines showed delayed leaf senescence. The ectopic expression of *OsNAC2* lead to an increase in ABA levels by directly upregulating the expression of ABA biosynthetic genes (*OsNCED3* and *OsZEP1*) while downregulating ABA catabolism (*OsABA8ox1*) (Mao et al., 2017). *OsNAC2* is the closest rice orthologue of the barley gene *HvNAC003* (Christiansen et al., 2011). Interestingly, the expression of *HvNAC003* was significantly upregulated at day 32 by $\log_2$FC 2.35 or 2.91, in the ARZ or BRZ respectively, followed by elevated expression levels during seminal root senescence (Appendix 3). Considering the temporally confined ABA peak at day 39, it is hypothesized that *HvNAC003* functions as an inducer of ABA biosynthesis, like its orthologue *OsNAC2* does in rice. *TaNAC29*, a NAC-type TF with 92% identity to *HvNAC023*, provoked an ABA-hypersensitive response when overexpressed in Arabidopsis, which was indicative of the involvement of *TaNAC29* in the ABA signaling pathway (Huang et al., 2015). Interestingly, *HvNAC023* displayed also a sharp upregulation at day 32, which temporally appeared before the ABA peak at day 39 (Appendix 3). Hence, *HvNAC023* might be involved in the ABA signaling pathway, as it is the case with the orthologue *TaNAC29* in wheat. The rice ABI5-Like1 (*ABL1*) gene, a TF involved in the regulation of ABA-mediated gene expression, directly binds to the promoter region of *OsWRKY69* (LOC_Os08g29660) (Yang et al., 2011). Thereby, Os*ABL1* can mediate ABA-dependent stimulation of *OsWRKY69* through direct activation. Notably, *HvWRKY30*, the barley orthologue of *OsWRKY69* (Mangelsen et al., 2008), was also significantly upregulated just before the appearance of the ABA peak, which may indicate an involvement of *HvWRKY30* in ABA signaling (Appendix 3).

Besides NACs and WRKYs, also AP2-type TFs showed remarkably altered changes in gene expression levels over time (Appendix 3). The role of AP2-type TFs in

ethylene-related signaling pathways has been studied intensively in Arabidopsis, but due to sequence variation and poor annotation, most of the AP2 genes in barley are difficult to classify, not allowing further interpretation. Instead, the present transcriptome study revealed strong upregulation of a gene encoding an enzyme catalyzing the rate-limiting step of ethylene biosynthesis, namely ACC oxidase, during root senescence. Together with the massive upregulation of AP2-related genes this implies that ethylene might act as a positive regulator of root senescence (Figure 3.27, Appendix 3). These TFs and especially those altered before appearance of the major root senescence phenotypes, i.e. root browning and cortical senescence, may be promising candidates for the regulation of root senescence.

Abscisic acid is important in many aspects of plant development, such as the induction of seed dormancy or the synthesis of seed storage proteins and lipids (Nambara and Marion-Poll, 2005). In vegetative tissues, ABA mediates responses to drought or salt to prevent water loss by stomatal closure (Xiong and Zhu, 2003). Particularly during developmental leaf senescence, after chlorophyll breakdown has begun, a dramatic increase in endogenous ABA levels has been observed (Aharoni and Richmond, 1978; Zhang et al., 2012). In daylily, the RNA-AFLP profile in ABA-treated flowers was similar to that in naturally senescing petals (Panavas et al., 1999). Moreover, exogenous ABA treatment has been shown to accelerate leaf and flower senescence (Onoue et al., 2000; Lee et al., 2011). These and other studies have clearly shown that ABA is a major player in organ senescence. Also in the present study, ABA concentrations increased in barley leaves when chlorophyll concentrations declined, and ABA levels kept increasing until chlorophyll breakdown was complete (for example in leaf number 4; Appendix 5). Surprisingly, a continuous induction of ABA levels was not observed during root senescence, although expression levels of two *HvNCED* genes were strongly upregulated at day 32 (Figure 3.23, Figure 3.24, Figure 3.25). Instead, a sharp and temporally confined ABA peak was detected at day 39, which was preceded and followed by a continuously low ABA level (Figure 3.13). Compared with ABA, time-dependent profiles of other hormones were different in that auxin and CKs decreased when root senescence set in at day 39, while SA increased especially after day 39 (Figure 3.13). This exceptional, time-dependent profile of ABA levels in barley roots coincided with the onset of senescence-related processes, such as the initiation of root cortical

senescence or root browning or the decline of nitrate uptake capacity, and implied that ABA might trigger the initiation of a coordinated senescence program in roots.

Interestingly, ABA also induces hydrogen peroxide (H_2O_2) formation in leaves, which is a confirmed trigger of leaf senescence (Zimmermann and Zentgraf, 2005). In the present study, the ABA peak in roots at day 39 was closely followed by a massive increase in the expression of genes belonging to oxidation-reduction-related GO terms (Figure 3.16, Figure 3.17). Among these genes were catalase1 and catalase2 genes (Appendix 6). In addition, catalase activity, which is induced upon H_2O_2, increased from day 46 on (Figure 3.7). This temporal sequence of events, ABA peak with subsequent H_2O_2 formation and oxidative stress responses, implied that ABA might trigger senescence processes in roots via H_2O_2 induction.

As revealed by transcriptome and metabolite analysis, tryptophan decarboxylase (*TDC*) and its product serotonin were strongly enhanced during root senescence. Overexpressing tryptophan decarboxylase, the rate-limiting enzyme of serotonin synthesis, increased serotonin concentrations and delayed leaf senescence in rice leaves, while its knockdown provoked early senescence (Kang et al., 2009). In cassava, two tryptophan decarboxylase genes, *MeTDC1* and *MeTDC2*, were upregulated by H_2O_2 treatment, which pointed to a potential role of serotonin in ROS scavenging (Wei et al., 2016). Furthermore, pathogen attack is also associated with serotonin accumulation. The rice *SL* (Sekiguchi lesion) mutant, which is defective in serotonin production, displayed increased susceptibility to *Bipolaris oryzae* infection, while this phenotype could be rescued by exogenous serotonin application (Ishihara et al., 2008). Interestingly, serotonin also accumulated in trichomes of *Cnidoscolus texanus*, which was supposed to serve as defense against herbivores (Lookadoo and Pollard, 1991). A *glutamine synthetase1;1* knockout line in rice, which is defective in the conversion of ammonium to glutamine, retarded shoot growth and over-accumulated ammonium and serotonin in both, leaves and roots. It was thus speculated that activation of serotonin biosynthesis is part of the metabolic reprogramming, which allows to avoid ammonium toxicity (Kusano et al., 2011). Taken together, these above-mentioned studies showed that serotonin can act as a negative regulator in senescence-, cell death- or stress-related processes. In the present study, the expression of tryptophan decarboxylase in barley was almost linearly upregulated in ARZ before day 39, which fell together with the accumulation of serotonin (Table 3.2, Figure 3.37). This implied that serotonin might serve similar

functions in root senescence as it does in leaf senescence. However, the temporal pattern of serotonin accumulation and of the corresponding biosynthesis genes indicated that serotonin synthesis is not directly related to the formation of ABA.

The present work shows that the recorded biological processes in aging seminal roots of barley are likely part of a senescence program. In particular the transcriptome analysis indicated that the recorded degenerative processes were under the control of a considerable number of TFs especially from the NAC-, WRKY- and AP2-type TF families. These TFs were temporally upregulated just before root senescence phenotypes appeared (chapter 4.4). Indeed, many orthologs of these barley TFs have been identified as prominent regulators of leaf senescence in other species, supporting the idea that the degenerative processes monitored in aging seminal roots resemble those observed during leaf senescence. Regarding the age when roots start senscing, day 39 turned out as a transition point for most of the phenotypic and physiological changes, since cortical senescence, arrested root elongation, protein degradation, decline of nitrate uptake capacity, initiation of nutrient remobilization-related processes as well as the sharp ABA peak were collectively observed or altered at this time (chapter 3.1, 3.2). Day 39 was also a transition point in the regulation of global gene expression as GO terms describing "oxidation-reduction processes" and "responses to oxidative stress" became enriched (chapter 3.3.3). Together with the above-mentioned events this indicated the initiation of degenerative processes in seminal roots. From a simplified viewpoint, barley seminal root development can be divided into two distinct phases: the first phase lasts from root emergence to day 39 and can be assigned as growth phase, while the second phase after day 39 can be assigned as senescence phase.

References

Adams TS, Eissenstat DM (2015) On the controls of root lifespan: assessing the role of soluble phenolics. Plant and Soil, 392**:** 301-308

Aharoni N, Richmond AE (1978) Endogenous gibberellin and abscisic acid content as related to senescence of detached lettuce leaves. Plant Physiology, 62**:** 224-228

Ahkami AH, Lischewski S, Haensch KT, Porfirova S, Hofmann J, Rolletschek H, Melzer M, Franken P, Hause B, Druege U (2009) Molecular physiology of adventitious root formation in Petunia hybrida cuttings: involvement of wound response and primary metabolism. New Phytologist, 181**:** 613-625

Armstrong W (1980) Aeration in higher plants. Advances in botanical research, 7**:** 225-332

Asseng S, Ritchie JT, Smucker AJM, Robertson MJ (1998) Root growth and water uptake during water deficit and recovering in wheat. Plant and Soil, 201**:** 265-273

Badri DV, Vivanco JM (2009) Regulation and function of root exudates. Plant, Cell & Environment, 32**:** 666-681

Balazadeh S, Siddiqui H, Allu AD, Matallana-Ramirez LP, Caldana C, Mehrnia M, Zanor M-I, Köhler B, Mueller-Roeber B (2010) A gene regulatory network controlled by the NAC transcription factor ANAC092/AtNAC2/ORE1 during salt-promoted senescence. The Plant Journal, 62**:** 250-264

Balazadeh S, Wu A, Mueller-Roeber B (2010) Salt-triggered expression of the ANAC092-dependent senescence regulon in Arabidopsis thaliana. Plant signaling & behavior, 5**:** 733-735

Baldi E, Wells CE, Marangoni B (2010) Nitrogen absorption and respiration in white and brown peach roots. Journal of plant Nutrition, 33**:** 461-469

Barber SA (1979) Corn residue management and soil organic matter. Agronomy Journal, 71**:** 625-627

Bartsch N (1987) Responses of root systems of young Pinus sylvestris and Picea abies plants to water deficits and soil acidity. Canadian Journal of Forest Research, 17**:** 805-812

Beers EP (1997) Programmed cell death during plant growth and development. Cell Death & Differentiation, 4

Bhalerao R, Keskitalo J, Sterky F, Erlandsson R, Björkbacka H, Birve SJ, Karlsson J, Gardeström P, Gustafsson P, Lundeberg J (2003) Gene expression in autumn leaves. Plant Physiology, 131**:** 430-442

Bieker S, Riester L, Stahl M, Franzaring J, Zentgraf U (2012) Senescence-specific Alteration of Hydrogen Peroxide Levels in Arabidopsis thaliana and Oilseed Rape Spring Variety Brassica napus L. cv. MozartF. Journal of Integrative Plant Biology, 54**:** 540-554

Bingham IJ (2007) Quantifying the presence and absence of turgor for the spatial characterization of cortical senescence in roots of Triticum aestivum (Poaceae). American journal of botany, 94**:** 2054-2058

Bohner A, Kojima S, Hajirezaei M, Melzer M, von Wirén N (2015) Urea retranslocation from senescing Arabidopsis leaves is promoted by DUR3-mediated urea retrieval from leaf apoplast. The Plant Journal, 84: 377-387

Bohner A, Kojima S, Hajirezaei M, Melzer M, Wirén N (2015) Urea retranslocation from senescing Arabidopsis leaves is promoted by DUR3-mediated urea retrieval from leaf apoplast. The Plant Journal, 81**:** 377-387

Bouma TJ, Yanai RD, Elkin AD, Hartmond U, Flores-Alva DE, Eissenstat DM (2001) Estimating age-dependent costs and benefits of roots with contrasting life span: comparing apples and oranges. New Phytologist, 150**:** 685-695

Bouranis D, Chorianopoulou S, Siyiannis V, Protonotarios V, Hawkesford M (2003) Aerenchyma formation in roots of maize during sulphate starvation. Planta, 217**:** 382-391

Brevedan RE, Egli DB (2003) Short Periods of Water Stress during Seed Filling, Leaf Senescence, and Yield of Soybean Published with the approval of the Director of the Kentucky Agric. Exp. Stn. as paper No. 03-06-001. Crop Science, 43: 2083-2088

Buchanan-Wollaston V, Page T, Harrison E, Breeze E, Lim PO, Nam HG, Lin JF, Wu SH, Swidzinski J, Ishizaki K (2005) Comparative transcriptome analysis reveals significant differences in gene expression and signalling pathways between developmental and dark/starvation-induced senescence in Arabidopsis. The Plant Journal, 42: 567-585

Burton AL, Lynch JP, Brown KM (2013) Spatial distribution and phenotypic variation in root cortical aerenchyma of maize (Zea mays L.). Plant and soil, 367**:** 263-274

Byeon Y, Park S, Lee HY, Kim YS, Back K (2014) Elevated production of melatonin in transgenic rice seeds expressing rice tryptophan decarboxylase. Journal of pineal research, 56**:** 275-282

Can S, Amasino RM (1997) Making sense of senescence. Plant Physiol, 113**:** 313-319

Cao J, Murch SJ, O'Brien R, Saxena PK (2006) Rapid method for accurate analysis of melatonin, serotonin and auxin in plant samples using liquid chromatography–tandem mass spectrometry. Journal of Chromatography A, 1134**:** 333-337

Chapin LJ, Jones ML (2009) Ethylene regulates phosphorus remobilization and expression of a phosphate transporter (PhPT1) during petunia corolla senescence. Journal of Experimental Botany, 60: 2179-2190

Cheng S, Cao L, Chen S, Zhu D, Wang X, Min S, Zhai H (2004) Conception of late--stage vigor super hybrid rice and its biological significance. Zhongguo shuidao kexue, 19**:** 280-284

Chimungu JG, Maliro MFA, Nalivata PC, Kanyama-Phiri G, Brown KM, Lynch JP (2015) Utility of root cortical aerenchyma under water limited conditions in tropical maize (Zea mays L.). Field Crops Research, 171**:** 86-98

Christiansen MW, Holm PB, Gregersen PL (2011) Characterization of barley (Hordeum vulgare L.) NAC transcription factors suggests conserved functions compared to both monocots and dicots. BMC Research Notes, 4**:** 302

Christiansen MW, Holm PB, Gregersen PL (2011) Characterization of barley (Hordeum vulgare L.) NAC transcription factors suggests conserved functions compared to both monocots and dicots. BMC Research Notes, 4**:** 1-13

Christiansen MW, Holm PB, Gregersen PL (2011) Characterization of barley (Hordeum vulgare L.) NAC transcription factors suggests conserved functions compared to both monocots and dicots. BMC Research Notes, 4**:** 1

Christiansen MW, Matthewman C, Podzimska-Sroka D, O'Shea C, Lindemose S, Møllegaard NE, Holme IB, Hebelstrup K, Skriver K, Gregersen PL (2016) Barley plants over-expressing the NAC transcription factor gene HvNAC005 show stunting and delay in development combined with early senescence. Journal of Experimental Botany, 67**:** 5259-5273

Coll NS, Vercammen D, Smidler A, Clover C, Van Breusegem F, Dangl JL, Epple P (2010) <div xmlns="http://www.w3.org/1999/xhtml">Arabidopsis Type I Metacaspases Control Cell Death</div>. Science, 330**:** 1393-1397

Comas LH, Anderson L, Dunst R, Lakso A, Eissenstat D (2005) Canopy and environmental control of root dynamics in a long-term study of Concord grape. New Phytologist, 167**:** 829-840

Comas LH, Eissenstat DM, Lakso AN (2000) Assessing root death and root system dynamics in a study of grape canopy pruning. New Phytologist, 147**:** 171-178

Cornish K, Zeevaart JAD (1985) Abscisic Acid Accumulation by Roots of Xanthium strumarium L. and Lycopersicon esculentum Mill. in Relation to Water Stress. Plant Physiology, 79**:** 653-658

Crafts-Brandner SJ, Egli DB (1987) Sink Removal and Leaf Senescence in Soybean: Cultivar Effects. Plant Physiology, 85**:** 662-666

Deacon J, Mitchell R (1985) Comparison of rates of natural senescence of the root cortex of wheat (with and without mildew infection), barley, oats and rye. Plant and Soil, 84**:** 129-131

Dela Fuente R, Leopold A (1968) Senescence processes in leaf abscission. Plant physiology, 43**:** 1496

Delorme VGR, McCabe PF, Kim D-J, Leaver CJ (2000) A Matrix Metalloproteinase Gene Is Expressed at the Boundary of Senescence and Programmed Cell Death in Cucumber. Plant Physiology, 123**:** 917-928

Demel RA, De Kruyff B (1976) The function of sterols in membranes. Biochimica et Biophysica Acta (BBA)-Reviews on Biomembranes, 457**:** 109-132

Díaz-Mendoza M, Velasco-Arroyo B, González-Melendi P, Martínez M, Díaz I (2014) C1A cysteine protease–cystatin interactions in leaf senescence. Journal of Experimental Botany, 65**:** 3825-3833

Djanaguiraman M, Annie Sheeba J, Durga Devi D, Bangarusamy U (2009) Cotton leaf senescence can be delayed by nitrophenolate spray through enhanced antioxidant defence system. Journal of Agronomy and Crop Science, 195**:** 213-224

Drew MC, He C-J, Morgan PW (1989) Decreased ethylene biosynthesis, and induction of aerenchyma, by nitrogen-or phosphate-starvation in adventitious roots of Zea mays L. Plant Physiology, 91**:** 266-271

Dun EA, Brewer PB, Beveridge CA (2009) Strigolactones: discovery of the elusive shoot branching hormone. Trends in plant science, 14**:** 364-372

Eason J, Ryan D, Watson L, Hedderley D, Christey M, Braun R, Coupe S (2005) Suppression of the cysteine protease, aleurain, delays floret senescence in Brassica oleracea. Plant molecular biology, 57**:** 645-657

Egli DB, Leggett JE, Duncan WG (1978) Influence of N Stress on Leaf Senescence and N Redistribution in Soybeans1. Agronomy Journal, 70**:** 43-47

Elliott G, Robson A, Abbott L (1993) Effects of phosphate and nitrogen application on death of the root cortex in spring wheat. New phytologist, 123**:** 375-382

Ernst M, Römheld V, Marschner H (1989) Estimation of phosphorus uptake capacity by different zones of the primary root of soil-grown maize (Zea mays L.). Journal of Plant Nutrition and Soil Science, 152**:** 21-25

Eshel A, Beeckman T (2013) Plant roots: the hidden half. CRC Press

Eveland AL, Jackson DP (2011) Sugars, signalling, and plant development. Journal of Experimental Botany,

Fan M, Zhu J, Richards C, Brown KM, Lynch JP (2003) Physiological roles for aerenchyma in phosphorus-stressed roots. Functional Plant Biology, 30**:** 493-506

Fischer AM, Gan S (2007) Nutrient remobilization during leaf senescence. Senescence processes in plants, 26**:** 87-107

Fusseder A (1987) The longevity and activity of the primary root of maize. Plant and Soil, 101**:** 257-265

Galau GA, Hughes DW, Dure L (1986) Abscisic acid induction of cloned cotton late embryogenesis-abundant (Lea) mRNAs. Plant molecular biology, 7**:** 155-170

Gan S (2008) Annual Plant Reviews, Senescence Processes in Plants, Vol 26. John Wiley & Sons

Gan S, Amasino RM (1995) Inhibition of leaf senescence by autoregulated production of cytokinin. Science, 270**:** 1986-1988

Gan S, Amasino RM (1995) Inhibition of leaf senescence by autoregulated production of cytokinin. Science, 270**:** 1986

Gepstein S, Sabehi G, Carp M-J, Haigui T, Nesher MFO, Yariv I, Dor C, Bassani M (2003) Large-scale identification of leaf senescence-associated genes. The Plant Journal, 36**:** 629-642

Gerbner G, Gross L, Signorielli N, Morgan M (1980) Aging with Television: Images on Television Drama and Conceptions of Social Reality. Journal of Communication, 30**:** 37-47

Gill RA, Jackson RB (2000) Global patterns of root turnover for terrestrial ecosystems. New phytologist, 147**:** 13-31

Grbić V, Bleecker AB (1995) Ethylene regulates the timing of leaf senescence in Arabidopsis. The Plant Journal, 8**:** 595-602

Gregory PJ, McGowan M, Biscoe PV, Hunter B (1978) Water relations of winter wheat: 1. Growth of the root system. The Journal of Agricultural Science, 91**:** 91-102

Guiboileau A, Sormani R, Meyer C, Masclaux-Daubresse C (2010) Senescence and death of plant organs: nutrient recycling and developmental regulation. Comptes rendus biologies, 333**:** 382-391

Guilbaud CS, Dalchau N, Purves DW, Turnbull LA (2015) Is 'peak N'key to understanding the timing of flowering in annual plants? New Phytologist, 205**:** 918-927

Guo F-Q, Crawford NM (2005) Arabidopsis Nitric Oxide Synthase1 Is Targeted to Mitochondria and Protects against Oxidative Damage and Dark-Induced Senescence. The Plant Cell, 17**:** 3436-3450

Guo Y, Cai Z, Gan S (2004) Transcriptome of Arabidopsis leaf senescence. Plant, cell & environment, 27**:** 521-549

Guo Y, Gan S (2006) AtNAP, a NAC family transcription factor, has an important role in leaf senescence. The Plant Journal, 46**:** 601-612

Gupta N, Gupta S, Kumar A (2000) Exogenous cytokinin application increases cell membrane and chlorophyll stability in wheat (Triticum aestivum L.). Cereal Research Communications**:** 287-291

Gutjahr C, Sawers RJ, Marti G, Andrés-Hernández L, Yang S-Y, Casieri L, Angliker H, Oakeley EJ, Wolfender J-L, Abreu-Goodger C (2015) Transcriptome diversity among rice root types during asymbiosis and interaction with arbuscular mycorrhizal fungi. Proceedings of the National Academy of Sciences, 112**:** 6754-6759

Hajirezaei MR, Takahata Y, Trethewey RN, Willmitzer L, Sonnewald U (2000) Impact of elevated cytosolic and apoplastic invertase activity on carbon metabolism during potato tuber development. Journal of Experimental Botany, 51**:** 439-445

Hanaoka H, Noda T, Shirano Y, Kato T, Hayashi H, Shibata D, Tabata S, Ohsumi Y (2002) Leaf Senescence and Starvation-Induced Chlorosis Are Accelerated by the Disruption of an Arabidopsis Autophagy Gene. Plant Physiology, 129**:** 1181-1193

He C-J, Morgan PW, Drew MC (1992) Enhanced Sensitivity to Ethylene in Nitrogen- or Phosphate-Starved Roots of Zea mays L. during Aerenchyma Formation. Plant Physiology, 98**:** 137-142

He CJ, Morgan PW, Drew MC (1996) Transduction of an Ethylene Signal Is Required for Cell Death and Lysis in the Root Cortex of Maize during Aerenchyma Formation Induced by Hypoxia. Plant Physiology, 112**:** 463-472

Heeraman D, Crown P, Juma N (1993) A color composite technique for detecting root dynamics of barley (Hordeum vulgare L.) from minirhizotron images. Plant and Soil, 157**:** 275-287

Heeraman DA, Crown PH, Juma NG (1993) A color composite technique for detecting root dynamics of barley (Hordeum vulgare L.) from minirhizotron images. Plant and Soil, 157**:** 275-287

Heyl A, Werner T, Schmülling T (2006) Cytokinin metabolism and signal transduction. Plant hormone signaling**:** 93-123

Himelblau E, Amasino RM (2001) Nutrients mobilized from leaves of Arabidopsis thaliana during leaf senescence. Journal of Plant Physiology, 158**:** 1317-1323

Hishi T, Takeda H (2005) Life cycles of individual roots in fine root system of Chamaecyparis obtusa Sieb. et Zucc. Journal of Forest Research, 10**:** 181-187

Ho C-L, Tan Y-C, Yeoh K-A, Ghazali A-K, Yee W-Y, Hoh C-C (2016) De novo transcriptome analyses of host-fungal interactions in oil palm (Elaeis guineensis Jacq.). BMC genomics, 17**:** 66

Hochholdinger F, Park WJ, Sauer M, Woll K (2004) From weeds to crops: genetic analysis of root development in cereals. Trends in Plant Science, 9**:** 42-48

Hochholdinger F, Tuberosa R (2009) Genetic and genomic dissection of maize root development and architecture. Current opinion in plant biology, 12**:** 172-177

Hochholdinger F, Woll K, Sauer M, Dembinsky D (2004) Genetic dissection of root formation in maize (Zea mays) reveals root-type specific developmental programmes. Annals of Botany, 93**:** 359-368

Hochholdinger F, Zimmermann R (2008) Conserved and diverse mechanisms in root development. Current opinion in plant biology, 11**:** 70-74

Holden J (1975) Use of nuclear staining to assess rates of cell death in cortices of cereal roots. Soil Biology and Biochemistry, 7**:** 333-334

Hörtensteiner S (2009) Stay-green regulates chlorophyll and chlorophyll-binding protein degradation during senescence. Trends in Plant Science, 14**:** 155-162

Huang Q, Wang Y, Li B, Chang J, Chen M, Li K, Yang G, He G (2015) TaNAC29, a NAC transcription factor from wheat, enhances salt and drought tolerance in transgenic Arabidopsis. BMC Plant Biology, 15**:** 268

Ishihara A, Hashimoto Y, Tanaka C, Dubouzet JG, Nakao T, Matsuda F, Nishioka T, Miyagawa H, Wakasa K (2008) The tryptophan pathway is involved in the defense responses of rice against pathogenic infection via serotonin production. The Plant Journal, 54**:** 481-495

Jackson VG (1922) Anatomical structure of the roots of barley. Annals of Botany**:** 21-40

Jeong K, Baten A, Waters DLE, Pantoja O, Julia CC, Wissuwa M, Heuer S, Kretzschmar T, Rose TJ (2016) Phosphorus remobilization from rice flag leaves during grain filling: an RNA-seq study. Plant Biotechnology Journal**:** n/a-n/a

Jing HC, Sturre MJ, Hille J, Dijkwel PP (2002) Arabidopsis onset of leaf death mutants identify a regulatory pathway controlling leaf senescence. The Plant Journal, 32**:** 51-63

Justin S, Armstrong W (1991) Evidence for the involvement of ethene in aerenchyma formation in adventitious roots of rice (Oryza sativa L.). New Phytologist, 118**:** 49-62

Kaneda T, Taga Y, Takai R, Iwano M, Matsui H, Takayama S, Isogai A, Che FS (2009) The transcription factor OsNAC4 is a key positive regulator of plant hypersensitive cell death. The EMBO Journal, 28**:** 926-936

Kang K, Kim Y-S, Park S, Back K (2009) Senescence-Induced Serotonin Biosynthesis and Its Role in Delaying Senescence in Rice Leaves. Plant Physiology, 150**:** 1380-1393

Kanjanaphachoat P, Wei B-Y, Lo S-F, Wang I-W, Wang C-S, Yu S-M, Yen M-L, Chiu S-H, Lai C-C, Chen L-J (2012) Serotonin accumulation in transgenic rice by over-expressing tryptophan decarboxlyase results in a dark brown phenotype and stunted growth. Plant Molecular Biology, 78**:** 525-543

Kato Y, Okami M (2010) Root growth dynamics and stomatal behaviour of rice (Oryza sativa L.) grown under aerobic and flooded conditions. Field Crops Research, 117**:** 9-17

Kermode AR (2011) Seed dormancy: methods and protocols. Humana Press

Kim JH, Woo HR, Kim J, Lim PO, Lee IC, Choi SH, Hwang D, Nam HG (2009) <div xmlns="http://www.w3.org/1999/xhtml">Trifurcate Feed-Forward Regulation of Age-Dependent Cell Death Involving miR164 in Arabidopsis</div>. Science, 323**:** 1053-1057

Kim JH, Woo HR, Kim J, Lim PO, Lee IC, Choi SH, Hwang D, Nam HG (2009) Trifurcate feed-forward regulation of age-dependent cell death involving miR164 in Arabidopsis. Science, 323**:** 1053-1057

Kim JI, Murphy AS, Baek D, Lee S-W, Yun D-J, Bressan RA, Narasimhan ML (2011) YUCCA6 over-expression demonstrates auxin function in delaying leaf senescence in Arabidopsis thaliana. Journal of Experimental Botany, 62**:** 3981-3992

KIRK J, Deacon J (1986) EARLY SENESCENCE OF THE ROOT CORTEX OF AGRICULTURAL GRASSES, AND OF WHEAT FOLLOWING ROOT AMPUTATION OR INFECTION BY THE TAKE-ALL FUNGUS. New phytologist, 104**:** 63-75

Knipfer T, Besse M, Verdeil J-L, Fricke W (2011) Aquaporin-facilitated water uptake in barley (Hordeum vulgare L.) roots. Journal of Experimental Botany, 62**:** 4115-4126

Kobayashi Y, Murata M, Minami H, Yamamoto S, Kagaya Y, Hobo T, Yamamoto A, Hattori T (2005) Abscisic acid-activated SNRK2 protein kinases function in the gene regulation pathway of ABA signal transduction by phosphorylating ABA response element-binding factors. The Plant Journal, 44**:** 939-949

Kojima M, Kamada-Nobusada T, Komatsu H, Takei K, Kuroha T, Mizutani M, Ashikari M, Ueguchi-Tanaka M, Matsuoka M, Suzuki K (2009) Highly sensitive and high-throughput analysis of plant hormones using MS-probe modification and liquid chromatography–tandem mass spectrometry: an application for hormone profiling in Oryza sativa. Plant and Cell Physiology, 50**:** 1201-1214

Kojima S, Bohner A, von Wirén N (2006) Molecular Mechanisms of Urea Transport in Plants. The Journal of Membrane Biology, 212**:** 83-91

Kokáš F, Vojta P, Galuszka P (2016) Dataset for transcriptional response of barley (Hordeum vulgare) exposed to drought and subsequent re-watering. Data in brief, 8**:** 334-341

Kokubun N, Ishida H, Makino A, Mae T (2002) The degradation of the large subunit of ribulose-1, 5-bisphosphate carboxylase/oxygenase into the 44-kDa fragment in the lysates of chloroplasts incubated in darkness. Plant and cell physiology, 43**:** 1390-1395

Konôpka B, Noguchi K, Sakata T, Takahashi M, Konôpková Z (2006) Fine root dynamics in a Japanese cedar (Cryptomeria japonica) plantation throughout the growing season. Forest Ecology and Management, 225**:** 278-286

Krassovsky I (1926) Physiological activity of the seminal and nodal roots of crop plants. Soil Science, 21**:** 307

Kraus M, Fusseder A, Beck E (1987) Development and replenishment of the P-depletion zone around the primary root of maize during the vegetation period. Plant and soil, 101**:** 247-255

Kusano M, Tabuchi M, Fukushima A, Funayama K, Diaz C, Kobayashi M, Hayashi N, Tsuchiya YN, Takahashi H, Kamata A, Yamaya T, Saito K (2011) Metabolomics data reveal a crucial role of cytosolic glutamine synthetase 1;1 in coordinating metabolic balance in rice. The Plant Journal, 66**:** 456-466

Lachno DR, Baker DA (1986) Stress induction of abscisic acid in maize roots. Physiologia Plantarum, 68**:** 215-221

Lal R (2004) Soil carbon sequestration impacts on global climate change and food security. science, 304**:** 1623-1627

Lascaris D, Deacon J (1991) Relationship between root cortical senescence and growth of wheat as influenced by mineral nutrition, Idriella bolleyi (Sprague) von Arx and pruning of leaves. New phytologist, 118**:** 391-396

Lavenus J, Goh T, Roberts I, Guyomarc'h S, Lucas M, De Smet I, Fukaki H, Beeckman T, Bennett M, Laplaze L (2013) Lateral root development in Arabidopsis: fifty shades of auxin. Trends in Plant Science, 18**:** 450-458

Lee IC, Hong SW, Whang SS, Lim PO, Nam HG, Koo JC (2011) Age-Dependent Action of an ABA-Inducible Receptor Kinase, RPK1, as a Positive Regulator of Senescence in Arabidopsis Leaves. Plant and Cell Physiology, 52**:** 651-662

Lee S, Seo PJ, Lee HJ, Park CM (2012) A NAC transcription factor NTL4 promotes reactive oxygen species production during drought-induced leaf senescence in Arabidopsis. The Plant Journal, 70**:** 831-844

Lefebvre V, North H, Frey A, Sotta B, Seo M, Okamoto M, Nambara E, Marion-Poll A (2006) Functional analysis of Arabidopsis NCED6 and NCED9 genes indicates that ABA synthesized in the endosperm is involved in the induction of seed dormancy. The Plant Journal, 45**:** 309-319

Letham D (1994) Cytokinins as phytohormones-sites of biosynthesis, translocation and function of translocated cytokinin. Cytokinins: chemistry, activity and function**:** 57-80

Li L, Liu C, Lian X (2010) Gene expression profiles in rice roots under low phosphorus stress. Plant Molecular Biology, 72**:** 423-432

Li Z, Peng J, Wen X, Guo H (2013) Ethylene-insensitive3 is a senescence-associated gene that accelerates age-dependent leaf senescence by directly repressing miR164 transcription in Arabidopsis. The Plant Cell, 25**:** 3311-3328

Liedgens M, Soldati A, Stamp P, Richner W (2000) Root Development of Maize (L.) as Observed with Minirhizotrons in Lysimeters. Crop Science, 40**:** 1665-1672

Liljeroth E (1995) Comparisons of early root cortical senescence between barley cultivars, Triticum species and other cereals. New Phytologist, 130**:** 495-501

Lim PO, Kim HJ, Gil Nam H (2007) Leaf senescence. Annu. Rev. Plant Biol., 58**:** 115-136

Lim PO, Woo HR, Nam HG (2003) Molecular genetics of leaf senescence in Arabidopsis. Trends in Plant Science, 8**:** 272-278

Lookadoo SE, Pollard AJ (1991) Chemical contents of stinging trichomes ofCnidoscolus texanus. Journal of Chemical Ecology, 17**:** 1909-1916

Lynch JP (2007) Roots of the second green revolution. Australian Journal of Botany, 55**:** 493-512

Lynch JP (2011) Root Phenes for Enhanced Soil Exploration and Phosphorus Acquisition: Tools for Future Crops. Plant Physiology, 156**:** 1041-1049

Lynch JP (2013) Steep, cheap and deep: an ideotype to optimize water and N acquisition by maize root systems. Annals of botany, 112**:** 347-357

Mangelsen E, Kilian J, Berendzen KW, Kolukisaoglu ÜH, Harter K, Jansson C, Wanke D (2008) Phylogenetic and comparative gene expression analysis of barley (Hordeum vulgare) WRKY transcription factor family reveals putatively retained functions between monocots and dicots. BMC genomics, 9**:** 194

Mao C, Lu S, Lv B, Zhang B, Shen J, He J, Luo L, Xi D, Chen X, Ming F (2017) A Rice NAC Transcription Factor Promotes Leaf Senescence via ABA Biosynthesis. Plant Physiology,

Marschner H (2011) Marschner's mineral nutrition of higher plants. Academic press

Martínez DE, Bartoli CG, Grbic V, Guiamet JJ (2007) Vacuolar cysteine proteases of wheat (Triticum aestivum L.) are common to leaf senescence induced by different factors. Journal of Experimental Botany, 58**:** 1099-1107

McKenzie BE, Peterson CA (1995) Root Browning in Pinus banksiana Lamb. and Eucalyptus pilularis Sm. 1. Anatomy and Permeability of the White and Tannin Zones. Botanica Acta, 108**:** 127-137

Merrill S, Black A, Bauer A (1996) Conservation tillage affects root growth of dryland spring wheat under drought. Soil science society of America journal, 60**:** 575-583

Mhamdi A, Queval G, Chaouch S, Vanderauwera S, Van Breusegem F, Noctor G (2010) Catalase function in plants: a focus on Arabidopsis mutants as stress-mimic models. Journal of Experimental Botany,

Miao Y, Laun T, Zimmermann P, Zentgraf U (2004) Targets of the WRKY53 transcription factor and its role during leaf senescence in Arabidopsis. Plant Molecular Biology, 55**:** 853-867

Millar AA, Smith MA, Kunst L (2000) All fatty acids are not equal: discrimination in plant membrane lipids. Trends in Plant Science, 5**:** 95-101

Morita MT (2010) Directional gravity sensing in gravitropism. Annual review of plant biology, 61**:** 705-720

Morris K, Mackerness SAH, Page T, John CF, Murphy AM, Carr JP, Buchanan-Wollaston V (2000) Salicylic acid has a role in regulating gene expression during leaf senescence. The Plant Journal, 23**:** 677-685

Morris K, Mackerness SAH, Page T, John CF, Murphy AM, Carr JP, Buchanan-Wollaston V (2000) Salicylic acid has a role in regulating gene expression during leaf senescence. The Plant Journal, 23**:** 677-685

Mrízová K, Jiskrová E, Vyroubalová Š, Novák O, Ohnoutková L, Pospíšilová H, Frébort I, Harwood WA, Galuszka P (2013) Overexpression of Cytokinin Dehydrogenase Genes in Barley (Hordeum vulgare cv. Golden Promise) Fundamentally Affects Morphology and Fertility. PLOS ONE, 8**:** e79029

Munné-Bosch S, Jubany-Marí T, Alegre L (2001) Drought-induced senescence is characterized by a loss of antioxidant defences in chloroplasts. Plant, Cell & Environment, 24**:** 1319-1327

Nagarajan VK, Jain A, Poling MD, Lewis AJ, Raghothama KG, Smith AP (2011) Arabidopsis Pht1;5 Mobilizes Phosphate between Source and Sink Organs and Influences the Interaction between Phosphate Homeostasis and Ethylene Signaling. Plant Physiology, 156**:** 1149-1163

Nambara E, Marion-Poll A (2005) Abscisic acid biosynthesis and catabolism. Annu. Rev. Plant Biol., 56**:** 165-185

Noh Y-S, Amasino RM (1999) Identification of a promoter region responsible for the senescence-specific expression of SAG12. Plant Molecular Biology, 41**:** 181-194

Noh Y-S, Amasino RM (1999) Regulation of developmental senescence is conserved between Arabidopsis and Brassica napus. Plant Molecular Biology, 41**:** 195-206

Nooden L, Kahanak G, Okatan Y (1979) Prevention of monocarpic senescence in soybeans with auxin and cytokinin: an antidote for self-destruction. Science, 206**:** 841-843

Noodén LD, Guiamét JJ, John I (1997) Senescence mechanisms. Physiologia Plantarum, 101**:** 746-753

Noodén LD, Singh S, Letham DS (1990) Correlation of xylem sap cytokinin levels with monocarpic senescence in soybean. Plant Physiology, 93**:** 33-39

Oh SA, Park JH, Lee GI, Paek KH, Park SK, Nam HG (1997) Identification of three genetic loci controlling leaf senescence in Arabidopsis thaliana. The Plant Journal, 12**:** 527-535

Okumura N, Nishizawa N-K, Umehara Y, Ohata T, Nakanishi H, Yamaguchi T, Chino M, Mori S (1994) A dioxygenase gene (Ids2) expressed under iron deficiency conditions in the roots of Hordeum vulgare. Plant Molecular Biology, 25**:** 705-719

Onoue T, Mikami M, Yoshioka T, Hashiba T, Satoh S (2000) Characteristics of the inhibitory action of 1, 1-dimethyl-4-(phenylsulfonyl) semicarbazide (DPSS) on ethylene production in carnation (Dianthus caryophyllus L.) flowers. Plant Growth Regulation, 30**:** 201-207

Ori N, Juarez MT, Jackson D, Yamaguchi J, Banowetz GM, Hake S (1999) Leaf senescence is delayed in tobacco plants expressing the maize homeobox gene knotted1 under the control of a senescence-activated promoter. The Plant Cell, 11**:** 1073-1080

Orlando Filho J (1985) Potassium nutrition of sugarcane. Potassium in Agriculture: 1045-1062

Otegui MS, Noh YS, Martinez DE, Vila Petroff MG, Andrew Staehelin L, Amasino RM, Guiamet JJ (2005) Senescence-associated vacuoles with intense proteolytic activity develop in leaves of Arabidopsis and soybean. The Plant Journal, 41**:** 831-844

Palmgren MG, Clemens S, Williams LE, Krämer U, Borg S, Schjørring JK, Sanders D (2008) Zinc biofortification of cereals: problems and solutions. Trends in Plant Science, 13**:** 464-473

Panavas T, Pikula A, Reid PD, Rubinstein B, Walker EL (1999) Identification of senescence-associated genes from daylily petals. Plant Molecular Biology, 40**:** 237-248

Parreno-de Guzman LE, Zamora OB (2008) Formation of root air spaces (aerenchyma) and root growth of lowland rice (Oryza sativa L.) varieties under different water regimes. Asia Life Sci, 17**:** 309-323

Parrott DL, Martin JM, Fischer AM (2010) Analysis of barley (Hordeum vulgare) leaf senescence and protease gene expression: a family C1A cysteine protease is specifically induced under conditions characterized by high carbohydrate, but low to moderate nitrogen levels. New Phytologist, 187**:** 313-331

Pearson JN, Rengel Z (1994) Distribution and remobilization of Zn and Mn during grain development in wheat. Journal of Experimental Botany, 45**:** 1829-1835

Pegadaraju V, Knepper C, Reese J, Shah J (2005) Premature Leaf Senescence Modulated by the Arabidopsis PHYTOALEXIN DEFICIENT4 Gene Is Associated with Defense against the Phloem-Feeding Green Peach Aphid. Plant Physiology, 139**:** 1927-1934

Pérez J, Munoz-Dorado J, de la Rubia T, Martinez J (2002) Biodegradation and biological treatments of cellulose, hemicellulose and lignin: an overview. International Microbiology, 5**:** 53-63

Pietola L, Alakukku L (2005) Root growth dynamics and biomass input by Nordic annual field crops. Agriculture, Ecosystems & Environment, 108: 135-144

Pietola LM (2005) Root growth dynamics of spring cereals with discontinuation of mouldboard ploughing. Soil and Tillage Research, 80**:** 103-114

Poole P (2017) Shining a light on the dark world of plant root–microbe interactions. Proceedings of the National Academy of Sciences, 114**:** 4281-4283

Porra R, Thompson W, Kriedemann P (1989) Determination of accurate extinction coefficients and simultaneous equations for assaying chlorophylls a and b extracted with four different solvents: verification of the concentration of chlorophyll standards by atomic absorption spectroscopy. Biochimica et Biophysica Acta (BBA)-Bioenergetics, 975**:** 384-394

Postma JA, Lynch JP (2010) Theoretical evidence for the functional benefit of root cortical aerenchyma in soils with low phosphorus availability. Annals of Botany**:** mcq199

Radin JW, Parker LL, Sell CR (1978) Partitioning of Sugar between Growth and Nitrate Reduction in Cotton Roots. Plant Physiology, 62: 550-553

Rahman H, Sabreen S, Alam S, Kawai S (2005) Effects of nickel on growth and composition of metal micronutrients in barley plants grown in nutrient solution. Journal of Plant Nutrition, 28**:** 393-404

Reape TJ, Molony EM, McCabe PF (2008) Programmed cell death in plants: distinguishing between different modes. Journal of experimental botany, 59**:** 435-444

Reuter D (1997) Plant analysis: an interpretation manual. CSIRO publishing

Richmond AE, Lang A (1957) Effect of kinetin on protein content and survival of detached Xanthium leaves. Science, 125**:** 650-651

Rivero RM, Kojima M, Gepstein A, Sakakibara H, Mittler R, Gepstein S, Blumwald E (2007) Delayed leaf senescence induces extreme drought tolerance in a flowering plant. Proceedings of the National Academy of Sciences, 104: 19631-19636

Robatzek S, Somssich IE (2001) A new member of the Arabidopsis WRKY transcription factor family, AtWRKY6, is associated with both senescence-and defence-related processes. The Plant Journal, 28: 123-133

Rogers W (1940) Root studies VIII. Apple root growth in relation to rootstock, soil, seasonal and climatic factors. Journal of Pomology and Horticultural Science, 17**:** 99-130

Saengwilai P, Nord EA, Chimungu JG, Brown KM, Lynch JP (2014) Root Cortical Aerenchyma Enhances Nitrogen Acquisition from Low-Nitrogen Soils in Maize. Plant Physiology, 166**:** 726-735

Sakamoto T, Kobayashi M, Itoh H, Tagiri A, Kayano T, Tanaka H, Iwahori S, Matsuoka M (2001) Expression of a Gibberellin 2-Oxidase Gene around the Shoot Apex Is Related to Phase Transition in Rice. Plant Physiology, 125**:** 1508-1516

Scarpeci TE, Zanor MI, Mueller-Roeber B, Valle EM (2013) Overexpression of AtWRKY30 enhances abiotic stress tolerance during early growth stages in Arabidopsis thaliana. Plant molecular biology, 83**:** 265-277

Schildhauer J, Wiedemuth K, Humbeck K (2008) Supply of nitrogen can reverse senescence processes and affect expression of genes coding for plastidic glutamine synthetase and lysine-ketoglutarate reductase/saccharopine dehydrogenase. Plant Biology, 10**:** 76-84

Schmittgen TD, Livak KJ (2008) Analyzing real-time PCR data by the comparative CT method. Nature protocols, 3**:** 1101-1108

Schneider H, Postma JA, Wojciechowski T, Kuppe C, Lynch J (2017) Root Cortical Senescence Improves Growth under Suboptimal Availability of N, P, and K. Plant Physiology,

Schneider H, Postma JA, Wojciechowski T, Kuppe C, Lynch J (2017) Root Cortical Senescence Improves Growth under Suboptimal Availability of N, P, and K. Plant Physiology**:** pp. 00648.02017

Schröder P, Abele C, Gohr P, Stuhlfauth-Roisch U, Grosse W (1999) Latest on enzymology of serotonin biosynthesis in walnut seeds. *In* Tryptophan, Serotonin, and Melatonin. Springer, pp 637-644

Seiler C, Harshavardhan VT, Rajesh K, Reddy PS, Strickert M, Rolletschek H, Scholz U, Wobus U, Sreenivasulu N (2011) ABA biosynthesis and degradation contributing to ABA homeostasis during barley seed development under control and terminal drought-stress conditions. Journal of Experimental Botany,

Tai H, Lu X, Opitz N, Marcon C, Paschold A, Lithio A, Nettleton D, Hochholdinger F (2015) Transcriptomic and anatomical complexity of primary, seminal, and crown roots highlight root type-specific functional diversity in maize (Zea mays L.). Journal of Experimental Botany,

Takahashi H, Yamauchi T, Rajhi I, Nishizawa NK, Nakazono M (2015) Transcript profiles in cortical cells of maize primary root during ethylene-induced lysigenous aerenchyma formation under aerobic conditions. Annals of botany, 115**:** 879-894

Tamura K, Stecher G, Peterson D, Filipski A, Kumar S (2013) MEGA6: molecular evolutionary genetics analysis version 6.0. Molecular biology and evolution, 30: 2725-2729

Thimm O, Bläsing O, Gibon Y, Nagel A, Meyer S, Krüger P, Selbig J, Müller LA, Rhee SY, Stitt M (2004) mapman: a user-driven tool to display genomics data sets onto diagrams of metabolic pathways and other biological processes. The Plant Journal, 37: 914-939

Thomas H (2013) Senescence, ageing and death of the whole plant. New Phytologist, 197**:** 696-711

Thomas H, Ougham HJ, Wagstaff C, Stead AD (2003) Defining senescence and death. Journal of Experimental Botany, 54**:** 1127-1132

Thomas H, Stoddart JL (1980) Leaf senescence. Annual review of plant physiology, 31**:** 83-111

Tukey Jr H (1970) The leaching of substances from plants. Annual review of plant physiology, 21**:** 305-324

Uga Y, Sugimoto K, Ogawa S, Rane J, Ishitani M, Hara N, Kitomi Y, Inukai Y, Ono K, Kanno N (2013) Control of root system architecture by DEEPER ROOTING 1 increases rice yield under drought conditions. Nature Genetics, 45**:** 1097-1102

Valenzuela-Estrada LR, Vera-Caraballo V, Ruth LE, Eissenstat DM (2008) Root anatomy, morphology, and longevity among root orders in Vaccinium corymbosum (Ericaceae). American Journal of Botany, 95**:** 1506-1514

Van Breusegem F, Dat JF (2006) Reactive oxygen species in plant cell death. Plant physiology, 141**:** 384-390

Van Steveninck RFM, Babare A, Fernando DR, Van Steveninck ME (1993) The binding of zinc in root cells of crop plants by phytic acid. Plant and Soil, 155**:** 525-528

Vetterlein D, Doussan C (2016) Root age distribution: how does it matter in plant processes? A focus on water uptake. Plant and Soil, 407**:** 145-160

Volder A, Smart DR, Bloom AJ, Eissenstat DM (2005) Rapid decline in nitrate uptake and respiration with age in fine lateral roots of grape: implications for root efficiency and competitive effectiveness. New Phytologist, 165**:** 493-502

Wagstaff C, Leverentz MK, Griffiths G, Thomas B, Chanasut U, Stead AD, Rogers HJ (2002) Cysteine protease gene expression and proteolytic activity during senescence of Alstroemeria petals. Journal of Experimental Botany, 53**:** 233-240

Wang P, Sun X, Chang C, Feng F, Liang D, Cheng L, Ma F (2013) Delay in leaf senescence of Malus hupehensis by long-term melatonin application is associated with its regulation of metabolic status and protein degradation. Journal of pineal research, 55**:** 424-434

Weaver LM, Gan S, Quirino B, Amasino RM (1998) A comparison of the expression patterns of several senescence-associated genes in response to stress and hormone treatment. Plant Molecular Biology, 37**:** 455-469

Webb K, Jensen E, Heywood S, Morris S, Linton P, Hooker J (2010) Gene expression and nitrogen loss in senescing root systems of red clover (Trifolium pratense). The Journal of Agricultural Science, 148**:** 579-591

Wei Y, Hu W, Wang Q, Liu W, Wu C, Zeng H, Yan Y, Li X, He C, Shi H (2016) Comprehensive transcriptional and functional analyses of melatonin synthesis genes in cassava reveal their novel role in hypersensitive-like cell death. Scientific reports, 6

Werner T, Motyka V, Laucou V, Smets R, Van Onckelen H, Schmülling T (2003) Cytokinin-Deficient Transgenic Arabidopsis Plants Show Multiple Developmental Alterations Indicating Opposite Functions of Cytokinins in the Regulation of Shoot and Root Meristem Activity. The Plant Cell, 15**:** 2532-2550

Wi SJ, Kim WT, Park KY (2006) Overexpression of carnation S-adenosylmethionine decarboxylase gene generates a broad-spectrum tolerance to abiotic stresses in transgenic tobacco plants. Plant Cell Reports, 25**:** 1111-1121

Witte C-P (2011) Urea metabolism in plants. Plant Science, 180**:** 431-438

Woo HR, Kim HJ, Nam HG, Lim PO (2013) Plant leaf senescence and death–regulation by multiple layers of control and implications for aging in general. J Cell Sci, 126**:** 4823-4833

Woo HR, Kim HJ, Nam HG, Lim PO (2013) Plant leaf senescence and death – regulation by multiple layers of control and implications for aging in general. Journal of Cell Science, 126**:** 4823-4833

Xiao S, Dai L, Liu F, Wang Z, Peng W, Xie D (2004) COS1: an Arabidopsis coronatine insensitive1 suppressor essential for regulation of jasmonate-mediated plant defense and senescence. The Plant Cell, 16**:** 1132-1142

Xiong L, Zhu J-K (2003) Regulation of abscisic acid biosynthesis. Plant physiology, 133**:** 29-36

Xiong Y, Contento AL, Bassham DC (2005) AtATG18a is required for the formation of autophagosomes during nutrient stress and senescence in Arabidopsis thaliana. The Plant Journal, 42**:** 535-546

Xu Y, Tian J, Gianfagna T, Huang B (2008) Effects of SAG12-ipt expression on cytokinin production, growth and senescence of creeping bentgrass (Agrostis stolonifera L.) under heat stress. Plant Growth Regulation, 57**:** 281

Yamauchi T, Rajhi I, Nakazono M (2011) Lysigenous aerenchyma formation in maize root is confined to cortical cells by regulation of genes related to generation and scavenging of reactive oxygen species. Plant signaling & behavior, 6**:** 759-761

YANG J, ZHANG J, HUANG Z, WANG Z, ZHU Q, LIU L (2002) Correlation of Cytokinin Levels in the Endosperms and Roots with Cell Number and Cell Division Activity during Endosperm Development in Rice. Annals of Botany, 90**:** 369-377

Yang X, Yang Y-N, Xue L-J, Zou M-J, Liu J-Y, Chen F, Xue H-W (2011) Rice ABI5-Like1 Regulates Abscisic Acid and Auxin Responses by Affecting the Expression of ABRE-Containing Genes. Plant Physiology, 156**:** 1397-1409

York LM, Lynch JP (2015) Intensive field phenotyping of maize (Zea mays L.) root crowns identifies phenes and phene integration associated with plant growth and nitrogen acquisition. Journal of experimental botany, 66**:** 5493-5505

York LM, Silberbush M, Lynch JP (2016) Spatiotemporal variation of nitrate uptake kinetics within the maize (Zea mays L.) root system is associated with greater nitrate uptake and interactions with architectural phenes. Journal of Experimental Botany,

Yoshida S (2003) Molecular regulation of leaf senescence. Current Opinion in Plant Biology, 6**:** 79-84

Yu P, Baldauf J, Lithio A, Marcon C, Nettleton D, Li C, Hochholdinger F (2016) Root type specific reprogramming of maize pericycle transcriptomes by local high nitrate results in disparate lateral root branching patterns. Plant Physiology,

Zentgraf U, Laun T, Miao Y (2010) The complex regulation of WRKY53 during leaf senescence of Arabidopsis thaliana. European journal of cell biology, 89**:** 133-137

Zhang H, Xue Y, Wang Z, Yang J, Zhang J (2009) Morphological and physiological traits of roots and their relationships with shoot growth in "super" rice. Field Crops Research, 113**:** 31-40

Zhang J, Shi Y, Zhang X, Du H, Xu B, Huang B (2017) Melatonin suppression of heat-induced leaf senescence involves changes in abscisic acid and cytokinin biosynthesis and signaling pathways in perennial ryegrass (Lolium perenne L.). Environmental and Experimental Botany, 138**:** 36-45

Zhang K, Gan S-S (2012) An abscisic acid-AtNAP transcription factor-SAG113 protein phosphatase 2C regulatory chain for controlling dehydration in senescing Arabidopsis leaves. Plant Physiology, 158**:** 961-969

Zhang K, Xia X, Zhang Y, Gan S-S (2012) An ABA-regulated and Golgi-localized protein phosphatase controls water loss during leaf senescence in Arabidopsis. The Plant Journal, 69**:** 667-678

Zhou X, Jiang Y, Yu D (2011) WRKY22 transcription factor mediates dark-induced leaf senescence in Arabidopsis. Molecules and cells, 31**:** 303-313

Zhu J, Brown KM, Lynch JP (2010) Root cortical aerenchyma improves the drought tolerance of maize (Zea mays L.). Plant, Cell & Environment, 33**:** 740-749

Zimmermann P, Heinlein C, Orendi G, Zentgraf U (2006) Senescence-specific regulation of catalases in Arabidopsis thaliana (L.) Heynh. Plant, Cell & Environment, 29**:** 1049-1060

Zimmermann P, Zentgraf U (2005) The correlation between oxidative stress and leaf senescence during plant development. Cellular and Molecular Biology Letters, 10**:** 515

Zobel R (1992) Root morphology and development. Journal of Plant Nutrition, 15**:** 677-684

Zonia LE, Stebbins NE, Polacco JC (1995) Essential Role of Urease in Germination of Nitrogen-Limited Arabidopsis thaliana Seeds. Plant Physiology, 107**:** 1097-1103

Appendix

Appendix1 The concentrations and contents of elements in seminal root during root aging
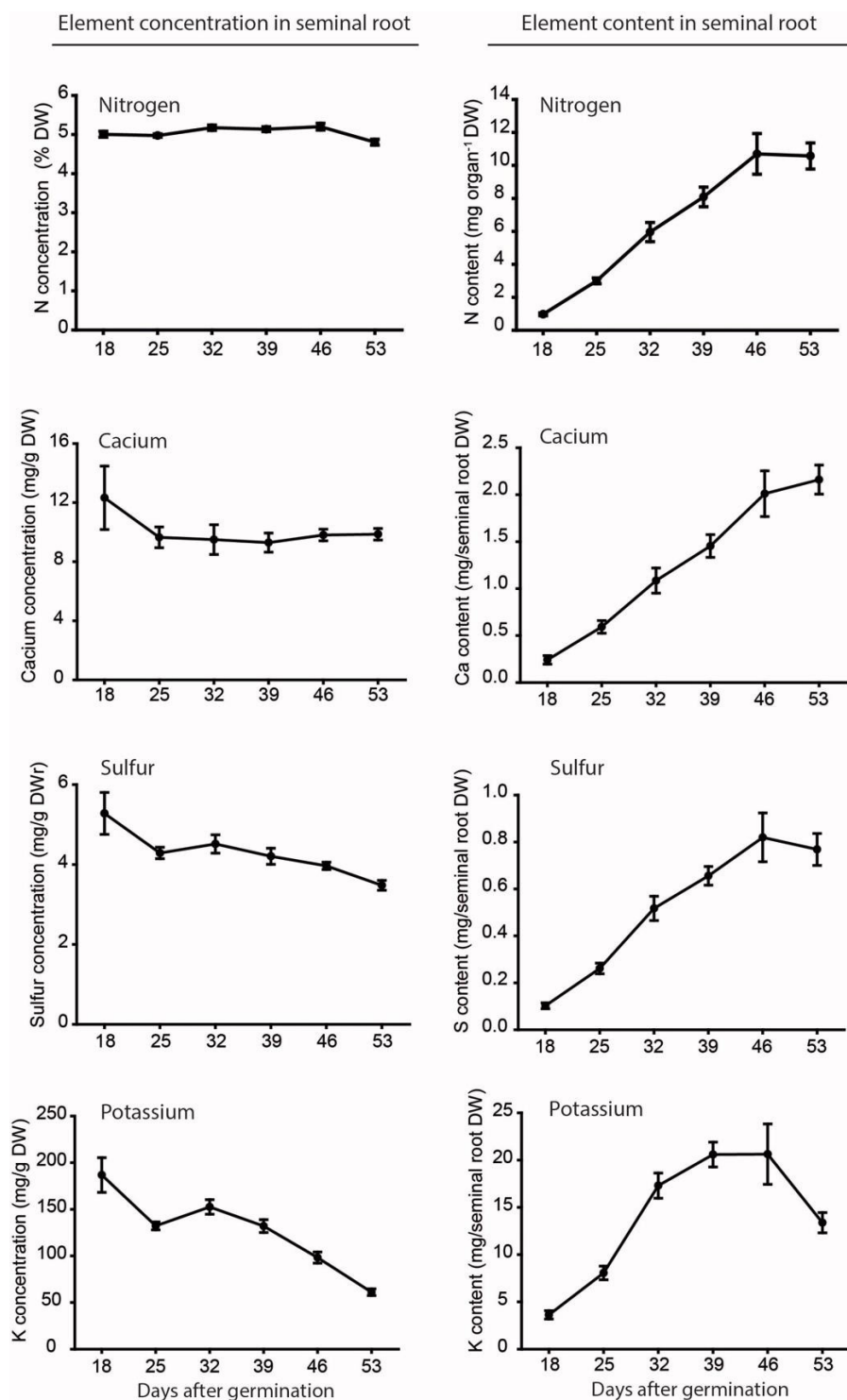
Element concentration in seminal root — Element content in seminal root
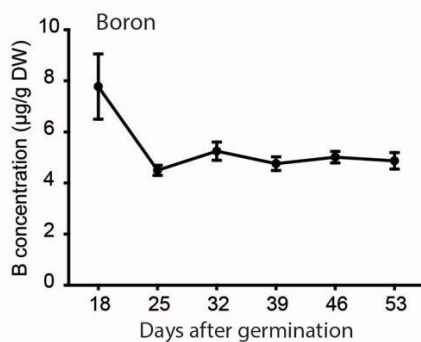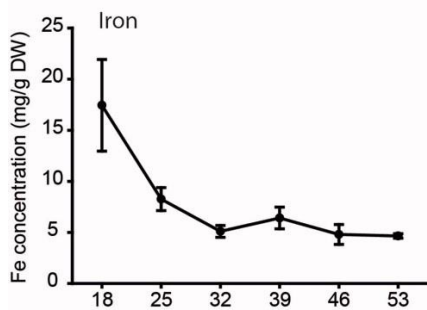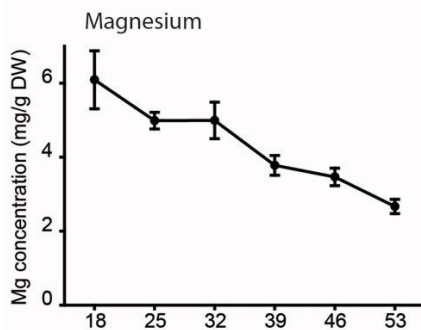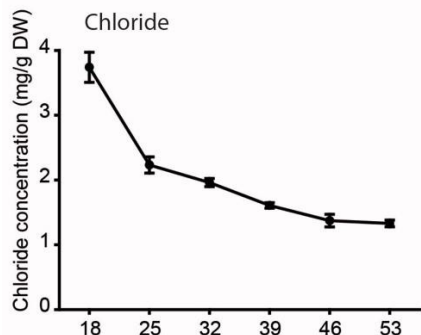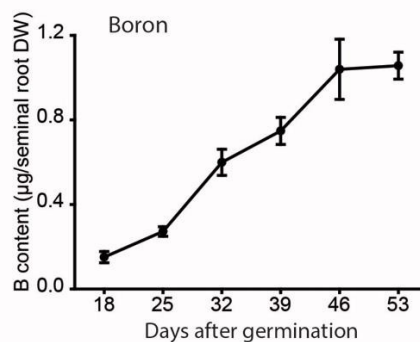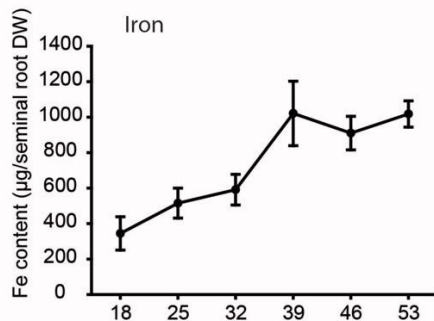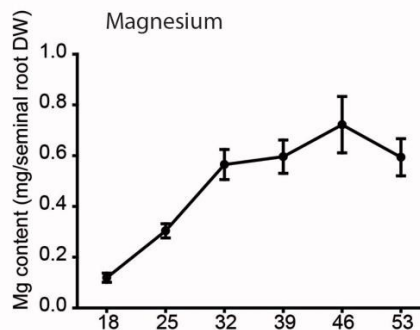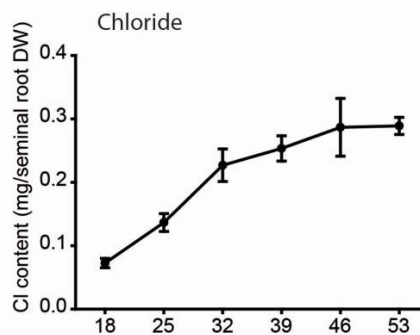
Chloride, Magnesium, Iron, Boron concentration and content plotted against Days after germination

Element concentration in seminal root

Element content in seminal root

Molybdenum

Molybdenum

Manganese

Manganese

Copper

Copper
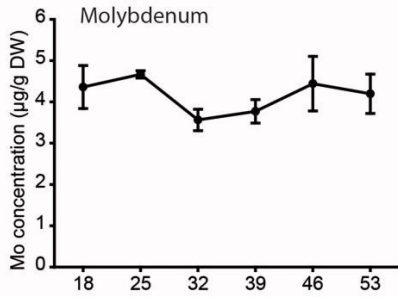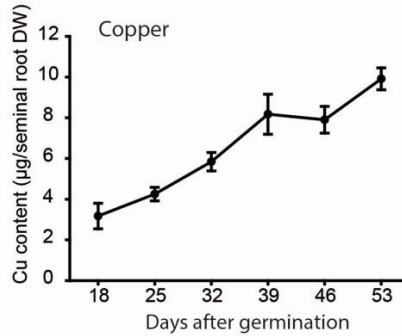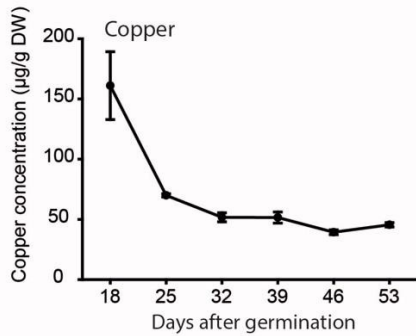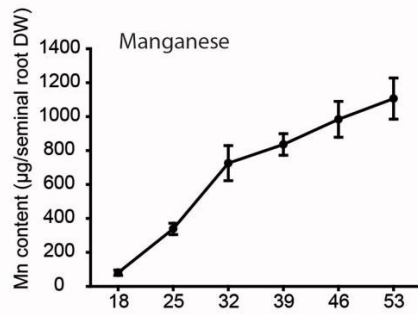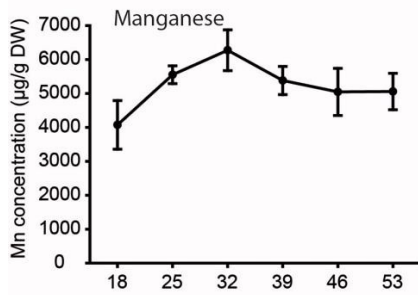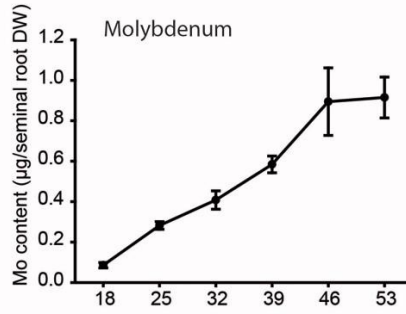
Phosphorus and zinc concentrations in the whole barley shoot

Phosphorus

Zinc
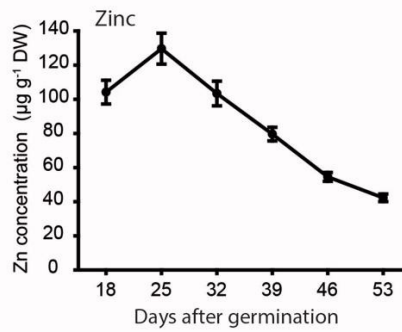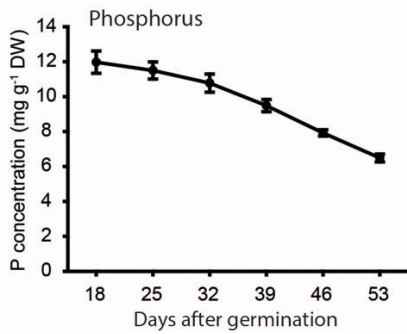
Appendix 2.102 Significant enriched GO terms in cluster 1 of
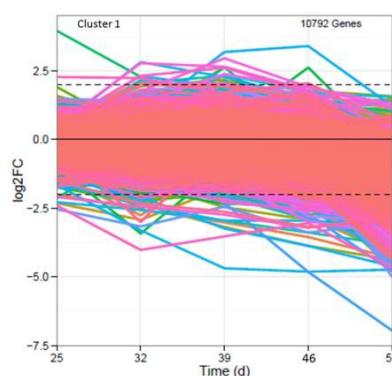
<table>
<tr><th colspan="5">Significant enriched GO terms in cluster 1 (10792 genes)
of apical root zone (ARZ)</th></tr>
<tr><td>GO:0007018</td><td>GO:0006556</td><td>GO:0015991</td><td>GO:0006099</td><td>GO:0030244</td></tr>
<tr><td>microtubule-based movement</td><td>adenosylmethionine biosynthetic process</td><td>ATP hydrolysis coupled proton transport</td><td>tricarboxylic acid cycle</td><td>cellulose biosynthetic process</td></tr>
<tr><td>0.000000036</td><td>0.000000084</td><td>0.000003</td><td>0.0000066</td><td>0.0000073</td></tr>
<tr><td>53 / 108</td><td>16 / 19</td><td>27 / 48</td><td>20 / 32</td><td>22 / 37</td></tr>
<tr><td>GO:0006886</td><td>GO:0010411</td><td>GO:0006564</td><td>GO:0009086</td><td>GO:0006098</td></tr>
<tr><td>intracellular protein transport</td><td>xyloglucan metabolic process</td><td>L-serine biosynthetic process</td><td>methionine biosynthetic process</td><td>pentose-phosphate shunt</td></tr>
<tr><td>0.000018</td><td>0.000018</td><td>0.000036</td><td>0.000073</td><td>0.000097</td></tr>
<tr><td>115 / 329</td><td>21 / 36</td><td>11 / 14</td><td>13 / 19</td><td>15 / 24</td></tr>
<tr><td>GO:0042546</td><td>GO:0009664</td><td>GO:0042026</td><td>GO:0019419</td><td>GO:0006096</td></tr>
<tr><td>cell wall biogenesis</td><td>plant-type cell wall organization</td><td>protein refolding</td><td>sulfate reduction</td><td>glycolytic process</td></tr>
<tr><td>0.00019</td><td>0.00052</td><td>0.00072</td><td>0.00093</td><td>0.00122</td></tr>
<tr><td>23 / 46</td><td>17 / 32</td><td>10 / 15</td><td>5 / 5</td><td>49 / 133</td></tr>
<tr><td>GO:0046112</td><td>GO:0006633</td><td>GO:0006270</td><td>GO:0019430</td><td>GO:0043648</td></tr>
<tr><td>nucleobase biosynthetic process</td><td>fatty acid biosynthetic process</td><td>DNA replication initiation</td><td>removal of superoxide radicals</td><td>dicarboxylic acid metabolic process</td></tr>
<tr><td>0.00188</td><td>0.00221</td><td>0.00258</td><td>0.00258</td><td>0.00328</td></tr>
<tr><td>13 / 24</td><td>45 / 123</td><td>8 / 12</td><td>8 / 12</td><td>34 / 89</td></tr>
<tr><td>GO:0015986</td><td>GO:0006434</td><td>GO:0006122</td><td>GO:0006086</td><td>GO:0046165</td></tr>
<tr><td>ATP synthesis coupled proton transport</td><td>seryl-tRNA aminoacylation</td><td>mitochondrial electron transport, ubiquinol to cytochrome c</td><td>acetyl-CoA biosynthetic process from pyruvate</td><td>alcohol biosynthetic process</td></tr>
<tr><td>0.00359</td><td>0.00374</td><td>0.00398</td><td>0.00441</td><td>0.00441</td></tr>
<tr><td>11 / 20</td><td>4 / 4</td><td>6 / 8</td><td>5 / 6</td><td>5 / 6</td></tr>
<tr><td>GO:0046434</td><td>GO:1901136</td><td>GO:0045892</td><td></td><td></td></tr>
<tr><td>organophosphate catabolic process</td><td>carbohydrate derivative catabolic process</td><td>negative regulation of transcription, DNA-templated</td><td></td><td></td></tr>
<tr><td>0.00526</td><td>0.00553</td><td>0.00587</td><td></td><td></td></tr>
<tr><td>8 / 13</td><td>20 / 47</td><td>11 / 21</td><td></td><td></td></tr>
</table>

Appendix 2.103 Significant enriched GO terms in cluster 2 of

Significant enriched GO terms in cluster 2 (9433 genes) of apical root zone (ARZ)				
GO:0006355	GO:0055114	GO:0019684	GO:0009690	GO:0071577
regulation of transcription, DNA-templated	oxidation-reduction process	photosynthesis, light reaction	cytokinin metabolic process	zinc II ion transmembrane transport
0.0000000401	0.000866	0.000122	0.000122	0.000455
273 / 1175	412 / 2083	7 / 9	7 / 9	8 / 13
GO:0006529	GO:0009611			
asparagine biosynthetic process	response to wounding			
0.000045	0.000822			
12 / 21	10 / 20			

Appendix 2.3 Significant enriched GO terms in cluster 3 of ARZ

Significant enriched GO terms in cluster 3 (3663 genes) of apical root zone (ARZ)				
		GO:0055085		
		transmembrane transport		
		0.0000392		
		75 / 903		

Appendix 2.4 Significant enriched GO terms in cluster 4 of ARZ

Significant enriched GO terms in cluster 4 (2565 genes) of apical root zone (ARZ)			
GO:0006468	GO:0006659	GO:0006355	GO:0006558
protein phosphorylation	phosphatidylserine biosynthetic process	regulation of transcription, DNA-templated	L-phenylalanine metabolic process
0.000000303	0.001082	0.00000996	0.0000408
136 / 1847	3 / 5	90 / 1175	8 / 28

Appendix 2.5 Significant enriched GO terms in cluster 5 of ARZ

Significant enriched GO terms in cluster 5 (164 genes) of apical root zone (ARZ)				
		GO:0006680		
		glucosylceramide catabolic process		
		0.000213		
		2 / 8		

Appendix 2.6 Significant enriched GO terms in cluster 1 of BRZ

Significant enriched GO terms in cluster 1 (7529 genes) of basal root zone (BRZ)				
GO:0006979	GO:0007018	GO:0007264	GO:0006334	GO:0006633
response to oxidative stress	microtubule-based movement	small GTPase mediated signal transduction	nucleosome assembly	fatty acid biosynthetic process
0.00000000654	0.000000000000206	0.002250	0.0000000311	0.000866
77 / 234	52 / 108	46 / 175	42 / 104	36 / 123
GO:0030244	GO:0051301	GO:0019953	GO:0000910	GO:0010411
cellulose biosynthetic process	cell division	sexual reproduction	cytokinesis	xyloglucan metabolic process
0.000000508	0.000430	0.000000183	0.0000671	0.000585
20 / 37	18 / 46	17 / 27	16 / 34	15 / 36
GO:0046274	GO:0006556	GO:0008299	GO:0006270	GO:0006555
lignin catabolic process	adenosylmethionine biosynthetic	isoprenoid biosynthetic process	DNA replication initiation	methionine metabolic process
0.000328	0.00000133	0.001854	0.00000125	0.002215
14 / 31	13 / 19	11 / 25	10 / 12	10 / 22
GO:0019419				
sulfate reduction				
0.000164				
5 / 5				

Appendix 2.7 Significant enriched GO terms in cluster 2 of BRZ
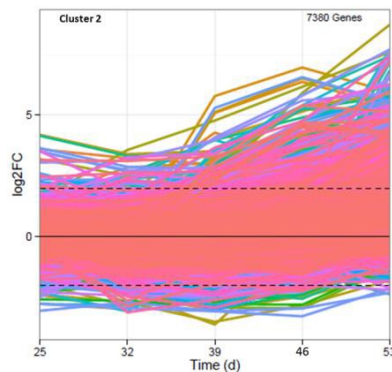
Significant enriched GO terms in cluster 2 (7380 genes) of basal root zone (BRZ)				
GO:0006355	GO:0071577	GO:0071805	GO:0045040	GO:0006529
regulation of transcription, DNA-templated	zinc II ion transmembrane transport	potassium ion transmembrane transport	protein import into mitochondrial outer membrane	asparagine biosynthetic process
0.00000917	0.0000588	0.000304	0.001306	0.000127
203 / 1175	8 / 13	21 / 73	4 / 5	10 / 21

Appendix 2.8 Significant enriched GO terms in cluster 3 of BRZ
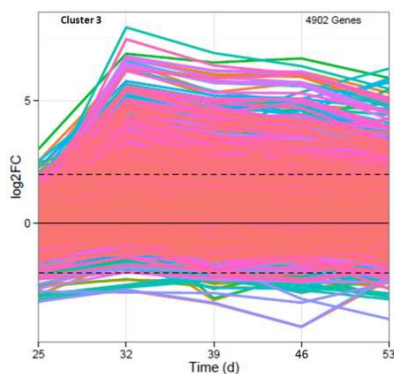
Significant enriched GO terms in cluster 3 (4902 genes) of basal root zone (BRZ)				
GO:0006468	GO:0016567	GO:0007205	GO:0006559	GO:0006887
protein phosphorylation	protein ubiquitination	protein kinase C-activating G-protein coupled receptor signaling pathway	L-phenylalanine catabolic process	exocytosis
$<1 \times 10^{-20}$	0.0000237	0.000000417	0.000000574	0.0000316
352 / 1847	27 / 111	12 / 22	11 / 19	16 / 50

Appendix 2.9 Significant enriched GO terms in cluster 4 of BRZ
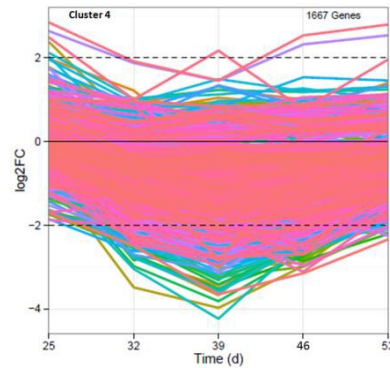
Significant enriched GO terms in cluster 4 (1667 genes) of basal root zone (BRZ)
No enriched GO terms in cluster 4 of BRZ

Appendix 2.10 Significant enriched GO terms in cluster 5 of BRZ
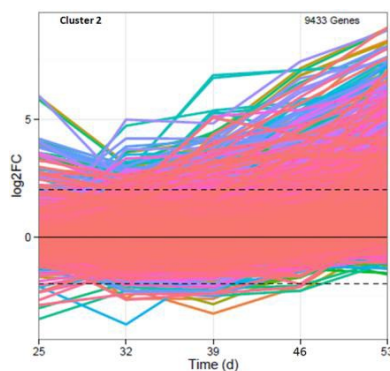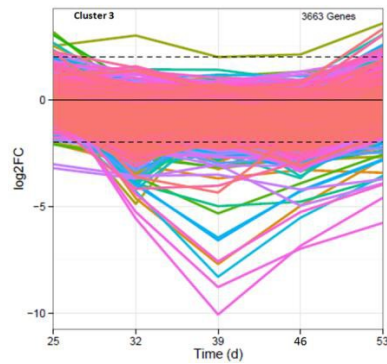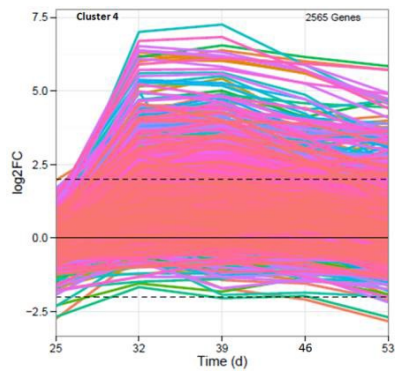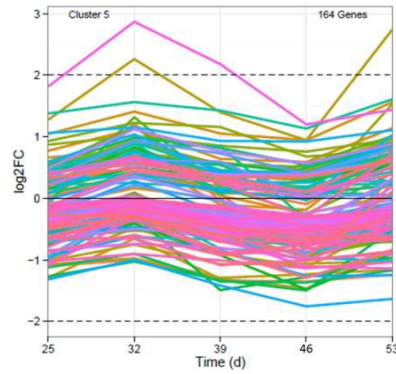

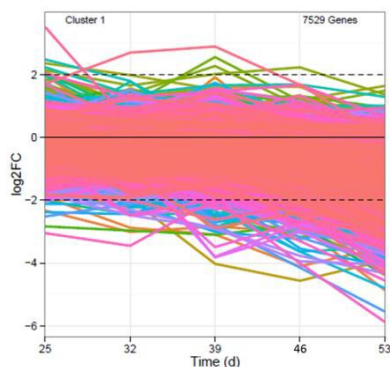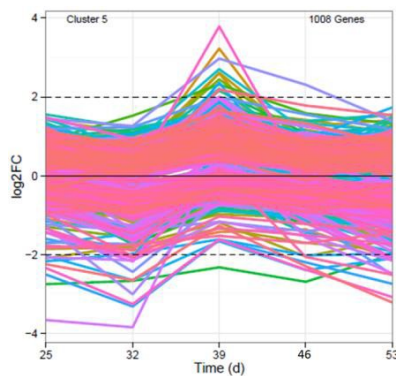|		Significant enriched GO terms in cluster 5 (1008 genes) of basal root zone (BRZ)		
		GO:0016125		
		sterol metabolic process		
		0.0000000542		
		4 / 4		

					Appendix table 3.1 Expressions of NAC transcription factor family in AZR over time		
logFC d25	logFC d32	logFC d39	logFC d42	logFC d53	ID	Harvest assembly ID	Putative orthologous
0.34	0.47	0.52	0.53	0.86	CUST_23467_PI399408534	35_27291	GRAB1 protein (wheat)
-0.82	-1.16	-0.78	-0.42	0.52	CUST_10542_PI399408534	35_13569	GRAB2 protein (wheat)
-0.33	0.02	0.25	0.79	2.01	CUST_8981_PI399408534	35_18477	GRAB2 protein (wheat)
-0.48	-0.12	0.11	0.59	1.80	CUST_15173_PI404877155	Contig9032_s_at	GRAB2 protein (wheat)
-0.09	-0.42	-0.27	-0.21	-0.06	CUST_12000_PI404877155	Contig5723_at	HvNAC002 (barley)
0.57	2.35	2.52	2.43	2.99	CUST_9618_PI404877155	Contig3361_at	HvNAC003 (barley)
1.83	1.79	1.99	3.91	5.62	CUST_9620_PI404877155	Contig3362_at	HvNAC004 (barley)
-0.50	0.26	0.39	1.65	2.71	CUST_3522_PI404877155	Contig14026_at	HvNAC005 (barley)
-0.31	-0.29	-0.38	0.43	2.19	CUST_12495_PI404877155	Contig6233_at	HvNAC006 (barley)
-0.01	0.48	0.73	0.64	0.92	CUST_423_PI404877155	Contig10340_at	HvNAC007 (barley)
0.00	0.80	0.91	1.34	2.75	CUST_15169_PI404877155	Contig9031_at	HvNAC008 (barley)
-0.11	0.30	0.36	0.73	1.52	CUST_1082_PI404877155	Contig11098_at	HvNAC013 (barley)
-0.20	-0.36	0.01	1.00	3.11	CUST_12740_PI404877155	Contig6484_at	HvNAC015 (barley)
-0.07	-0.16	0.04	0.09	0.36	CUST_11552_PI404877155	Contig5241_at	HvNAC016 (barley)
-0.28	-0.48	-0.10	-0.33	1.00	CUST_300_PI404877155	Contig10172_at	HvNAC020 (barley)
1.27	3.49	3.61	5.60	6.90	CUST_3182_PI404877155	Contig13658_at	HvNAC023 (barley)
-1.77	-1.84	-1.73	-1.91	-1.61	CUST_6630_PI404877155	Contig19673_at	HvNAC033 (barley)
-0.11	1.14	1.36	1.02	1.05	CUST_12015_PI404877155	Contig5740_at	HvNAC035 (barley)
-0.31	-0.43	-0.62	-0.66	-0.21	CUST_1626_PI404877155	Contig11856_at	HvNAC039 (barley)
0.37	1.81	1.89	1.58	1.48	CUST_4325_PI404877155	Contig15251_at	HvNAC040 (barley)
0.03	0.62	0.72	0.77	1.06	CUST_3434_PI404877155	Contig13898_at	HvNAC048 (barley)
-0.09	0.18	0.15	0.33	0.45	CUST_22698_PI399408534	35_14840	NAC domain protein (barley)
-0.07	0.14	0.15	1.69	3.62	CUST_15188_PI399408534	35_27594	NAC domain protein (wheat)
0.05	1.39	1.58	1.38	1.84	CUST_842_PI399408534	35_405	NAC domain protein (wheat)
-0.11	0.16	0.32	-0.04	0.55	CUST_22610_PI399408534	35_22454	NAC transcription factor (barley)
-0.06	0.31	0.73	1.53	3.43	CUST_728_PI399408534	35_425	NAC domain protein 48 (rice)
-0.29	-0.30	-0.07	-0.36	1.12	CUST_15149_PI399408534	35_3855	NAC domain protein 71 (rice)
-0.45	-0.28	0.08	-0.06	1.15	CUST_788_PI399408534	35_415	NAC domain protein 71 (rice)
-0.19	0.94	1.17	0.94	0.98	CUST_11316_PI399408534	35_2260	NAC domain protein 74 (rice)
0.25	1.35	1.42	1.36	0.92	CUST_1388_PI399408534	35_37892	NAC domain protein 74 (rice)
0.10	1.18	1.05	0.68	0.24	CUST_7857_PI404877155	Contig2318_at	NAC domain protein 78 (rice)
0.45	0.80	0.67	1.45	0.23	CUST_20153_PI399408534	35_14941	NAC transcription factor (barley)
-0.55	-1.27	-1.07	-1.21	-0.83	CUST_7018_PI399408534	35_43081	NAC transcription factor (barley)
-0.10	-1.11	-0.68	-1.05	-0.76	CUST_2083_PI399408534	35_23678	NAC transcription factor (barley)
0.80	2.47	2.69	4.59	5.85	CUST_18124_PI399408534	35_5915	NAC transcription factor (barley)
-0.95	-1.38	-1.32	-0.90	-0.27	CUST_20019_PI399408534	35_24730	NAC transcription factor (barley)
-0.76	-1.06	-1.21	-0.65	0.12	CUST_28257_PI399408534	35_7768	NAC transcription factor

							(barley)
-0.73	-1.37	-1.59	-1.08	0.20	CUST_8899_PI399408534	35_4511	NAC014 gene (barley)
0.14	0.18	0.22	0.58	0.89	CUST_15193_PI399408534	35_19996	NAC023 gene (barley)
0.14	0.65	0.64	0.56	0.45	CUST_26733_PI399408534	35_17366	NAC2 protein-like (rice)
-0.10	0.11	0.68	1.41	3.41	CUST_127_PI399408534	35_498	NAC23 (Sugarcane)
-0.09	0.28	0.72	1.42	3.49	CUST_33083_PI399408534	35_518	NAC23 (Sugarcane)
-0.15	0.02	0.15	0.13	0.50	CUST_19097_PI404877155	HZ01D23u_s_at	NAC-like protein (rice)
-0.36	0.77	0.43	0.52	-0.19	CUST_24932_PI399408534	35_6147	NAM -like protein (arabidopsis)
-0.29	-0.48	-0.51	-0.27	0.63	CUST_28318_PI399408534	35_45754	Nam-like protein 17 (Petunia)
-0.05	0.99	1.05	0.97	0.51	CUST_7862_PI404877155	Contig2318_s_at	nam-like protein 2 (Petunia)
-0.17	0.69	0.44	0.35	1.21	CUST_17020_PI399408534	35_4213	NAM-related protein 1 (maize)
0.50	1.82	2.00	1.76	1.76	CUST_10652_PI399408534	35_21150	OsNAC protein-like (rice)
0.09	-0.30	0.22	1.12	3.15	CUST_12499_PI404877155	Contig6235_s_at	OsNAC6 protein (rice)
-0.53	-0.76	-1.20	-0.52	0.08	CUST_33367_PI399408534	35_16659	Putative OsNAC4 (rice)
-0.81	-1.15	-1.37	-0.65	-0.12	CUST_4930_PI399408534	35_21369	NAC domain protein (rice)
-0.66	-0.74	-0.41	0.71	2.77	CUST_32838_PI399408534	35_544	NAC domain protein (rice)
0.42	0.08	0.02	-0.04	-1.07	CUST_9860_PI404877155	Contig3584_at	NAC transcription factor (rice)
-0.71	0.39	0.50	1.65	2.47	CUST_13637_PI399408534	35_21015	Putative NAM protein (rice)
-0.53	-0.36	-0.25	0.08	0.93	CUST_14554_PI399408534	35_30327	Putative NAM protein (rice)
-0.39	0.08	-0.24	0.12	1.02	CUST_24370_PI399408534	35_38789	Putative NAM protein (rice)
-0.24	0.16	0.32	1.42	3.02	CUST_18119_PI399408534	35_5916	Putative NAM protein (rice)
0.13	0.10	0.04	0.43	0.78	CUST_19562_PI404877155	rbah54n13_s_at	Putative NAM protein (rice)
-0.42	-0.77	-0.52	0.35	1.60	CUST_16977_PI399408534	35_18187	PutativeNAM protein (rice)
-0.23	-0.80	-0.80	-0.68	0.00	CUST_13401_PI399408534	35_6587	Putative OsNAC4 (rice)
-0.18	-0.65	-0.81	-1.09	-1.62	CUST_27795_PI399408534	35_32050	Similarity to NAM (arabidopsis)

Appendix table 3.2 Expressions of NAC transcription factor family in BRZ over time							
logFC d25	logFC d32	logFC d39	logFC d46	logFC d53	ID	Harvest assembly ID	Putative orthologous
0.05	0.76	0.34	0.47	0.44	CUST_23467_PI399408534	35_27291	GRAB1 protein (wheat)
1.06	2.91	2.58	2.55	2.17	CUST_9618_PI404877155	Contig3361_at	HvNAC003 (barley)
2.06	1.91	2.18	3.28	4.89	CUST_9620_PI404877155	Contig3362_at	HvNAC004 (barley)
0.41	0.94	0.94	1.57	1.57	CUST_3522_PI404877155	Contig14026_at	HvNAC005 (barley)
-0.32	0.20	-0.36	0.44	1.42	CUST_12495_PI404877155	Contig6233_at	HvNAC006 (barley)
0.21	0.96	0.69	0.76	0.90	CUST_423_PI404877155	Contig10340_at	HvNAC007 (barley)
0.29	0.96	0.56	0.80	1.29	CUST_15169_PI404877155	Contig9031_at	HvNAC008 (barley)
0.13	0.15	0.06	0.21	0.33	CUST_11552_PI404877155	Contig5241_at	HvNAC016 (barley)
-0.07	-0.16	-0.24	-0.20	1.10	CUST_300_PI404877155	Contig10172_at	HvNAC020 (barley)
1.36	3.68	3.66	5.10	5.74	CUST_3182_PI404877155	Contig13658_at	HvNAC023 (barley)
0.38	1.68	1.19	1.05	1.13	CUST_12015_PI404877155	Contig5740_at	HvNAC035 (barley)
0.38	-0.24	-0.22	-0.81	-0.79	CUST_1626_PI404877155	Contig11856_at	HvNAC039 (barley)
0.43	1.89	1.61	1.49	1.43	CUST_4325_PI404877155	Contig15251_at	HvNAC040 (barley)
0.48	1.05	1.05	1.13	0.99	CUST_3434_PI404877155	Contig13898_at	HvNAC048 (barley)

0.01	0.75	0.42	0.48	0.41	CUST_22698_PI399408534	35_14840	NAC domain protein (barley)
0.22	0.45	0.42	1.19	2.18	CUST_15188_PI399408534	35_27594	NAC domain protein (wheat)
0.38	2.00	1.68	1.60	1.54	CUST_842_PI399408534	35_405	NAC domain protein (wheat)
0.54	0.77	0.67	0.54	0.57	CUST_22610_PI399408534	35_22454	NAC transcription factor (barley)
0.06	0.25	0.27	1.16	2.07	CUST_728_PI399408534	35_425	NAC domain protein 48 (rice)
-0.11	-0.05	-0.17	-0.32	1.10	CUST_15149_PI399408534	35_3855	NAC domain protein 71 (rice)
0.44	1.64	1.11	1.09	1.15	CUST_11316_PI399408534	35_2260	NAC domain protein 74 (rice)
0.24	1.54	1.29	0.88	0.81	CUST_1388_PI399408534	35_37892	NAC domain protein 74 (rice)
0.15	0.71	0.46	0.50	0.41	CUST_11383_PI399408534	35_40255	NAC domain protein 82-like (rice)
0.89	1.73	1.21	0.90	0.73	CUST_7862_PI404877155	Contig2318_s_at	nam-like protein 2 (Petunia)
-0.38	-1.13	-1.41	-1.36	-1.09	CUST_7018_PI399408534	35_43081	NAC transcription factor (barley)
-0.33	-0.73	-0.81	-0.50	-0.09	CUST_2083_PI399408534	35_23678	NAC transcription factor (barley)
1.15	2.99	2.87	4.42	4.93	CUST_18124_PI399408534	35_5915	NAC transcription factor (barley)
-0.50	-1.04	-0.92	-0.81	-0.67	CUST_8899_PI399408534	35_4511	NAC014 gene (barley)
0.31	0.81	0.67	0.50	0.48	CUST_26733_PI399408534	35_17366	NAC2 protein-like (rice)
0.12	0.22	0.39	1.23	2.13	CUST_127_PI399408534	35_498	NAC23 (Sugarcane)
-0.02	0.24	0.34	1.11	2.02	CUST_33083_PI399408534	35_518	NAC23 (Sugarcane)
0.17	0.47	0.28	0.42	0.57	CUST_19097_PI404877155	HZ01D23u_s_at	NAC-like protein (rice)
0.66	0.40	0.68	0.28	0.46	CUST_24932_PI399408534	35_6147	NAM -like protein (arabidopsis)
-0.06	0.70	0.34	0.45	0.42	CUST_16694_PI404877155	HF01A04w_s_at	nam-like protein 2 (Petunia)
0.15	0.25	1.79	0.39	1.03	CUST_17020_PI399408534	35_4213	NAM-related protein 1 (maize)
0.36	1.79	1.49	1.46	1.44	CUST_10652_PI399408534	35_21150	OsNAC protein-like (rice)
0.12	-0.25	-0.07	0.87	1.92	CUST_12499_PI404877155	Contig6235_s_at	OsNAC6 protein (rice)
-0.19	-0.78	-0.68	-0.71	-1.08	CUST_9860_PI404877155	Contig3584_at	NAC transcription factor (rice)
0.92	1.35	1.48	1.78	1.78	CUST_13637_PI399408534	35_21015	Putative NAM protein (rice)
0.00	0.74	0.41	1.21	1.78	CUST_18119_PI399408534	35_5916	Putative NAM protein (rice)
-0.28	-0.33	-0.12	0.42	0.96	CUST_16977_PI399408534	35_18187	Putative NAM protein (rice)
-0.52	-0.60	-1.06	-0.63	-1.05	CUST_13401_PI399408534	35_6587	Putative OsNAC4 (rice)
-0.43	-0.67	-0.41	-1.15	-0.89	CUST_27795_PI399408534	35_32050	Similarity to NAM (arabidopsis)

Appendix table 3.3 Expressions of WRKY transcription factor family in ARZ over time							
logFC d25	logFC d32	logFC d39	logFC d46	logFC d53	ID	Harvest assembly ID	Putative orthologous
0.75	2.97	3.00	2.89	2.85	CUST_10681_PI404877155	Contig4386_at	HvWRKY1 (barley)
-0.09	0.10	0.26	0.03	0.57	CUST_26661_PI399408534	35_17374	HvWRKY10 (barley)
-0.01	0.34	0.13	-0.02	0.51	CUST_4774_PI404877155	Contig16040_at	HvWRKY10 (barley)
0.18	-0.99	-1.28	-1.72	-1.33	CUST_34023_PI399408534	35_5370	HvWRKY13 (barley)
-0.02	-1.26	-1.17	-1.98	-1.55	CUST_2857_PI404877155	Contig13268_at	HvWRKY13 (barley)
0.41	-0.30	-0.33	-0.34	1.00	CUST_24665_PI399408534	35_38750	HvWRKY14 (barley)
0.08	0.39	0.33	0.08	0.61	CUST_20662_PI399408534	35_31880	HvWRKY15 (barley)
0.50	1.84	1.56	1.34	0.76	CUST_23349_PI399408534	35_41558	HvWRKY17 (barley)
0.14	1.96	1.65	1.27	0.58	CUST_5200_PI399408534	35_23506	HvWRKY18 (barley)
1.23	4.48	3.58	3.91	3.34	CUST_25882_PI399408534	35_3498	HvWRKY19 (barley)

0.56	2.66	2.19	1.87	1.24	CUST_288_PI404877155	Contig10167_at	HvWRKY19 (barley)
0.16	2.63	2.68	2.28	1.82	CUST_10684_PI404877155	Contig4387_at	HvWRKY2 (barley)
0.90	4.18	3.63	3.79	3.10	CUST_292_PI404877155	Contig10168_at	HvWRKY20 (barley)
0.54	3.00	3.42	2.94	1.73	CUST_9289_PI399408534	35_30519	HvWRKY22 (barley)
0.57	3.29	3.03	2.44	1.14	CUST_5003_PI399408534	35_15931	HvWRKY23 (barley)
0.35	2.59	2.98	1.89	1.07	CUST_7241_PI404877155	Contig21110_at	HvWRKY23 (barley)
0.31	1.47	1.64	0.93	0.48	CUST_19656_PI399408534	35_38900	HvWRKY27 (barley)
0.75	2.39	2.61	2.48	1.98	CUST_19454_PI399408534	35_4162	HvWRKY28 (barley)
0.38	-0.06	-0.09	-0.76	-0.83	CUST_31210_PI399408534	35_12329	HvWRKY29 (barley)
-0.44	1.38	2.38	2.55	2.55	CUST_15438_PI399408534	35_9124	HvWRKY3 (barley)
0.28	2.64	2.84	1.89	1.04	CUST_28428_PI399408534	35_10252	HvWRKY30 (barley)
0.73	2.54	2.60	2.54	2.05	CUST_1791_PI404877155	Contig12005_at	HvWRKY30 (barley)
-0.31	2.04	2.49	2.72	2.58	CUST_15828_PI399408534	35_13381	HvWRKY31 (barley)
-0.08	0.58	1.13	1.26	1.32	CUST_2686_PI399408534	35_4766	HvWRKY32 (barley)
-0.02	0.50	0.87	1.28	1.38	CUST_4727_PI404877155	Contig15957_at	HvWRKY32 (barley)
-0.15	0.36	-0.02	-0.47	0.32	CUST_615_PI399408534	35_18794	HvWRKY34 (barley)
-0.40	-0.14	-0.42	-0.66	0.05	CUST_4058_PI399408534	35_49737	HvWRKY34 (barley)
-0.18	0.21	-0.04	-0.49	0.28	CUST_552_PI404877155	Contig10471_at	HvWRKY34 (barley)
-0.21	-0.05	-0.54	-0.41	-1.38	CUST_16216_PI399408534	35_11153	HvWRKY36 (barley)
-0.16	-0.64	-0.50	-0.31	0.08	CUST_2943_PI404877155	Contig13375_at	HvWRKY39 (barley)
0.35	1.04	1.21	1.09	0.72	CUST_6969_PI404877155	Contig20450_at	HvWRKY4 (barley)
-0.13	0.20	0.15	0.30	0.82	CUST_28735_PI399408534	35_5543	HvWRKY42 (barley)
-0.06	0.11	0.08	0.35	0.85	CUST_4579_PI404877155	Contig15657_at	HvWRKY42 (barley)
-0.14	1.29	1.64	0.88	0.95	CUST_25852_PI399408534	35_41493	HvWRKY43 (barley)
-0.05	-0.06	0.07	0.09	0.36	CUST_13512_PI404877155	Contig7243_at	HvWRKY46, SUSIBA2 (barley)
-0.02	0.61	0.81	0.96	0.68	CUST_30953_PI399408534	35_22133	HvWRKY48 (barley)
0.10	0.79	0.58	0.92	0.02	CUST_12297_PI399408534	35_10813	HvWRKY49 (barley)
0.70	2.82	3.57	2.23	1.06	CUST_10702_PI399408534	35_6690	HvWRKY5 (barley)
-0.37	0.84	1.31	0.24	-0.59	CUST_6135_PI404877155	Contig18462_at	HvWRKY5 (barley)
0.06	2.69	2.47	2.63	2.05	CUST_6105_PI399408534	35_30633	HvWRKY53 (barley)
0.09	1.73	2.05	1.33	0.55	CUST_24759_PI399408534	35_38742	HvWRKY55 (barley)
-0.29	-0.26	-0.38	-0.15	0.55	CUST_14016_PI404877155	Contig7798_at	HvWRKY7 (barley)
0.06	0.19	-0.15	0.18	0.48	CUST_23802_PI399408534	35_25080	HvWRKY8 (barley)
0.06	-0.13	-0.15	0.18	0.40	CUST_7812_PI404877155	Contig23011_at	HvWRKY8 (barley)
-0.06	0.05	0.34	0.22	1.07	CUST_3689_PI399408534	35_24053	HvWRKY9 (barley)
-0.08	-0.15	0.32	0.04	0.78	CUST_7620_PI404877155	Contig22226_at	HvWRKY9 (barley)
0.81	3.04	2.96	2.88	2.83	CUST_4979_PI399408534	35_15934	Putative WRKY1 (barley)
-0.58	-1.10	-1.20	-0.99	-0.59	CUST_1832_PI399408534	35_25884	Putative WRKY11 (barley)
1.24	3.26	2.82	2.39	1.62	CUST_25869_PI399408534	35_3499	Putative WRKY20 (barley)
0.18	2.08	2.14	1.70	1.79	CUST_13771_PI404877155	Contig7517_at	putative WRKY19 (wheat)
0.31	3.32	3.40	2.53	1.00	CUST_4998_PI399408534	35_15932	Putative WRKY2 (Barley)
-0.16	1.57	1.53	0.85	0.17	CUST_4987_PI399408534	35_15933	Putative WRKY2 (barley)
0.35	0.83	1.26	1.06	0.89	CUST_4786_PI399408534	35_23566	Putative WRKY49 (wheat)
0.87	2.68	2.86	3.26	2.52	CUST_22737_PI399408534	35_22430	Putative WRKY70 (rice)
-0.49	1.20	1.48	1.83	1.57	CUST_6901_PI404877155	Contig20358_at	putative WRKY70 (rice)

-0.40	0.95	1.56	2.48	2.10	CUST_11939_PI399408534	35_30409	Putative WRKY70 (Setaria italica)
-0.07	-0.02	-0.08	0.07	0.44	CUST_19223_PI404877155	rbaal15j13_s_at	SUSIBA2 (barley)
-0.14	-0.47	-0.35	0.11	0.34	CUST_26012_PI399408534	35_20111	WRKY13 (wheat)
-0.30	-0.72	-1.03	-0.17	0.88	CUST_7128_PI399408534	35_25699	WRKY17 (Brachypodium distachyon)

Appendix table 3.4 Expressions of WRKY transcription factor family in BRZ over time

logFC d25	logFC d32	logFC d39	logFC d46	logFC d53	ID	Harvest assembly ID	Putative orthologous
1.30	4.22	3.66	3.83	3.10	CUST_10681_PI404877155	Contig4386_at	HvWRKY1 (barley)
0.19	0.83	0.54	0.68	0.73	CUST_26661_PI399408534	35_17374	HvWRKY10 (barley)
0.13	0.87	0.57	0.50	0.58	CUST_4774_PI404877155	Contig16040_at	HvWRKY10 (barley)
-1.12	-1.68	-1.69	-2.53	-2.28	CUST_34023_PI399408534	35_5370	HvWRKY13 (barley)
-0.81	-1.42	-1.52	-2.55	-1.96	CUST_2857_PI404877155	Contig13268_at	HvWRKY13 (barley)
-1.45	-0.23	-0.72	0.36	0.06	CUST_24665_PI399408534	35_38750	HvWRKY14 (barley)
-0.04	1.27	0.43	0.63	0.88	CUST_20662_PI399408534	35_31880	HvWRKY15 (barley)
0.82	2.10	2.08	2.20	1.44	CUST_23349_PI399408534	35_41558	HvWRKY17 (barley)
0.73	2.96	2.54	2.73	1.71	CUST_5200_PI399408534	35_23506	HvWRKY18 (barley)
1.96	5.10	4.57	5.06	3.49	CUST_25882_PI399408534	35_3498	HvWRKY19 (barley)
1.17	3.53	3.32	3.29	2.28	CUST_288_PI404877155	Contig10167_at	HvWRKY19 (barley)
0.41	3.79	2.75	2.83	2.17	CUST_10684_PI404877155	Contig4387_at	HvWRKY2 (barley)
1.85	4.82	4.48	4.92	3.57	CUST_292_PI404877155	Contig10168_at	HvWRKY20 (barley)
-0.78	-0.15	-0.56	-1.32	-1.84	CUST_5579_PI399408534	35_260	HvWRKY21 (barley)
0.73	3.98	3.02	2.81	2.25	CUST_9289_PI399408534	35_30519	HvWRKY22 (barley)
0.27	4.44	3.14	3.24	1.86	CUST_5003_PI399408534	35_15931	HvWRKY23 (barley)
0.74	3.73	2.96	2.41	1.58	CUST_7241_PI404877155	Contig21110_at	HvWRKY23 (barley)
-0.06	1.87	1.26	1.14	0.69	CUST_19656_PI399408534	35_38900	HvWRKY27 (barley)
1.27	3.15	2.75	2.58	2.29	CUST_19454_PI399408534	35_4162	HvWRKY28 (barley)
0.04	-0.57	-0.24	-1.03	-1.07	CUST_31210_PI399408534	35_12329	HvWRKY29 (barley)
0.19	2.74	2.54	2.43	2.54	CUST_15438_PI399408534	35_9124	HvWRKY3 (barley)
0.66	3.72	3.00	2.35	1.48	CUST_28428_PI399408534	35_10252	HvWRKY30 (barley)
1.26	3.26	2.95	2.66	2.29	CUST_1791_PI404877155	Contig12005_at	HvWRKY30 (barley)
-0.07	2.93	2.23	2.62	1.85	CUST_15828_PI399408534	35_13381	HvWRKY31 (barley)
-0.01	0.95	0.82	0.83	0.86	CUST_2686_PI399408534	35_4766	HvWRKY32 (barley)
0.06	0.87	0.69	0.87	0.82	CUST_4727_PI404877155	Contig15957_at	HvWRKY32 (barley)
-0.17	0.49	0.23	0.33	0.87	CUST_615_PI399408534	35_18794	HvWRKY34 (barley)
-0.19	0.25	0.00	0.16	0.45	CUST_4058_PI399408534	35_49737	HvWRKY34 (barley)
-0.18	0.36	0.18	0.37	0.92	CUST_552_PI404877155	Contig10471_at	HvWRKY34 (barley)
-0.08	1.37	0.29	0.72	0.61	CUST_6_PI399408534	35_21548	HvWRKY37 (barley)
1.02	2.18	1.81	1.62	1.25	CUST_6969_PI404877155	Contig20450_at	HvWRKY4 (barley)
-0.10	0.70	0.34	0.11	-0.25	CUST_34596_PI399408534	35_5307	HvWRKY41 (barley)
0.47	0.55	0.57	0.51	0.67	CUST_28735_PI399408534	35_5543	HvWRKY42 (barley)
0.31	0.20	0.26	0.34	0.53	CUST_4579_PI404877155	Contig15657_at	HvWRKY42 (barley)
0.61	2.92	2.08	2.13	1.79	CUST_25852_PI399408534	35_41493	HvWRKY43 (barley)

					ID	Harvest assembly ID	Putative orthologous
0.12	0.83	0.20	0.58	0.53	CUST_24813_PI399408534	35_8337	HvWRKY45 (barley)
-0.69	-0.30	-0.76	-0.61	-0.38	CUST_18872_PI399408534	35_17610	HvWRKY46, SUSIBA2 (barley)
0.02	-0.02	-0.06	0.15	0.27	CUST_13512_PI404877155	Contig7243_at	HvWRKY46, SUSIBA2 (barley)
0.35	0.90	0.83	0.85	0.08	CUST_30953_PI399408534	35_22133	HvWRKY48 (barley)
-0.20	1.98	0.98	1.08	0.49	CUST_12297_PI399408534	35_10813	HvWRKY49 (barley)
0.84	2.99	2.79	1.93	0.77	CUST_10702_PI399408534	35_6690	HvWRKY5 (barley)
-0.03	2.01	1.52	0.98	0.05	CUST_6135_PI404877155	Contig18462_at	HvWRKY5 (barley)
0.15	3.39	2.89	2.88	1.36	CUST_6105_PI399408534	35_30633	HvWRKY53 (barley)
0.20	2.26	1.78	1.51	0.94	CUST_24759_PI399408534	35_38742	HvWRKY55 (barley)
0.07	0.64	0.44	0.17	0.03	CUST_26978_PI399408534	35_2987	HvWRKY7 (barley)
0.15	-0.21	0.03	0.25	0.39	CUST_23802_PI399408534	35_25080	HvWRKY8 (barley)
0.13	-0.32	-0.10	0.07	0.50	CUST_7812_PI404877155	Contig23011_at	HvWRKY8 (barley)
0.38	0.47	0.47	0.61	0.85	CUST_3689_PI399408534	35_24053	HvWRKY9 (barley)
1.25	4.05	3.53	3.58	2.89	CUST_4979_PI399408534	35_15934	Putative WRKY1 (barley)
1.07	3.69	3.33	3.25	2.17	CUST_25869_PI399408534	35_3499	Putative WRKY20 (barley)
0.62	2.75	2.17	2.09	1.75	CUST_13771_PI404877155	Contig7517_at	putative WRKY19 (wheat)
0.29	3.74	2.96	2.41	1.12	CUST_4998_PI399408534	35_15932	Putative WRKY2 (Barley)
-0.03	2.79	1.57	1.28	0.25	CUST_4987_PI399408534	35_15933	Putative WRKY2 (barley)
-0.01	0.41	0.18	0.25	0.47	CUST_17956_PI399408534	35_5928	Putative WRKY40 (wheat)
0.85	1.97	1.59	1.39	1.14	CUST_4786_PI399408534	35_23566	Putative WRKY49 (wheat)
1.91	4.77	4.19	4.18	2.86	CUST_22737_PI399408534	35_22430	Putative WRKY70 (rice)
0.39	3.14	2.89	2.82	1.69	CUST_6901_PI404877155	Contig20358_at	putative WRKY70 (rice)
0.61	2.93	2.90	3.31	2.45	CUST_11939_PI399408534	35_30409	Putative WRKY70 (Setaria italica)
0.10	0.06	0.05	0.29	0.39	CUST_19223_PI404877155	rbaal15j13_s_at	SUSIBA2 (barley)
0.31	-0.02	0.05	0.42	0.36	CUST_26012_PI399408534	35_20111	WRKY13 (wheat)

Appendix table 3.5 Expressions of AP2 transcription factor family in ARZ over time							
logFC d25	logFC d32	logFC d39	logFC d46	logFC d53	ID	Harvest assembly ID	Putative orthologous
-0.06	-0.81	-0.86	-0.95	-0.73	CUST_25791_PI399408534	35_10361	AP2-like protein (wheat)
0.51	0.66	0.64	0.87	1.12	CUST_25636_PI399408534	35_10376	AP2-like protein (Brachypodium distachyon)
0.53	2.15	1.74	1.30	-0.46	CUST_10562_PI399408534	35_11386	AP2-like protein (Brachypodium distachyon)
-0.26	-0.21	-0.46	-0.24	1.30	CUST_4187_PI399408534	35_12046	AP2-like protein (Brachypodium distachyon)
-0.26	0.00	-0.18	-0.07	-0.77	CUST_22416_PI399408534	35_14873	HvERF1 (barley)
0.35	7.00	7.25	5.88	4.56	CUST_21491_PI399408534	35_15343	AP2-like protein (maize)
0.12	3.23	3.07	2.35	1.88	CUST_21470_PI399408534	35_15344	AP2-like protein (maize)
1.47	1.96	2.02	3.23	4.82	CUST_21469_PI399408534	35_15346	AP2-like protein (Setaria italica)
0.75	2.70	2.74	2.35	1.71	CUST_21457_PI399408534	35_15347	HvCBF6 (barley)
0.62	1.90	1.71	1.91	2.13	CUST_21455_PI399408534	35_15349	AP2-like protein (Brachypodium distachyon)
-0.32	-0.69	-1.00	-1.31	-0.85	CUST_10530_PI399408534	35_15743	AP2-like protein (barley)
-0.27	-0.02	-0.01	-0.38	-0.89	CUST_10515_PI399408534	35_15744	AP2-like protein (Dasypyrum villosum)
-0.07	0.01	-0.09	0.47	0.80	CUST_8063_PI399408534	35_15804	AP2-like protein (Brachypodium distachyon)
0.71	0.63	0.94	1.63	2.21	CUST_11715_PI399408534	35_16192	AP2-like protein (maize)

0.15	0.43	0.71	0.98	1.69	CUST_11705_PI399408534	35_16193	AP2-like protein (rice)
0.82	0.64	0.64	1.50	2.76	CUST_11691_PI399408534	35_16194	AP2-like protein (Setaria italica)
-0.13	1.83	1.61	1.09	0.98	CUST_11670_PI399408534	35_16195	AP2-like protein (rice)
-0.71	-0.83	-0.81	-1.20	-1.80	CUST_68_PI399408534	35_17054	AP2-like protein (Brachypodium distachyon)
0.08	0.18	0.35	0.51	1.07	CUST_34760_PI399408534	35_17070	AP2-like protein (barley)
-0.48	-0.82	-0.96	-0.91	-1.04	CUST_29402_PI399408534	35_17276	Spark target of EAT1-B1 (TOE1-B1) (wheat)
-0.49	-0.66	-0.49	-0.63	-0.08	CUST_10317_PI399408534	35_17946	AP2-like protein (wheat)
-0.23	-0.30	-0.27	-0.08	0.52	CUST_11489_PI399408534	35_18391	AP2-like protein (Brachypodium distachyon)
-0.23	-0.82	-0.81	0.11	0.66	CUST_23688_PI399408534	35_19676	AP2-like protein (wheat)
0.26	0.18	-0.04	0.51	0.31	CUST_22953_PI399408534	35_20232	AP2-like protein (rice)
1.02	2.05	1.83	2.11	5.31	CUST_17783_PI399408534	35_20400	AP2-like protein (rice)
-0.45	-0.64	-0.04	-0.19	-0.30	CUST_13049_PI399408534	35_21072	AP2-like protein (rice)
0.85	1.89	1.86	1.56	1.83	CUST_7581_PI399408534	35_21287	AP2-like protein (Brachypodium distachyon)
-0.55	-1.15	-1.21	-1.73	-3.31	CUST_26610_PI399408534	35_21853	HvBCBF1 (barley)
1.56	4.04	3.93	3.16	2.07	CUST_31855_PI399408534	35_23852	HvCBF3 (barley)
-0.81	-1.66	-0.54	-1.49	-0.75	CUST_21171_PI399408534	35_27336	AP2-like protein (Brachypodium distachyon)
-0.21	-0.65	-0.81	-1.13	-1.99	CUST_10085_PI399408534	35_27746	AP2-like protein (Brachypodium distachyon)
-0.72	-1.71	-2.10	-2.08	-1.51	CUST_14091_PI399408534	35_28072	AP2-like protein (barley)
0.13	-0.09	-0.04	0.45	0.98	CUST_27509_PI399408534	35_2919	AP2-like protein (Brachypodium distachyon)
-0.31	1.06	0.77	0.19	0.06	CUST_3147_PI399408534	35_30770	HvCBF11 (barley)
0.61	2.45	2.67	2.20	1.39	CUST_784_PI399408534	35_30843	HvCBF10b (barley)
-0.08	-0.09	0.02	0.22	1.05	CUST_28978_PI399408534	35_31564	AP2-like protein (Brachypodium distachyon)
-0.07	-0.20	-0.32	0.43	0.44	CUST_26674_PI399408534	35_31626	AP2-like protein (Brachypodium distachyon)
0.15	1.77	1.77	1.35	1.17	CUST_26236_PI399408534	35_3452	AP2-like protein (Thinopyrum intermedium)
0.06	0.16	-0.11	0.29	1.00	CUST_28758_PI399408534	35_39060	AP2-like protein (maize)
0.37	1.34	1.46	0.89	0.62	CUST_18237_PI399408534	35_39429	AP2 domain CBF protein (wheat)
0.30	0.70	1.00	0.85	0.31	CUST_26647_PI399408534	35_41404	AP2-like protein (barley)
0.06	-0.05	-0.04	0.23	0.87	CUST_14827_PI399408534	35_41882	AP2-like protein (rice)
-0.03	-0.43	-0.57	-0.65	-1.63	CUST_32814_PI399408534	35_4932	HvCBF7 (barley)
1.39	5.60	5.62	4.87	3.23	CUST_20709_PI399408534	35_5832	HvCBF1 (barley)
0.19	0.22	0.14	0.24	0.87	CUST_5456_PI399408534	35_6844	AP2-like protein (Brachypodium distachyon)
0.39	0.39	0.29	0.49	1.64	CUST_28904_PI399408534	35_7703	AP2-like protein (barley)
0.10	0.36	0.42	0.37	-1.21	CUST_25041_PI399408534	35_8313	AP2-like protein (Brachypodium distachyon)
1.21	2.70	2.63	2.24	1.27	CUST_24795_PI399408534	35_8339	AP2-like protein (rice)
0.22	0.22	0.09	0.70	0.89	CUST_8091_PI399408534	35_8945	AP2-like protein (rice)
-0.04	1.34	1.50	0.99	0.86	CUST_554_PI404877155	Contig10472_at	AP2-like protein (wheat)
0.05	-0.42	-0.73	-0.76	-1.54	CUST_1434_PI404877155	Contig11552_at	HvCBF7 (barley)
-0.12	-0.78	-0.76	0.15	0.68	CUST_2537_PI404877155	Contig12940_at	AP2-like protein (wheat)
-0.19	-0.16	0.06	0.59	2.34	CUST_5813_PI404877155	Contig17873_at	AP2-like protein (Brachypodium distachyon)
1.68	4.09	3.86	3.04	2.01	CUST_6519_PI404877155	Contig19472_at	HvCBF3 (barley)
0.69	0.52	1.09	1.94	3.10	CUST_6647_PI404877155	Contig19699_at	AP2-like protein (Setaria italica)
0.10	-0.40	-0.57	-0.56	-0.94	CUST_6985_PI404877155	Contig20485_at	AP2-like protein (Brachypodium distachyon)

					ID		Putative orthologous
0.75	-0.34	0.46	0.43	1.84	CUST_8294_PI404877155	Contig24555_at	AP2-like protein (maize)
0.68	1.80	2.19	2.08	2.32	CUST_8338_PI404877155	Contig2470_s_at	AP2-like protein (Brachypodium distachyon)
0.50	1.38	1.59	0.95	1.88	CUST_8378_PI404877155	Contig2481_s_at	AP2-like protein (rice)
-0.14	0.05	-0.02	-0.30	-0.37	CUST_10149_PI404877155	Contig3865_at	AP2-like protein (barley)
0.55	1.39	1.54	1.70	1.62	CUST_12926_PI404877155	Contig6636_at	AP2-like protein (wheat)
0.02	0.59	0.60	0.65	1.30	CUST_12997_PI404877155	Contig6727_at	AP2 transcriptional activator DRF1 (barley)
0.13	0.21	0.19	0.53	0.59	CUST_13292_PI404877155	Contig6987_at	AP2-like protein (Brachypodium distachyon)
0.24	0.75	0.71	1.11	1.84	CUST_13741_PI404877155	Contig7483_at	AP2-like protein (rice)
0.68	1.62	1.92	1.77	1.88	CUST_13968_PI404877155	Contig7722_at	AP2-like protein (barley)
0.28	0.33	0.44	0.34	-0.15	CUST_14526_PI404877155	Contig8357_at	AP2-like protein (barley)
-0.43	-0.94	-0.99	-1.02	-1.27	CUST_14558_PI404877155	Contig8369_at	Spark target of EAT1-B1 (TOE1-B1) (wheat)
-0.28	-0.22	-0.29	-0.06	0.60	CUST_15918_PI404877155	Contig9762_at	AP2-like protein (Brachypodium distachyon)
0.69	0.47	1.12	2.94	4.86	CUST_16599_PI404877155	HB26N23r_at	AP2-like protein (rice)
0.10	0.25	0.58	1.14	1.95	CUST_16951_PI404877155	HP01H17w_at	AP2-like protein (rice)

Appendix table 3.6 Expressions of AP2 transcription factor family in BRZ over time

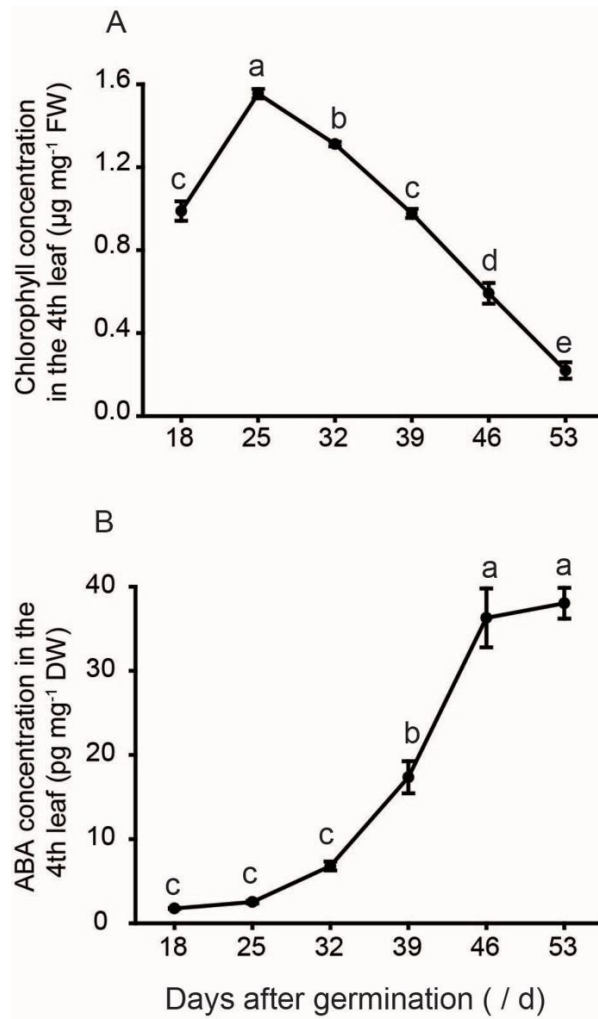| logFC d25	logFC d32	logFC d39	logFC d46	logFC d53	ID	Harvest assembly ID	Putative orthologous
-0.05	-0.43	-0.51	-0.53	-0.85	CUST_25791_PI399408534	35_10361	AP2-like protein (wheat)
0.51	2.93	1.84	1.73	0.56	CUST_10562_PI399408534	35_11386	AP2-like protein (Brachypodium distachyon)
-0.44	-0.37	0.03	-0.58	-1.26	CUST_21498_PI399408534	35_15342	AP2-like protein (rice)
0.86	8.00	6.96	6.42	5.50	CUST_21491_PI399408534	35_15343	AP2-like protein (maize)
0.30	4.17	3.23	2.94	2.16	CUST_21470_PI399408534	35_15344	AP2-like protein (maize)
1.35	2.62	2.12	2.66	3.54	CUST_21469_PI399408534	35_15346	AP2-like protein (Setaria italica)
1.06	3.14	2.72	2.60	1.76	CUST_21457_PI399408534	35_15347	HvCBF6 (barley)
1.34	2.63	2.48	2.66	2.15	CUST_21455_PI399408534	35_15349	AP2-like protein (Brachypodium distachyon)
0.05	-0.02	0.02	0.17	0.39	CUST_10627_PI399408534	35_15732	AP2-like protein (wheat)
-0.20	0.50	0.04	0.03	0.95	CUST_10530_PI399408534	35_15743	AP2-like protein (barley)
-0.37	0.14	-0.09	-0.42	-0.69	CUST_10515_PI399408534	35_15744	AP2-like protein (Dasypyrum villosum)
0.29	0.34	0.20	0.62	0.71	CUST_8063_PI399408534	35_15804	AP2-like protein (Brachypodium distachyon)
0.42	1.01	0.95	1.23	1.64	CUST_11705_PI399408534	35_16193	AP2-like protein (rice)
0.06	0.86	0.21	0.70	0.89	CUST_11691_PI399408534	35_16194	AP2-like protein (Setaria italica)
0.07	1.76	1.29	1.23	0.44	CUST_11670_PI399408534	35_16195	AP2-like protein (rice)
0.38	0.35	0.37	0.63	1.10	CUST_34760_PI399408534	35_17070	AP2-like protein (barley)
-0.15	-0.53	-0.60	-0.37	-0.80	CUST_29402_PI399408534	35_17276	Spark target of EAT1-B1 (TOE1-B1) (wheat)
-0.33	0.33	-0.06	0.46	1.03	CUST_10317_PI399408534	35_17946	AP2-like protein (wheat)
0.39	0.38	0.71	1.76	2.56	CUST_30696_PI399408534	35_18932	AP2-like protein (rice)
0.29	-0.82	-0.66	0.21	0.72	CUST_23688_PI399408534	35_19676	AP2-like protein (wheat)
0.21	1.32	1.79	2.38	5.47	CUST_17783_PI399408534	35_20400	AP2-like protein (rice)
-0.09	0.44	0.49	1.30	0.73	CUST_13049_PI399408534	35_21072	AP2-like protein (rice)
0.99	2.18	1.96	1.65	1.90	CUST_7581_PI399408534	35_21287	AP2-like protein (Brachypodium distachyon)

-0.33	-1.00	-0.96	-1.34	-1.46	CUST_26610_PI399408534	35_21853	HvBCBF1 (barley)
1.77	4.65	4.42	3.99	3.19	CUST_31855_PI399408534	35_23852	HvCBF3 (barley)
-0.37	-0.82	-0.95	-1.15	-1.88	CUST_10085_PI399408534	35_27746	AP2-like protein (Brachypodium distachyon)
-1.00	-2.25	-2.14	-2.18	-2.18	CUST_14091_PI399408534	35_28072	AP2-like protein (barley)
0.31	-0.13	0.19	0.66	0.84	CUST_27509_PI399408534	35_2919	AP2-like protein (Brachypodium distachyon)
-0.29	-0.72	-0.65	-0.53	-0.54	CUST_14012_PI399408534	35_30385	AP2-like protein (rice)
0.00	1.74	1.08	0.75	0.60	CUST_3147_PI399408534	35_30770	HvCBF11 (barley)
0.22	3.51	2.68	2.55	2.07	CUST_784_PI399408534	35_30843	HvCBF10b (barley)
-0.32	0.30	-0.19	0.52	1.22	CUST_32762_PI399408534	35_30982	AP2-like protein (Setaria italica)
0.46	0.08	0.74	0.88	1.48	CUST_28978_PI399408534	35_31564	AP2-like protein (Brachypodium distachyon)
0.09	0.14	-0.01	0.57	0.69	CUST_26674_PI399408534	35_31626	AP2-like protein (Brachypodium distachyon)
0.19	2.84	2.29	2.22	1.52	CUST_26236_PI399408534	35_3452	AP2-like protein (Thinopyrum intermedium)
0.16	2.01	1.44	1.47	1.32	CUST_18237_PI399408534	35_39429	AP2 domain CBF protein (wheat)
0.16	0.86	0.97	0.77	0.52	CUST_26647_PI399408534	35_41404	AP2-like protein (barley)
-0.25	0.60	-0.03	0.49	1.15	CUST_14827_PI399408534	35_41882	AP2-like protein (rice)
-0.10	-0.94	-0.77	-1.43	-1.97	CUST_32814_PI399408534	35_4932	HvCBF7 (barley)
1.56	6.49	5.73	5.60	4.79	CUST_20709_PI399408534	35_5832	HvCBF1 (barley)
0.05	-0.17	-0.08	0.04	2.01	CUST_28904_PI399408534	35_7703	AP2-like protein (barley)
-0.28	-0.26	0.07	-0.47	-1.21	CUST_25041_PI399408534	35_8313	AP2-like protein (Brachypodium distachyon)
1.16	3.01	2.69	2.90	2.16	CUST_24795_PI399408534	35_8339	AP2-like protein (rice)
0.04	2.35	1.86	1.79	1.29	CUST_554_PI404877155	Contig10472_at	AP2-like protein (wheat)
-0.14	-1.01	-0.94	-1.49	-2.15	CUST_1434_PI404877155	Contig11552_at	HvCBF7 (barley)
0.32	-0.87	-0.73	0.22	0.71	CUST_2537_PI404877155	Contig12940_at	AP2-like protein (wheat)
-0.03	0.18	0.05	0.21	0.34	CUST_4341_PI404877155	Contig15309_at	AP2-like protein (Brachypodium distachyon)
-0.02	0.57	0.55	1.30	0.77	CUST_6102_PI404877155	Contig18390_at	AP2-like protein (wheat)
1.73	4.57	4.28	3.75	2.96	CUST_6519_PI404877155	Contig19472_at	HvCBF3 (barley)
0.67	0.71	0.33	0.81	0.95	CUST_6647_PI404877155	Contig19699_at	AP2-like protein (Setaria italica)
-0.03	-1.02	-0.43	-0.47	-1.12	CUST_6985_PI404877155	Contig20485_at	AP2-like protein (Brachypodium distachyon)
0.22	0.33	0.09	0.51	1.63	CUST_8294_PI404877155	Contig24555_at	AP2-like protein (maize)
1.27	2.70	2.50	2.82	2.63	CUST_8338_PI404877155	Contig2470_s_at	AP2-like protein (Brachypodium distachyon)
-0.31	1.19	1.41	1.56	0.58	CUST_8378_PI404877155	Contig2481_s_at	AP2-like protein (rice)
-0.27	0.09	-0.07	-0.26	-0.40	CUST_10149_PI404877155	Contig3865_at	AP2-like protein (barley)
0.94	1.88	1.94	2.19	1.60	CUST_12926_PI404877155	Contig6636_at	AP2-like protein (wheat)
0.48	0.74	0.85	0.90	1.29	CUST_12997_PI404877155	Contig6727_at	AP2 transcriptional activator DRF1 (barley)
0.38	0.09	0.33	0.67	0.56	CUST_13292_PI404877155	Contig6987_at	AP2-like protein (Brachypodium distachyon)
0.32	1.09	1.04	1.19	1.57	CUST_13741_PI404877155	Contig7483_at	AP2-like protein (rice)
1.03	2.24	2.21	2.33	2.18	CUST_13968_PI404877155	Contig7722_at	AP2-like protein (barley)
-0.13	-0.62	-0.60	-0.38	-0.89	CUST_14558_PI404877155	Contig8369_at	Spark target of EAT1-B1 (TOE1-B1) (wheat)
0.29	0.46	0.69	1.86	2.69	CUST_16599_PI404877155	HB26N23r_at	AP2-like protein (rice)

Appendix 4 Expression of *HvNAC005* in ARZ and BRZ during root aging

Tissue	ID	logFC d25	logFC d32	logFC d39	logFC d46	logFC d53
Basal root zone	CUST_3522_PI404877155	0.41	0.94	0.94	1.57	1.57
Apical root zone	CUST_3522_PI404877155	-0.50	0.26	0.39	1.65	2.71

Appendix 5 The chlorophyll and ABA concentrations during senescence of the 4th leaf

Appendix 6 Expressions of catalase-like genes in ARZ and BRZ overtime

Basal root zone (BRZ)							
logFC d25	logFC d32	logFC d39	logFC d46	logFC d53	ID	Harvest assembly ID	Annotation
-0.20	0.63	0.46	1.62	3.04	CUST_102088_PI40352 4517	35_2912 27	Catalase 1 (Arabidopsis thaliana)
-0.56	0.30	0.15	0.93	1.89	CUST_154793_PI40352 4517	35_432 47	Catalase isozyme 2 (Hordeum vulgare)
0.67	1.79	2.30	3.51	4.83	CUST_178732_PI40352 4517	35_497 11	Catalase isozyme 2 (Hordeum vulgare)
-0.24	0.28	0.30	0.40	0.90	CUST_51832_PI403524 517	35_147 71	Catalase 1 (Triticum aestivum)
0.19	1.41	1.93	3.13	4.45	CUST_51835_PI403524 517	35_147 72	Catalase isozyme 2 (Hordeum vulgare)
0.65	1.57	2.08	3.38	4.74	CUST_51837_PI403524 517	35_147 73	Catalase isozyme 2 (Hordeum vulgare)
0.61	1.66	2.12	3.38	4.69	CUST_51848_PI403524 517	35_147 75	Catalase (Acacia ampliceps)

Apical root zone (ARZ)							
logFC d25	logFC d32	logFC d39	logFC d46	logFC d53	ID	Harvest assembly ID	Annotation
1.19	0.91	1.20	2.89	4.01	CUST_102088_PI40352 4517	35_2912 7	Catalase 1 (Arabidopsis thaliana)
-0.19	-0.37	-0.73	-0.38	0.20	CUST_109829_PI40352 4517	35_3120 9	Catalase isozyme 1 (Hordeum vulgare)
0.23	0.69	1.00	0.77	0.71	CUST_133877_PI40352 4517	35_3757 5	Catalase-like (Burkholderia phytofirmans)
1.14	0.11	0.36	1.61	2.60	CUST_154793_PI40352 4517	35_4324 7	Catalase isozyme 2 (Hordeum vulgare)
4.06	3.07	4.45	6.55	7.98	CUST_178732_PI40352 4517	35_4971 1	Catalase isozyme 2 (Hordeum vulgare)
-0.10	-0.28	-0.26	-0.07	0.54	CUST_3106_PI4035245 17	35_844	Catalase isozyme 1 (Hordeum vulgare)
4.17	3.00	4.20	6.47	8.10	CUST_51835_PI403524 517	35_1477 2	Catalase isozyme 2 (Hordeum vulgare)
2.94	2.03	3.14	5.36	6.94	CUST_51837_PI403524 517	35_1477 3	Catalase isozyme 2 (Hordeum vulgare)
3.79	2.72	3.87	6.13	7.65	CUST_51848_PI403524 517	35_1477 5	Catalase (Acacia ampliceps)

Curriculum Vitae

Personal information

Name: Zhaojun Liu

Email: liu@ipk-gatersleben.de , lzjdeyouxiang@126.com

Institution: Molecular Plant Nutrition group, The Leibniz Institute of Plant Genetics and Crop Plant Research (IPK), Gatersleben, Germany

Education background

09.2005 – 07.2009

Bachelor of Forestry, Northwest A&F University, China

09.2009 – 07.2012

Master of Silviculture, supervisor: Prof. Dr. Zhao Zhong, Northwest A&F University, China, master thesis: Proteomic study for adventitious root formation of *Xanthoceras sorbifolia* cuttings

10.2012 – Present

PhD of Biology, supervisor: Prof. Dr. Nicolaus von Wiren. Molecular plant nutrition group, IPK, Germany. PhD project: Characterization of root senescence in barley

Scholarships and awards

11.08.2012 – 13.09.2012

Short-stay scholarship, Hokkaido University, Japan

Supervisor: Prof. Dr. Koike Takayoshi

02.06.2015 – 05.06.2015

The Best Talk, Biotechnology journal award sponsored by Wiley

Plant Science Student Conference, Halle, Germany

https://msbi.ipb-halle.de/pssc2015/

05.10.2016 – 07.10.2016

The Best Talk

9th International PhD School of Plant Development, Retzbach, Germany

http://plant-development.org/history.html

26.01.2017 – 26.03.2017

EU COST action scholarship, Short-Term Scientific Missions

Project: Proteomic analysis for barley root senescence

Supervisor: Prof. Dr. Sebastien Carpentier, KU Leuven, Belgium

Scientific activity and training

30.06.2013 – 06.07.2013

EPPN summer school on plant phenotyping

Biological research center (BRC), Szeged, Hungary

10.11.2014 – 14.11.2015

Poster, 7th European Workshop on plant senescence, Denmark

14.09.2015 – 17.09.2015

Barlomics summer school, IPK, Germany

02.11.2015 – 06.11.2015

Root phenotyping winter school, Jülich, Germany

12.09.2016 – 15.09.2016

Biodiversity training course. Supervisor: Prof. Dr. Nico Eisenhauer

German Centre for Integrative Biodiversity Research (iDiv), Leipzig

29.05.2017 – 01.06.2017

Poster, the 8th international symposium on root development. Umea, Sweden

Publication

Zhaojun Liu, Sheng Zhang, Zhong Zhao, Boyong Zhang, Jianwei Zong. Optimization of Two-dimensional Gel Electrophoresis for Proteome from the Phloem of *Xanthoceras sorbifolia*. Journal of Northwest Forestry University, 2012, 27(3): 55 - 61.

Zhaojun Liu. Construction of artificial wetlands in south of Shaanxi. Shaanxi Forest Science and Technology, 2008, (4): 135 - 137.

Xiaobin Song, **Zhaojun Liu**. Analysis of *Cryphonectria parasitica* in Southern Shaanxi Based on Quantitative Theory (I). Journal of Northwest Forestry University, 2010, 25(6): 122 -125.

Zong Jianwei, Yang Yuhua, Zhao Zhong, **Liu Zhaojun**, Zhang Sheng. Effects of Exogenous IBA on the root morphology indices of *Xanthoceras sorbifolia* bunge by hardwood cuttings. Northern Horticulture, 2012 (23): 11 -14.

Ma W, Schubert V, Martis M M, Hause G, **Liu Z**, Shen Y, Conrad U, Shi W, Scholz U, Taudien S, Cheng Z, Houben A. The distribution of alpha-kleisin during meiosis in the holocentromeric plant *Luzula elegans*. Chromosome Research, 2016, 24(3): 393 – 405.

Eidesstattliche Erklärung / *Declaration under Oath*

Ich erkläre an Eides statt, dass ich die Arbeit selbstständig und ohne fremde Hilfe verfasst, keine anderen als die von mir angegebenen Quellen und Hilfsmittel benutzt und die den benutzten Werken wörtlich oder inhaltlich entnommenen Stellen als solche kenntlich gemacht habe.

I declare under penalty of perjury that this thesis is my own work entirely and has been written without any help from other people. I used only the sources mentioned and included all the citations correctly both in word or content.

_____
Datum / Date

_____
Unterschrift des Antragstellers /

Signature of the applicant

Erklärung über bestehende Vorstrafen und anhängige Ermittlungsverfahren /

Declaration concerning Criminal Record and Pending Investigations

Hiermit erkläre ich, dass ich weder vorbestraft bin noch dass gegen mich Ermittlungsverfahren anhängig sind. / *I hereby declare that I have no criminal record and that no preliminary investigations are pending against me.*

_____	_____
Datum / Date	Unterschrift des Antragstellers
	/ *Signature of the applicant*